The Department of Geodetic Science
Report No. 77

Super-wide-angle Photography and Its Application in Highway Mapping

by
Sanjib K. Ghosh
and
Everett H. Ramey

Research Sponsored by
State of Ohio
Department of Highways
Columbus, Ohio 43215

In Cooperation with
U.S. Department of Commerce
Bureau of Public Roads

Agreement No. 1485
RF Project No. 2159

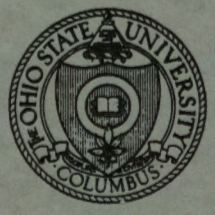

THE OHIO STATE UNIVERSITY
RESEARCH FOUNDATION
COLUMBUS, OHIO 43212

September 1966

RF Project No. 2159

FINAL TECHNICAL REPORT

by

THE OHIO STATE UNIVERSITY
RESEARCH FOUNDATION
1314 Kinnear Road
Columbus, Ohio 43212

On:

SUPER-WIDE-ANGLE PHOTOGRAPHY
AND
ITS APPLICATION IN HIGHWAY MAPPING

Sponsor: State of Ohio
Department of Highways
Columbus, Ohio 43215

In Cooperation with

U. S. Department of Commerce
Bureau of Public Roads

Research Period: January, 1966 to September, 1966

Prepared by: Dr. Sanjib K. Ghosh
and
Mr. Everett H. Ramey

Submitted by: Dr. Sanjib K. Ghosh
Project Supervisor, Photogrammetry
Department of Geodetic Science

Date: September 1966

FOREWORD

This report was prepared by Dr. Sanjib K. Ghosh, Research Project Supervisor and Mr. Everett H. Ramey, Research Assistant, Department of Geodetic Science, The Ohio State University under State of Ohio, Department of Highways contract (in cooperation with the U. S. Bureau of Public Roads) dated January 3, 1966, this being The Ohio State University Research Foundation Project No. 2159. Project period: January 3, 1966; extended to September 30, 1966.

The project was administered under the direction of Mr. P. E. Masheter, and Mr. C. R. Hanes in charge of Engineering Research and Development, Ohio Department of Highways with Mr. L. O. Herd, Chief of the Aerial Engineering Section, the Ohio Department of Highways as the liaison representative.

OSURF Project No. 2159 covers research performed by Dr. Sanjib K. Ghosh, Project Supervisor, Messrs. Everett H. Ramey, John Y. C. Wang, and John F. Kenefick, Research Assistants; Mr. Fletcher W. Twitty, Technical Assistant; Mrs. Vera N. Hoff, Secretary, and Mrs. Erma A. Findlay, Clerk Typist.

Sincere appreciation is extended to Mr. Lloyd O. Herd, Chief of the Aerial Engineering Section of the Ohio Department of Highways for his interest and enthusiasm for this research. Similar appreciation is also due the members of Mr. Herd's staff: Messrs. Don Jennings, Jack Strahle and William G. Prescott.

The assistance and cooperation of the Topographic Division Research Center, U. S. Geological Survey, McLean, Virginia for furnishing the diapositives which were used in this study is thankfully acknowledged.

The opinions, findings and conclusions expressed in this publication are those of the authors and not necessarily those of the State of Ohio or the Bureau of Public Roads.

TABLE OF CONTENTS

TABLE OF CONTENTS
(continued)

LIST OF TABLES

LIST OF ILLUSTRATIONS

LIST OF ILLUSTRATIONS
(continued)

1. INTRODUCTION

1.1 Purpose and Objectives

The super-wide-angle single lens aerial camera is a recent development in photogrammetry. With its development has come a new family of instruments and procedures to handle the photography with angular coverage of 120°. In some cases, existing instruments and procedures have been modified to accomodate use of the super-wide-angle photography.

The super-wide-angle (SWA) system has been successfully used for many problems in mapping, but principally for small and medium scales. The group of Ohio State University researchers working with Dr. Ghosh undertook for the Ohio Department of Highways the study of super-wide-angle photography for use in highway mapping. It is intended to present a complete report of this study in the following pages.

The objectives of this study are:

To evaluate super-wide-angle (SWA) photography for highway surveying and mapping with special reference to the equipment presently available with the Ohio Highway Department (particularly the Nistri-Bendix Analytical plotter AP/C) with a view to improving the present mapping system.

The entire study is comprised of three broad aspects:

1) A general study of the SWA system and a theoretical analysis of the obtainable observational accuracy as compared to the standard (wide angle) system of photography.

2) A study and analysis of the AP/C system of handling photogrammetric problems. This study was required in view of the very recent development of this analytical plotter, which had not been thus far thoroughly evaluated by any agency. This led to establishing a procedure for handling SWA photographs with the AP/C.

3) A test of the procedure by using SWA photographs taken of a controlled test area with an RC9 camera (manufactured by Wild-Heerbrugg, Ltd.), which is the only SWA camera available commercially in the free world. A comparative study is made between results obtained from aerotriangulations at the Nistri-Bendix AP/C and at the Wild A7 stereo instruments.

1.2 The Super-wide-angle Photography

1.2.1 Comparative Study between SWA and WA Systems, General

Lenses are classified as to their field of coverage with super-wide-angle denoting an angle of coverage greater than 100°. In the case of the RC9 camera built by the Wild Company, the angle of coverage is 120°. This is the camera that is presently in limited use to the United States and Canada and is the one used for this study.

Wide-angle photography as used in photogrammetric mapping generally has an angle of coverage of 90° with a focal length of approximately 150 mm and with a 9 x 9 inch or 23 x 23 cm format. In the RC9 camera the 9 x 9 inch format has been retained and the focal length was changed accordingly to approximately 88 mm. Thus, a great advantage in coverage is achieved. For a given flight height, the RC9 photograph covers three times the area of that by the wide-angle photograph as shown in Figure 1.1. But based on performance tests the same accuracy claimed for RC9 photography is as obtained for wide-angle photography--if the flight height is reduced by a ratio of 5/6: 1. The advantage thus gained is the area mapped is then two times that of wide-angle photography, which is still a very significant factor.

Another comparison is significant: the coverage in a single strip with conventional 60% overlap. Here with forward overlap u = 60%,

$A = a \cdot \frac{h}{f}$ with $a_1 = a_2$ for 9 x 9 inch plates. In terms of the plates:

$$\frac{A_1}{A_2} = \frac{a_1 \cdot h}{f_1} \Big/ \frac{a_2 \cdot h}{f_2} = \frac{f_2}{f_1} = \frac{150}{88} = 1.71$$ shown in Figure 1.2.

or, the gain for the super-wide-angle is 1.71 times the wide angle.

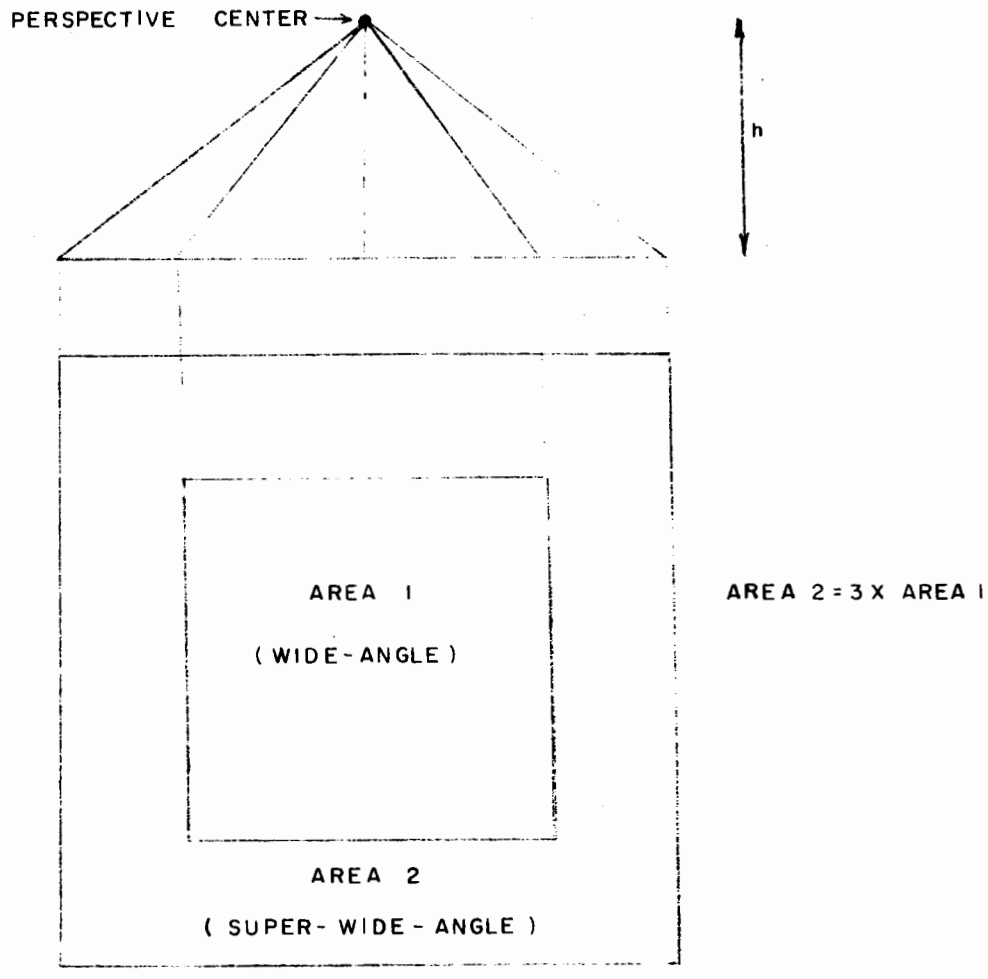

Figure 1.1. Comparison of Areas of RC9 and Wide-angle Photographs

Of more significance is the relationship in base-height ratios between the two, because this is the important item in measuring elevations. Here $b = (1 - u)A$. Thus, the base height ratio is increased in same ratio, or 1.71. Where

$$h = \frac{A}{a} f \text{ and } b = (1 - u)A, \quad b/h = \frac{(1 - u)A}{A \cdot f} \cdot a = \frac{.4 \times 230}{88} = 1.05$$

for super-wide-angle photography compared to 0.6 for wide-angle for $u = 60\%$.

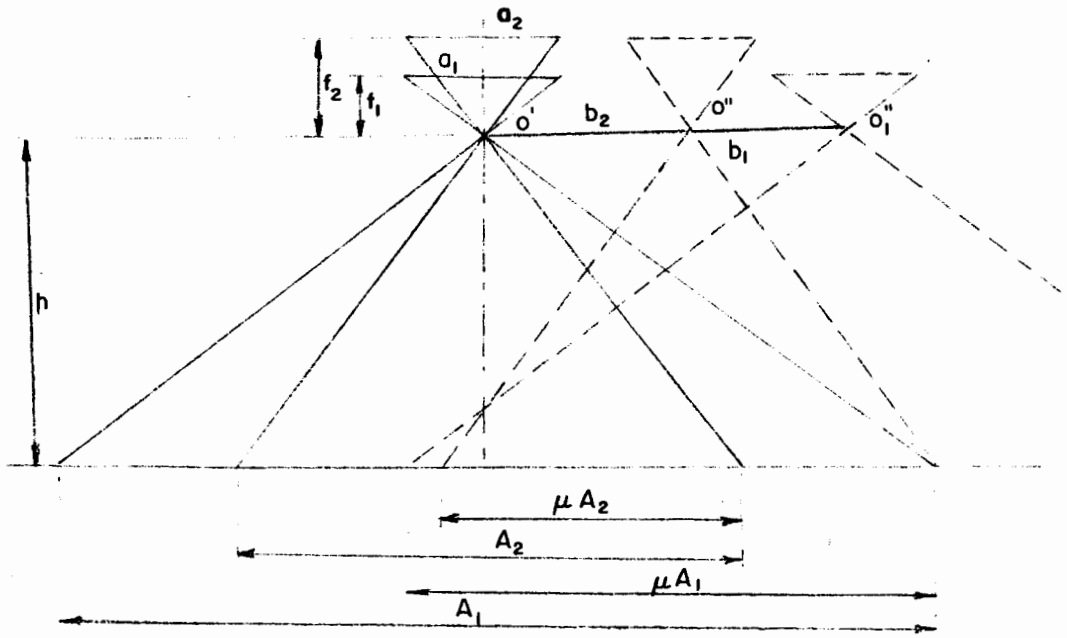

Figure 1.2. Base-height Relations for RC9 and Wide-angle Photographs

Thus, there are important advantages with super-wide-angle photography. The angle of coverage has been shown to be the optimum [29]. The economy of having fewer photographs, fewer models, less photo materials, less flight time and less ground control is most appealing. However, the super-wide-angle photographs have been indicated to be inferior in other respects [36]. Some favorable results have been reported both by using conventional analogue photogrammetric equipment and by using analytical techniques. [7, 22, 23, 36.]

The RC9 photograph has more distortion than the highest quality wide-angle photograph of the same area coverage. This results from two causes: (1) the lens has greater distortion; and (2) the larger angle of coverage in the RC9 results in larger effects in earth curvature and atmospheric refraction. Thus to have some means to correct for distortions is a necessary requirement in the use of RC9 photographs. Corrector plates have been used to do this; an analytical approach might be better.

1.2.2 Comparative Study Between SWA and WA Systems, Empirical Observations.

In a series of tests conducted by USAE/GIMRADA [8] results of two systems were compared. System 1) utilizing aerial pictures taken with the Wild RC9 camera and using the Wild Autograph A9 (i.e., SWA system). System 2) utilizing aerial pictures taken with a KC-1 camera and using the Wild Autograph A7 (i.e., WA system).

The results of these tests are given briefly below:

a) Grid model flatness test:

Standard deviation in the scale of the picture:

SWA system : 7 μ

WA system : 9 μ

b) Terrain model flatness tests:

At equal photographic altitude (results attributed to small scale of photographs, and additional photographic process involved in reducing the plates).

Standard deviation in the scale of the picture:

SWA system : 14 μ

WA system : 17 μ

c) Stereotriangulation test:

With aerotriangulation missions flown at a flying height of 20,000 feet in a strip length of more than 22 linear miles the standard residual errors are (in feet).

System	X	Y	Z
SWA	12.0	12.1	9.4
WA	7.6	11.4	7.7

These cannot be compared directly because the picture scales are different. After standardizing the SWA system to the WA system base by multiplying the figures with a factor 0.582 (= 88.5/152 i.e., the ratio between the two focal lengths) we obtain the standard errors:

System	X	Y	Z
SWA	7.0	7.1	5.5
WA	7.6	11.4	7.7

These figures without any unit assigned, may be used for the purpose of comparison.

All these prove the superiority of the SWA system over the standard WA system.

1.2.3 Comparative Study Between SWA and WA Systems; Accuracy of Relative Orientation

The accuracy of the compiled map in a photogrammetric system is directly related to the accuracy of orientation of individual stereo models, in which, again the accuracy of relative orientation contributes the major factor [11].

The accuracy of relative orientation depends on

a) the quality of restitution instrument
b) the quality of the photography
c) the ability of the operator
d) the theoretically considered observational errors.

The first three items are beyond the scope of the present study. Furthermore, these items cannot be analyzed in the SWA system without obtaining considerable empirically obtained data.

The effect of the observational errors in relative orientation may be analyzed from the variance-covariance matrices as suggested by Ghosh [11].

For this theoretical study, the following assumptions are made:

a) Parallax observations at the model points have the same weight.
b) Parallax observations are uncorrelated.
c) Dependent method of Relative Orientation (i.e., using the elements of only one projector camera) with the right-hand side camera.
d) Flat terrain (where, generally speaking, the ruggedness of the terrain is less than 10 per cent of the flying height).
e) Numerical Relative orientation.

This study is made in two cases:

i) With six model points for orientation (points Nos. 1, 2, 3, 4, 5 and 6 in Figure 1.3) where points 1 and 2 are left and right nadir points respectively).

ii) With nine points in the model for orientation (i.e., points 7, 8 and 9 added to the previous six points in Figure 1.3).

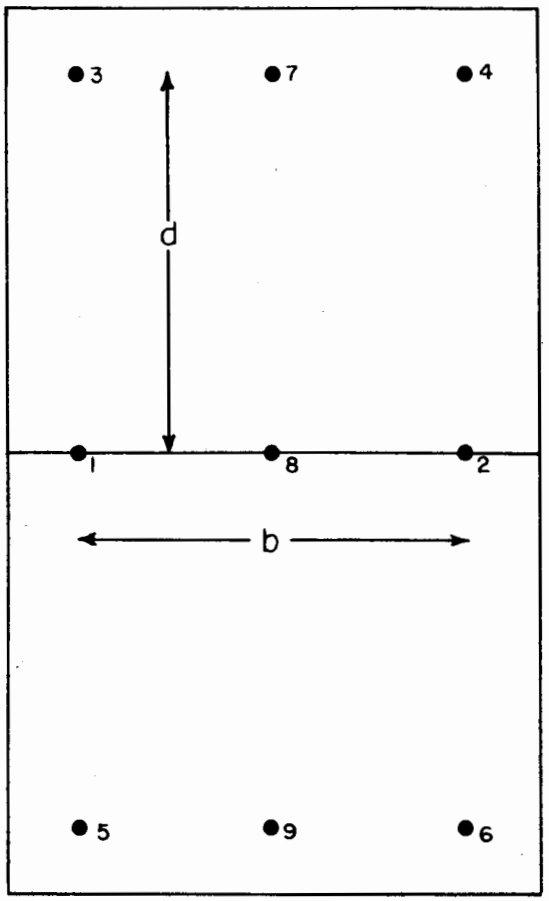

Figure 1.3. Location of Model Points For Relative Orientation

The variance-covariance matrix with six points is given in Table 1.1.

Table 1.1

Variance-covariance Matrix, Numerical
Relative Orientation, Six Points

	Q_{by}	Q_{bz}	Q_{κ}	Q_{φ}	Q_{ω}
Q_{by}	$\frac{1}{6}$	0	0	0	0
Q_{bz}		$\frac{Z^2}{2d^2}$	0	$-\frac{Z^2}{2bd^2}$	0
Q_{κ}			$\frac{2}{3b^2}$	0	0
Q_{φ}				$\frac{Z^2}{b^2d^2}$	0
Q_{ω}					$\frac{3Z^2}{4d^4}$

Here, b is the model base, which considering 60% overlap and considering the scale of the model as the same as that in the picture, is

92 mm $\cong$ 0.09 m.

d is the distance of the points 3, 4, 5, 6, 7 and 9 from the base in the model and

$d = (\frac{a}{2} - 10)$ mm = 105 mm $\cong$ 0.10 m.

Z is the projection distance of the terrain surface in the model and

Z = f = 88.5 mm $\cong$ 0.09 m.

Substituting these numerical values is obtained Table 1.2.

Table 1.2

Numerical Substitution of Table 1.1
for SWA Photography

	Q_{by}	Q_{bz}	Q_{κ}	Q_{φ}	Q_{ω}
Q_{by}	0.17	0	0	0	0
Q_{bz}		0.4	0	-4.5	0
Q_{κ}			82.3	0	0
Q_{φ}				100.0	0
Q_{ω}					60.7

These values in the case of WA photography are:

$b = 92$ mm $\cong 0.09$ m, $d = 105$ mm $\cong 0.10$ m, $z = f \cong 150$ mm $= 0.15$ m.

Substituting these values is obtained Table 1.3.

Table 1.3

Numerical Substitution of Table 1.1
for WA Photography

	Q_{by}	Q_{bz}	Q_{κ}	Q_{φ}	Q_{ω}
Q_{by}	0.17	0	0	0	0
Q_{bz}		1.12	0	-12.5	0
Q_{κ}			82.3	0	0
Q_{φ}				277.8	0
Q_{ω}					168.7

A comparison of Tables 1.2 and 1.3 indicates that by using SWA photography there is no improvement over the WA photography in elements by and κ, whereas, there are definite improvements in the elements bz, φ and ω; even the correlation between φ and bz is reduced, i.e., except for by and κ the improvement is roughly three times in each case.

Similar variance-covariance matrix with nine points is given in Table 1.4.

Table 1.4

Variance-covariance Matrix, Numerical Relative Orientation, Nine Points

	Q_{by}	Q_{bz}	Q_{κ}	Q_{φ}	Q_{ω}
Q_{by}	$\frac{1}{9}$	0	0	0	0
Q_{bz}		$\frac{5Z^2}{12d^2}$	0	$-\frac{Z^2}{2bd^2}$	0
Q_{κ}			$\frac{2}{3b^2}$	0	0
Q_{φ}				$\frac{Z^2}{b^2d^2}$	0
Q_{ω}					$\frac{Z^2}{2d^4}$

Proper numerical substitutions in Table 1.4 give Table 1.5 for SWA and Table 1.6 for WA.

Table 1.5

Numerical Substitution of Table 1.4
for SWA Photography

	Q_{by}	Q_{bz}	Q_{κ}	Q_{φ}	Q_{ω}
Q_{by}	0.11	0	0	0	0
Q_{bz}		0.34	0	-4.5	0
Q_{κ}			82.3	0	0
Q_{φ}				100.0	0
Q_{ω}					40.5

Table 1.6

Numerical Substitution of Table 1.4
for WA Photography

	Q_{by}	Q_{bz}	Q_{κ}	Q_{φ}	Q_{ω}
Q_{by}	0.11	0	0	0	0
Q_{bz}		1.12	0	-12.5	0
Q_{κ}			82.3	0	0
Q_{φ}				277.8	0
Q_{ω}					112.5

A comparison of Tables 1.5 and 1.6 also indicates that, in the case of using nine points for numerical orientation of the stereo model, there is no improvement over WA photography by using SWA photography in the same elements by and κ, whereas, there is definite improvement in the accuracies of elements bz, φ and ω as well as in the correlation between φ and bz.

These studies indicate that SWA photography is definitely capable of yielding better accuracy and better efficiency than the standard WA photography.

2. THE ANALYTICAL SYSTEM

The requirements for highway mapping presents a challenge to the photogrammetrist because of the small tolerances imposed, especially for elevations. Scales generally range from 1" = 200' to 1" = 40' or 50' for location and construction maps with elevations measured to as little as 0.1 ft and contours to 2 ft interval. Thus a low flight altitude with many large scale models and much ground control are required. Any improvement in the accuracy of the system will therefore have an important consequence economically. This is accomplished in several ways:

1) By the use of a measuring device with higher reading accuracy accomplished

a) by measuring to smaller increments such as one micron for most comparators; and

b) by increasing the fidelity of measurements through calibration of the comparator.

2) By offering a means to correct measurements made on a photograph for known systematic errors which include

a) radial lens distortion-- symmetrical, and possibly asymmetric or tangential-- with more accuracy than is done in analogue devices;

b) film distortion-- by measuring to fiducial marks positions of which have been determined in the camera by calibration study;

c) effects of atmospheric refraction and earth curvature by correcting with a more accurate mathematical method; and

d) possibly still other corrections such as other camera or comparator errors determined by calibration studies.

All these corrections are feasible with electronic computers. In the past they have been either neglected altogether or else handled in a less rigorous manner.

2.1 The AP/C System

The AP/C (Analytical Plotter/Commercial, see Figure 2.1) combines a two-plate precision comparator, built by the Nistri Company of Italy, with an on-line electronic computer, built by the Bendix Corporation of the United States of America.

It was designed and built under the supervision of the National Research Council of Canada. Being a new system, a description of its function is in order. However, no attempt is made to describe in detail its mechanical and electronic complexities.

There are three basic components to the AP/C: (1) the computer with its associated electrical equipment, (2) the optical-mechanical viewing unit, essentially a two-plate comparator, and (3) the plotting table. With the computer unit is a typewriter with a punched-tape reader and punch-out routines (Figure 2.1). The computer is small (approximately 2,000 word memory), fully transistorized, and very fast.

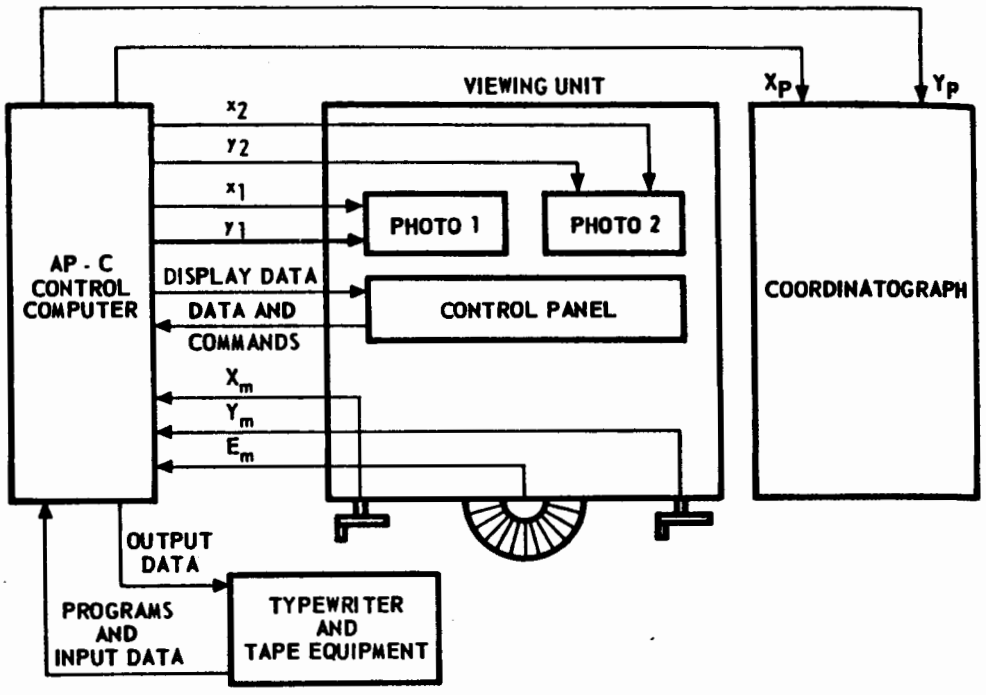

Figure 2.1 System Diagram for AP/C

The functions of the system as depicted in Figure 2.1 are described below:

The computer receives input data as model coordinates from the hand wheels (X_m, Y_m) and the footwheel (E_m) from the operator's control panel (data commands) and from the typewriter and tape unit (generally programs and subprograms are entered). In turn, the computer might cause print-out of data or punch out of data at the typewriter and tape unit. It sends commands to servos to keep the photographs properly positioned and oriented for viewing by the operator. It might also display various data at the operator's control panel. Finally, the computer commands servos for plotting at the coordinatograph.

The photogrammetric solutions on AP/C can perhaps be shown by describing a typical operation procedure. First refer to Figure 2.2 for a presentation of the coordinate systems used. The usual case in photogrammetry might begin with photograph coordinates. Then, after applying corrections and transformations, model coordinates are obtained. Here, with AP/C it is handled in the inverse manner as the computer is reacting to commands from hand wheels and the footwheel -- the model coordinates X_m, Y_m, E_m for model point P. These coordinates are translated to the perspective center O_1 by airbase components b_x, b_y, b_z to the coordinate system X_c, Y_c, Z_c. Orientation elements κ, ω, φ are next applied sequentially in this given order to rotate to the coordinate system X''', Y''', Z''' still at model scale. A scaling by factor f/z''' converts to photograph coordinates x, y, z (=f).

The systematic corrections to coordinates have not been considered so far. These are applied in a similar manner as the transformations above. First the model coordinates are corrected for earth curvature which depends on X_m and Y_m and some scale constant S_G to correct the model coordinate E_m. The atmospheric refraction depends on the X_c, Y_c from the nadir point and on the E_m for the point. Earth curvature and refraction corrections are added to obtain Z_c. Finally, corrections for lens distortion and film shrinkage are applied to the photo coordinates to furnish the operator his correct stereoscope model for viewing.

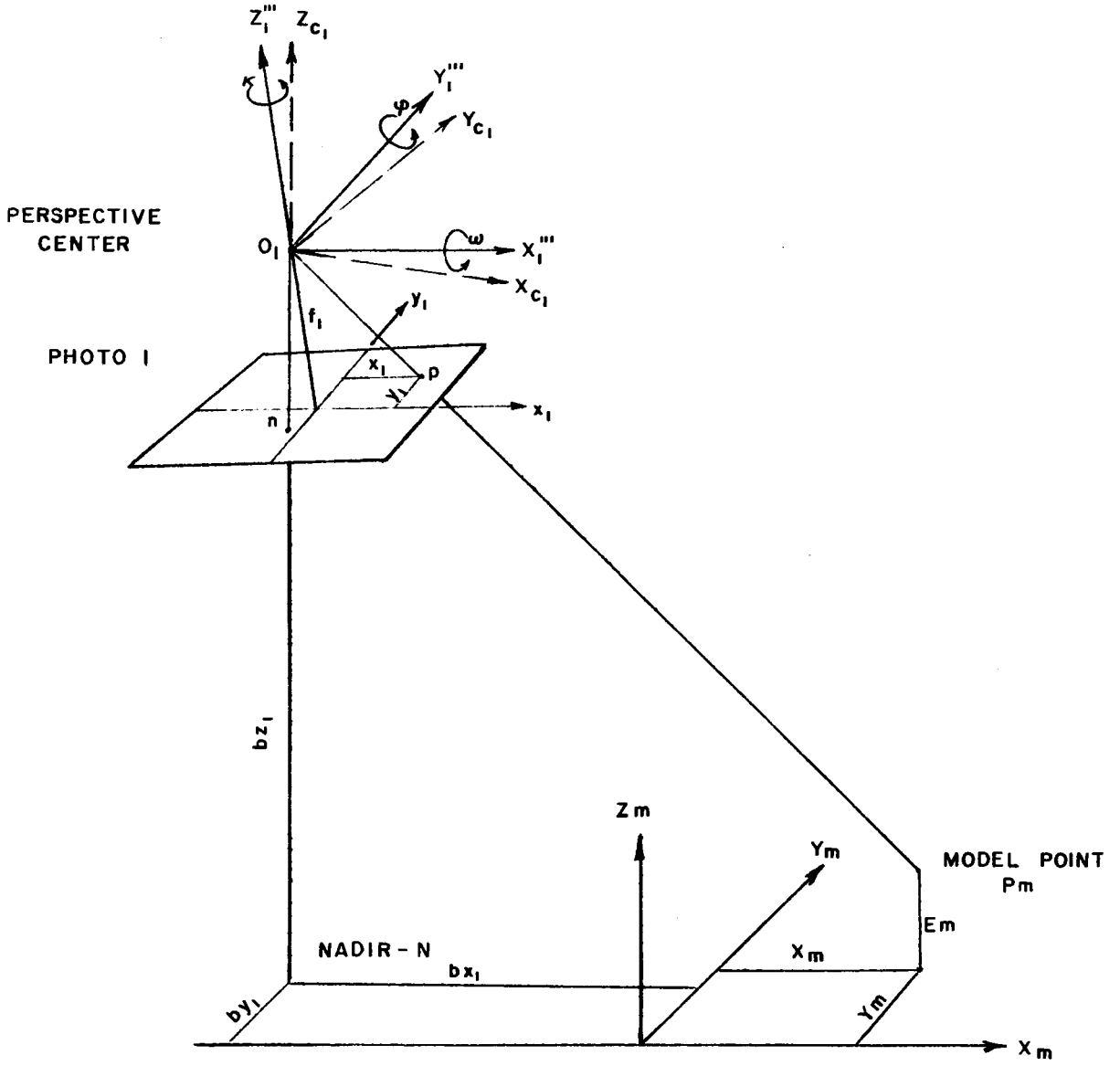

Figure 2.2 Coordinate Systems in AP/C

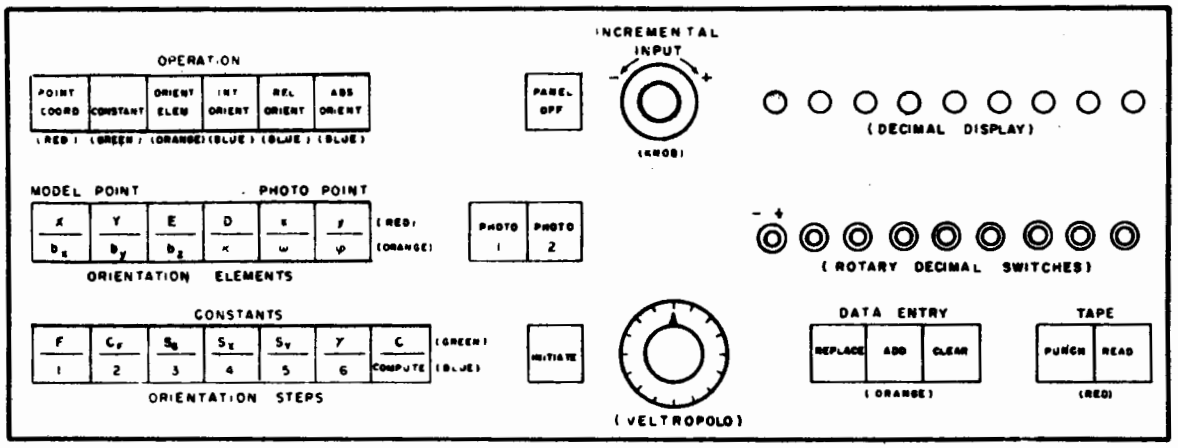

Figure 2.3 Operator's Control Panel in AP/C

The above cycle is performed for each photograph as the operator moves about the model space---either by hand wheels and foot-wheel, or by the Veltropolo slewing device (which actually permits slewing accurately in any desired azimuth). These computations comprise the biggest effort of the computer and are designated as the "Real-Time" Program. Intermixed with the cycles for the real-time program are computations with several subroutines. The real-time program is executed at the rate of 30 times per second and the operator's control panel is also interrogated by the computer at 30 times per second. The subroutines (display data, lens and film corrections for each photo, and model corrections for each photo) cycle 5 to 6 times per second. Thus, many computations, such as for relative orientation, appear instantaneous to the operator because of the speed of execution.

The Operator's Control Panel is depicted in Figure 2.3; the diagram is self explanatory. This is the chief means by which the operator communicates with the computer and the program. The push-button switches are arranged in a nice color scheme to aid in executing each operation. There is also some interlocking of switches such that only one operation may be active at a given time.

Some features of the stereoviewer unit are mentioned. The maximum plate size is 9 x 9 inch. The plates are entered in the plate holders, against stops, to approximately align the plates to the flight axis. The plates are viewed at 10 or 14 times magnification using a 25-micron measuring dot. Focal lengths up to 3344 mm can be accommodated with some limits on the orientation angles.

The AP/C can function as a monocular or as a stereo comparator in which case the output would be in photograph coordinates. The computer would then serve only a readout function. However, the real function for which the system was designed is that of a stereoplotter which furnishes model coordinates corrected for known systematic errors. To obtain model coordinates using measured photograph coordinates entails several steps: (1) A refinement of coordinates for systematic effects, (2) A computation of relative orientation, (3) A space intersection computation and a computation to scale and level the model, or an orientation to some coordinate system. Thus, the AP/C stereoplotter

offers distinct advantages in doing the steps directly. It has, however, some limitations because the built-in-programs or computer capacity may impose limits in the handling of redundant observations in correcting for systematic effects. An analysis of some of these factors is attempted in this study. More details of operating procedures are outlined under appropriate headings.

3. THE TEST PROCEDURE

It was fortunate for this study that the U. S. Geological Survey furnished diapositives of one of its RC9 cameras for a test area of Arizona. The scale was approximately 1:17,000 (h = 5000 ft) which approaches the desired large scale for highway mapping. Also, an abundance of premarked control stations cover five of the six photographs. (See Figure 3.1.)

The control layout of the area was designed for photogrammetric uses and was established as a joint effort of the Army Map Service and the U. S. Geological Survey. Two of the models of this strip are each controlled by four horizontal control stations and over 40 vertical control stations. These approximately cover the full extent of the models and are near ideal to study the elevation errors in the entire model area. All control was targeted in advance of photography by either 6- or 9-ft square panels.

The objectives of the test were to measure the inherent or residual errors in the RC9 - AP/C system, and later to compare these results with those obtained from RC9 - Wild A7 system. Thus, the test was done with absolute orientation for the high-density controlled area. This confined the error to within each model so as not to introduce any propagated error.

As a secondary step, the entire strip was done to test for propagated error in aerotriangulation. Actually, this is a small number of models for this test but it should show some pattern of error propagation as measurements are taken to microns.

The photography was printed with corrector plates for symmetrical lens distortion and for earth curvature and atmospheric refraction.

Figure 3.1 Layout for Test Strip, AMS Arizona Test Area

The latter corrector plate used was for 10,000 ft altitude whereas the flight height was 5,000 ft. A computed correction was made to compensate for this over-correction of the plate in the AP/C system.

The photographs were prepared for these tests in the following manner. First, a row of three pass points were drilled approximately on the normal flight line through the photograph center. A templet was used to maintain some symmetry in the location of these pass points. Coding of the photograph points was made by using a five digit number as follows: First two digits for the number of the photograph on which the point was identified, next digit used for classifying the point, and the last two digits to denote the serial number within the above grouping. Classification numbers: o - photo reference numbers with serial numbers: o - for center or nadir, and 1 through 4 - for fiducial mark numbers; 1 - horizontal control point; 2 - vertical control point; 3 - pass points; and 4 and up - any other groupings desired (not used in this example).

3.1 Interior Orientation

The interior orientation on the AP/C is the first step in the photogrammetric solution. The photograph is entered into the plate carrier to coincide with stops along two edges. The photograph is placed with the x-axis in the general direction of the flight axis-- actually some Kappa rotation can be added to the initial photograph to correct for crab of the flight line.

The operator is led by the computer by a semiautomatic routine to the vicinity of each of the fiducial marks. He completes bringing the measuring dot into exact coincidence with the fiducial marks by the "incremental" switch. Once all four marks are visited in this manner, he pushes the "compute" button; and then "initiate" button to apply the computation. This puts him at the centroid of the fiducial marks and furnishes him with a display of the coordinates for each mark with the centroid as reference. Also as part of this procedure, the initial value of "kappa", b_x, and b_y are computed for the photograph. These values will be further incremented, along with "omega", "phi" and b_z, during relative and absolute orientations. At this point the factor C_f (explained later in Section 3.2.2) is also computed and entered; and if applicable, any

calibrated offset in the principal point.

One of the weaknesses in interior orientation is the difficulty of obtaining absolute measurements for the fiducial marks. In this case, calibration was done with substitute fiducial marks. Even with care, the failure to accurately observe on the fiducial marks might introduce an error of 10 microns-- which affects plate centering and film distortion corrections.

Corrections affecting the images on the photograph and handled as part of the interior orientation problem are lens distortion, film shrinkage, earth curvature, atmospheric refraction and principal point offset. In the AP/C these are applied at different times in the solution than is sometimes done [15, 26]. The general scheme for the application in the AP/C system is outlined in Section 2.1. A departure from this was made for this test in the use of corrector plates. This is discussed in some detail in Section 3.5.

3.2 Film Distortion

3.2.1 Calibration of Fiducial System

To obtain reference positions for the fiducial marks, a flash exposure was made with a glass photographic plate at the focal plane position in the camera. Precision measurements of this plate were furnished by the Coast and Geodetic Survey. Ten measurements were made on each mark with an accuracy of pointing of 3.9 microns or 1.2 microns as the accuracy of the mean. (See Appendix A-2). These measuring errors run much higher than the measuring capability of the instrument--Mann Monocular Comparator with least count of 1 micron. This is because of the difficulty of accurately measuring fiducial marks-- even though this comparator has a measuring mark especially designed for this type of fiducial mark.

It is difficult to accurately measure the intersection of the legs of the fiducial mark of this camera with the dot-shaped measuring mark of the AP/C plotter. Thus, a substitute fiducial mark was selected (Figure 3.2). This required a calibration to determine the offsets (Δx, Δy) for each substitute fiducial mark from the true fiducial mark center and a precise reference for the principal point from these substitute marks.

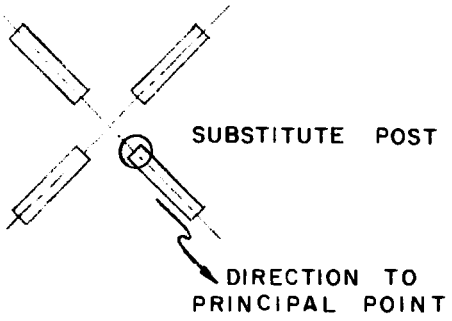

Figure 3.2 Substitute Fiducial Mark

For this calibration, a set of five measurements on each leg of the fiducial marks and five measurements on the substitute marks were made. The equation for the mean line defined by opposite legs of the fiducial marks were determined by a least-squares procedure using the ten observations. The intersection of the lines was obtained by the simultaneous solution of the two equations.

The principal point of the photograph is the origin of the photograph coordinate system and is determined by the intersection of the lines connecting opposite fiducial marks. But in the AP/C system the centroid of the fiducial marks is determined in interior orientation. Thus, it is always necessary to determine the offset of the principal point from this centroid position. In using a substitute mark, one must determine the principal point offset from the centroid of the substitute system. All data, including errors of the procedure in this computation are included in Appendix A-2.

The principal offset is entered by the operator's panel in conjunction with interior orientation-separate entries required for each photograph. The operator must be mindful of the orientation of his photographs on the instrument-- relative to that by which he calibrated the fiducial system [6]. Otherwise the offset can be applied in

opposite sense. Perhaps an easy way to keep this straight is to show by sketch, when calibration is done, the relationship of the offset to the fiducial marks. Then in operation the operator identifies the fiducial mark numbers by the dial edge of the photograph and determines which direction of the model coordinates correctly moves the principal point offset. (Figure 3.3)

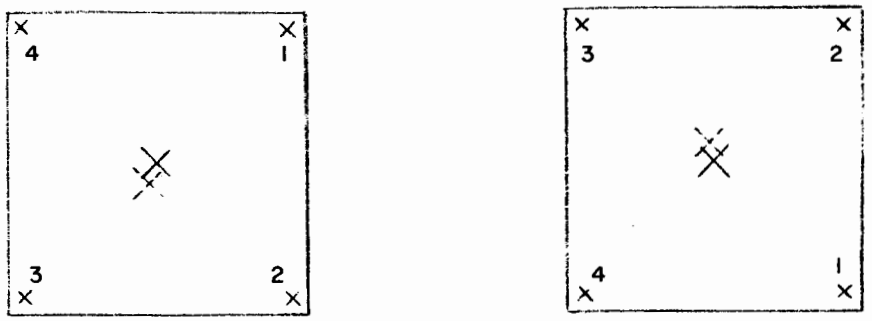

NEGATIVE OR KELSH DIAPOSITIVE CONTACT DIAPOSITIVE

Figure 3.3 Orientations for Photographs

3.2.2 Correction for Film Distortion

A constant for correcting for differential film shrinkage is computed for each photograph. It is based on the ratio of measured values between x and y coordinates to the ratio determined by the calibration routine, as outlines under Section 3.2.1. The correction is applied only to y coordinates, which brings them to the correct ratio with the x coordinates. Some further change in coordinates is possible with the b_z element. However, this introduces incorrect geometry in the photograph and could have a systematic effect in the aerotriangulation. A better procedure would be to change the focal length of the cameras, as is done in the analogue photogrammetric systems. The measured fiducial marks could give data for this. Then the focal length entered in the computer would be

$$f = \frac{(\Delta x) + (\Delta y)_{(\text{measured})}}{(\Delta x) + (\Delta y)_{(\text{calibrated})}} \cdot f_{(\text{calibrated})}$$

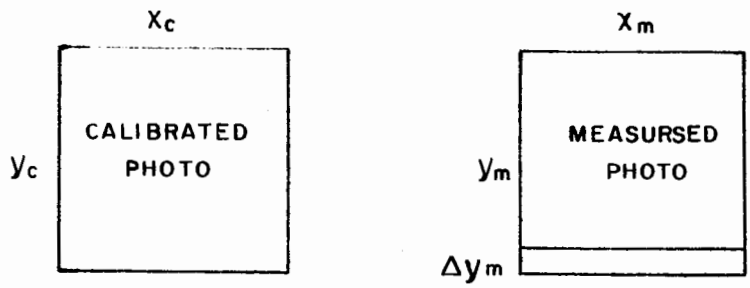

Figure 3.4 The Film Distortion Factor

The equation for the film distortion correction can be derived as follows:

We seek a correction Δy_m, in y_m to satisfy the condition, $\frac{x_m}{y_m - \Delta y_m} = \frac{x_c}{y_c}$. Actually we need a correction factor, $C_F = \frac{\Delta y_m}{y_m}$

such that $C_F \cdot y_m = \Delta y_m$. From above equations, $y_m - \Delta y_m = x_m \cdot \frac{y_c}{x_c}$.

Divide by y_m and rearrange to obtain $C_F = \frac{\Delta y_m}{y_m} = 1 - \frac{x_m}{y_m} \cdot \frac{y_c}{x_c}$

(The equation in this form is credited to Mr. D. J. Jennings, Ohio Highway Department.).

The data for this computation is obtained at the centering phase of interior orientation. The computation is done by desk calculator for each photograph of a strip and is based in the Δx's and Δy's between the measured fiducial marks of the photograph. The ratio y_c/x_c is obtained during the calibration of the fiducial system and becomes a constant for the camera.

It should also be noted that the procedure outlined here does not correct for a trapezoidal shrinkage pattern. However, as shown by Lampton [27], using a mean scale to four fiducial marks gives about as good results in correcting for film shrinkage as making an exact fit to the four marks. In the procedure here, differential scale in two directions is allowed so it can be assumed that no significant loss of accuracy is incurred.

3.3 Lens Distortion

In the AP/C system, corrections for lens distortion are computed by use of a stored function table whereby the distortion is expressed as a function of the radial distance from the principal point of the photograph. Correction equation: $\Delta x_L = x \cdot d(\frac{r}{D})$, where r is the radial distance, D is a scale factor as will be more clearly shown in an example, x is a photo coordinate from the principal point, and $d(\frac{r}{D})$, is the distortion function. Similarly, Δy_L is computed.

Corrections are applied only for symmetric radial distortion--asymmetric and tangential distortion being ignored. The following computation for the lens distortion table for camera No. 367 demonstrates the procedure. Figure 3.5 shows the actual calibration distortion curve and the series of linear approximations as used by the computer.

The method of approximating the lens distortion function might introduce a slight systematic error. The linear segments in this example generally approximate the actual graph (mean curve) within about 5 microns (Figure 3.5). It is more significant that camera No. 367 had asymmetric distortion as great as 20 microns. These distortions can not be corrected with the present procedure of the AP/C. Also significant is the principal point offset. [6].

In practice, RC9 photography might have lens distortion removed when printing diapositives by use of a corrector plate. One set of the photography used in this test strip was actually printed with such a plate. Even though most of the lens distortion was removed by this process, residual errors as large as 15 microns remain. This is based on calibration data furnished by the U. S. Geological Survey and is shown in Table 3.1. The significance of such a systematic error is

obvious and this example clearly indicates the need for accurate calibration. In using the test photography the residual distortion was removed by computing a function by the conventional method of AP/C, as discussed in Section 3.5.

The procedure for computing the lens distortion function in the AP/C is outlined below:

1) Divide the mean distortion curve (or similarly by use of a table of distortions) into eight (or less) convenient segments. For a 9 x 9 inch plate, we are interested in corrections for distortions up to about 160 mm. So, we choose an interval of 20 mm--our scale factor D. Sometimes the shape of the curve might impose a different value for D.

2) For each even interval, defined by r/D, determine the distortion function, d, as (distortion) /r, Table 3.2. A graph is helpful for this and for additional steps -- Figure 3.6.

3) Determine a linear equation, using slope-intercept form $y = mx + b$, for each segment of the distortion function, d.

4) Compute or scale the slope and intercept for each segment as computer input for the function d(S) and d(I) in Table 3.2. These values are next scaled to the binary system and combined into single words for entry in the AP/C -- the remaining rows of Table 3.2.

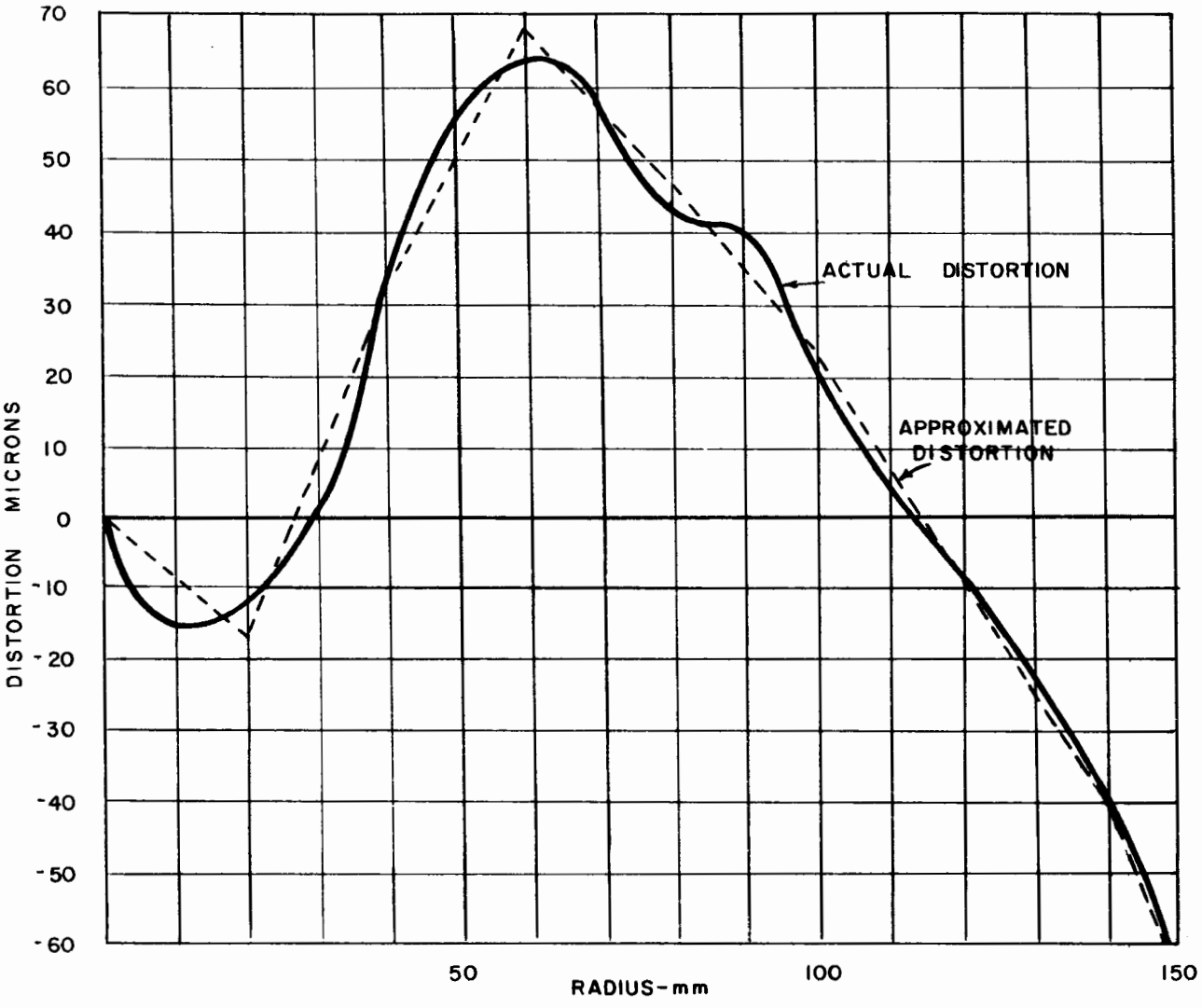

Figure 3.5 Distortion Curve
with
Approximation for AP/C

TABLE 3.1

Lens Distortion after use of Corrector Plate
(Computed from Data furnished by USGS
for
Camera RC9 Super-Aviogon SAg5-Ca 367)

Grid Radius (mm)	Measured Grid Radius (mm)	Printer Distortion (mm)	Lens Distortion (mm)	Error in Correction (mm)
20	20.007	+ .007	- .012	- .005
40	39.965	- .035	+ .031	- .004
60	59.925	- .075	+ .064	- .011
80	79.941	- .059	+ .043	- .016
100	99.971	- .029	+ .023	- .006
120	120.000	.000	- .008	- .008
130	130.027	+ .027	- .023	+ .004
140	140.055	+ .055	- .040	+ .015
150	150.080	+ .080	- .070	+ .010
155	155.103 (?)	+ .103	-	+ .007

TABLE 3.2

Computations for Lens Distortion Function

	20	40	60	80	100	120	140	148
Distortion	-.012	+.030	+.064	+.042	+.022	-.008	-.040	-.061
r/D	1	2	3	4	5	6	7	7.4
$d = \frac{Dist}{r} \cdot 10^{-4}$	-6	7.5	10.66	5.25	2.2	-.66	-2.86	-4.12
r/D Bracket	0-1	1-2	2-3	3-4	4-5	5-6	6-7	7-8(r=160)
d(S)	-6	+13.5	3.16	-5.41	-3.05	-2.86	-2.20	-3.15
d(I)	0	-19.5	+1.18	26.89	17.45	16.50	12.54	19.19
d(S)/8	-.75	1.69	.40	-.68	-.38	-.36	-.28	-.39
d(I)/8	0	-2.44	.15	3.36	2.18	2.06	1.57	2.40
d(S)/8·(104.85)	-79	177	42	-71	-40	-38	-29	-41
d(I)(26.21)	0	-64	4	88	57	54	41	63
d(S)'=d(S)+1024	945	1201	1066	953	984	986	995	983
$\frac{d(I)'}{} = \frac{d(I)}{8}(2048)$	0	-131 072	8192	180 224	116 736	110 592	83 968	129 024
(Subtract -d(I)' from 67108864)		66 977 792						
Σ(d(I)'+d(S)')	945	66 976 993	9250	181 177	117 720	111 578	84 963	130 007

Function d = distortion/r ; r = radial distance ; d(S) = slope of d- curve ; d(I) = intercept of d- curve

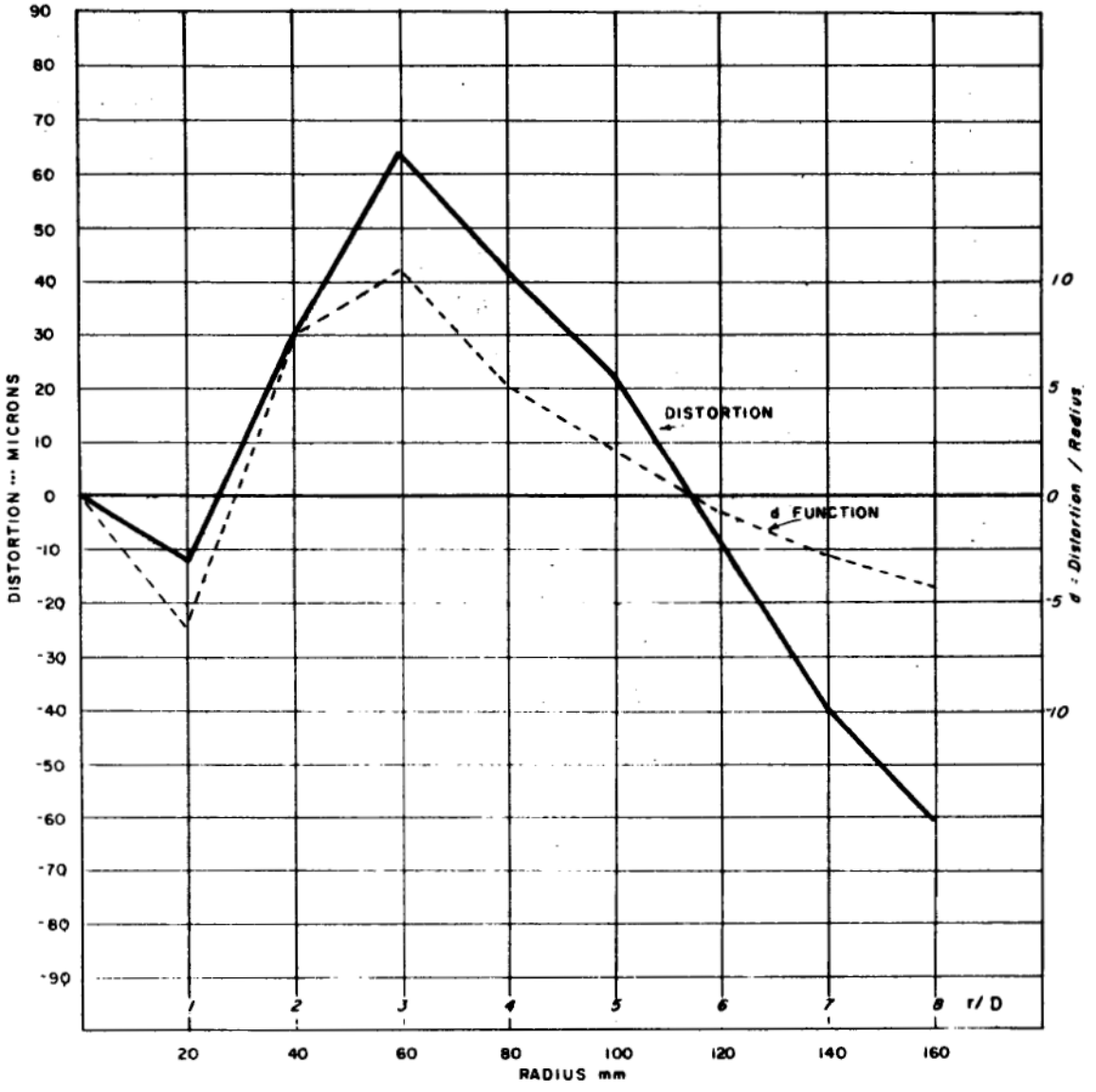

Figure 3.6 Distortion and Distortion Function Without Corrector Plate

3.4 Earth Curvature and Atmospheric Refraction

As outlined under Section 2 the distortions resulting from earth curvature and atmospheric refraction are removed by correcting the model coordinate, E_m. This appears to be the best place to correct for these effects and is geometrically valid for convergent photography. This is because the distortions are corrected using the line of camera station to nadir point as reference and in shifting the direction ray to the corrected E_m in model space. See Figure 2.2.

The corrections are indicated in their order and their significance to super-wide-angle photography becomes obvious in each case. The corrections in each case are applied using model scale. Thus, a factor S_G is entered initially which sets up a table of parameters for the equations. The earth's radius is reduced to model scale and the flight height h is computed by relationship f/h = scale.

The effect of earth curvature is depicted in Figure 3.7. Here the correction applied to radial distance in the photogrammetric model is negative (see also [4]):

$$\Delta Z_c = \simeq \frac{1}{2R} (X_m^2 + Y_m^2)$$

Where R is the earth's radius at model scale, and

$R = \frac{\text{Radius of Earth}}{S_G}$. The correction for curvature for the E_m coordinate is first computed - the E_m using coordinates X_m and Y_m . By means of the transformation equations, the corresponding shift in the photograph coordinates are then computed.

Atmospheric refraction is similarly computed in model space but using the lens-nadir line for reference. The equations solved are [2]:

$$D_{m_i} = [A_i - B_i \cdot E_m + f(E_m)][1 + \tan^2 \theta_{n_i}]$$

where $f(E_m) = LE_m^2 + ME_m + N$ and $\tan^2 \theta_{n_i} = \frac{X_{c_i}^2 + Y_{c_i}^2}{Z_{c_i}^2}$

The parameters A_i, B_i are computed using a stored program at the time that S_G is entered and are based on flight elevation, and θ is the angle

between the nadir direction and model point. The function $f(E_m)$ is the parabolic representation for the refraction effect due to the ground elevation as shown by Laurila [28].

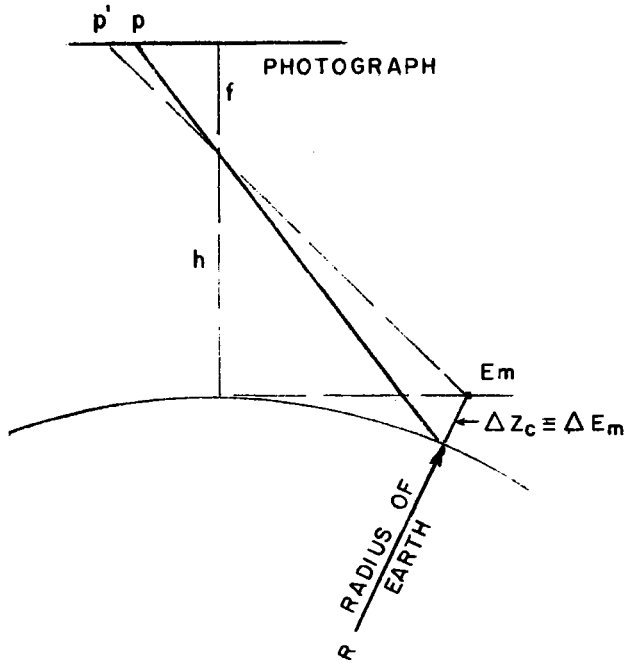

Figure 3.7 Earth Curvature Effects

These correction terms are likewise computed by a stored computer program. The parameters A, B, L, M, and N are based on a standard atmosphere. Figure 3.8 shows the correction. The measured coordinate E_m must be increased by amount ΔD_m to give photographed ray depicted by point P.

Both the atmospheric refraction correction and the earth curvature correction are combined with the b_z to give the model correction term [2].

$$\Delta Z_{m_i} = \Delta D_{m_i} + \Delta Z_{c_i} - b_{z_i} .$$

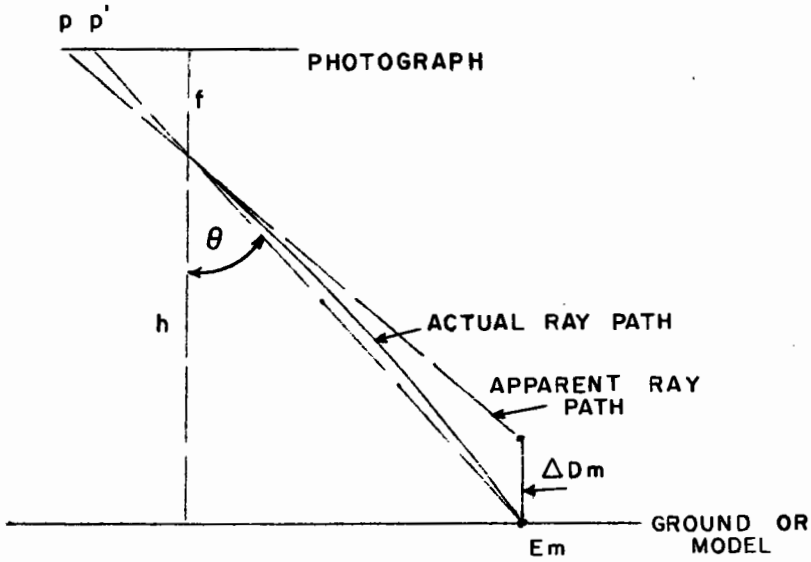

Figure 3.8 Atmospheric Refraction Effects

In the AP/C system the curvature and refraction effects are ignored for scales of 1:5000 and larger. For RC9 photography this constitutes a flight height of only 440 meters. Using refraction tables [29] for ground elevation of 0 km, and h = 0.5 km (approximately 440 m) the distortions are computed for an angle from the nadir of 60 grads (54°) or a radius of 121 mm and for an angle of 65 grads (58.5°), radius of 144 mm. Curvature was also computed for these radii as outlined in Section 3.5. Values are as follows:

Radius	121 mm	144 mm
Refraction	2 μm	4 μm
Curvature	7	12
Net effect	5	8

Whereas no effect would be realized for wide-angle photography where $\theta \leq 45^{\circ}$, the effects are measurable for RC9 photography. However, such an effect could generally be ignored for ordinary work without much effect on accuracy.

3.5 Use of Corrector Plates

The use of corrector plates to remove distortions due to lens, earth curvature and atmospheric refraction is one non-analytical approach to this problem. This can be done either in the compilation stage or at the time the diapositives are printed. The latter was done for the test strip used for this project. The using of the procedure at this time offers economic advantages because one printer can supply many compilation instruments to save costs for corrector plates.

The use of corrector plates has limitations. Agencies generally economize by operating with the minimum number of corrector plates and thus not cover every flight altitude. As an example, for this test strip, a plate for a flight altitude of 10,000 feet was used where the actual flight height was 5,000 feet, or an approximate flight elevation of 6,000 feet. This offers an interesting example for study of the residual systematic effects of such an application.

In applying these corrections which are residual to the use of the improper corrector plate, a new lens distortion tape was prepared to include the residual lens distortion corrections. This is valid if the photographs are considered to be vertical.

The formula for earth curvature effects used in this study is [4]:

$$ds = -\frac{hs^3}{2Rf^2}$$

where s is the residual distance from the principal point of the photograph, h = the flight altitude, f = focal length of taking camera, and R = the radius of the earth in the same units as h . As the sign indicates, the distortion effect is linear in h, it can be rewritten as:

$$ds = +\frac{h_c \cdot s^3}{2Rf^2} - \frac{h \cdot s^3}{2Rf^2} = \frac{(h_c - h)s^3}{2Rf^2}$$

where h_c is the camera elevation corresponding to the corrector plate, a d being a correction, is plus in sign. Another form for the same basic equation might be,

$$ds = \frac{s^3}{2Rf^2} = -\frac{(\text{scale No.}) \cdot s^3}{2Rf}$$

where the scale number is the reciprocal of the representative fraction of scale. Using this equation we can see that for a given scale, the distortions for two cameras varies inversely as their focal lengths, or distortions for RC9 are 150/88 times as large as wide-angle photographs.

For the test strip with h_c = 10,000 ft. and h = 5,000 ft:

$$ds = \frac{1524 \cdot s^3}{2 \cdot 7371000 \cdot (88.23)^2} = 1.54272 \times 10^{-8}\,\text{mm}^{-2} \cdot s^3$$

From this expression is obtained ds corresponding to several values of s:

s	10	20	30	40	50	60	70	80	90	100	110	120	130	140	160mm
ds	0	0.2	0.4	1.0	2.0	3.4	5.3	7.9	11.3	15.5	20.6	26.6	33.9	42.4	63.2μm

The refraction effects were obtained by use of tables [29]. Here it was necessary to convert from angular measure (in grads) to millimeters or microns on the plate (with f = 88.23 mm). But values were first interpolated for the camera height and ground elevation for the set of photographs. Because the atmospheric refraction is small at lower altitudes, the interpolation procedure used here introduced no significant error--perhaps 1 to 2 centesimal seconds of arc. Some gain in accuracy is achieved by computing the atmospheric refraction and earth curvature separately.

After computing the values above, they were plotted on a graph, Figure 3.9. These data were then combined with those of Table 3.1, residual lens distortion, to produce a new lens distortion function, Figure 3.10, with computations as shown in Table 3.3.

As may be noted, the distortions remaining for these conditions run to over 50 microns. Thus the exercise is a worthwhile one. The procedure was fairly straight-forward to apply if calibration data on printing are available. However, it seems that an easier and more

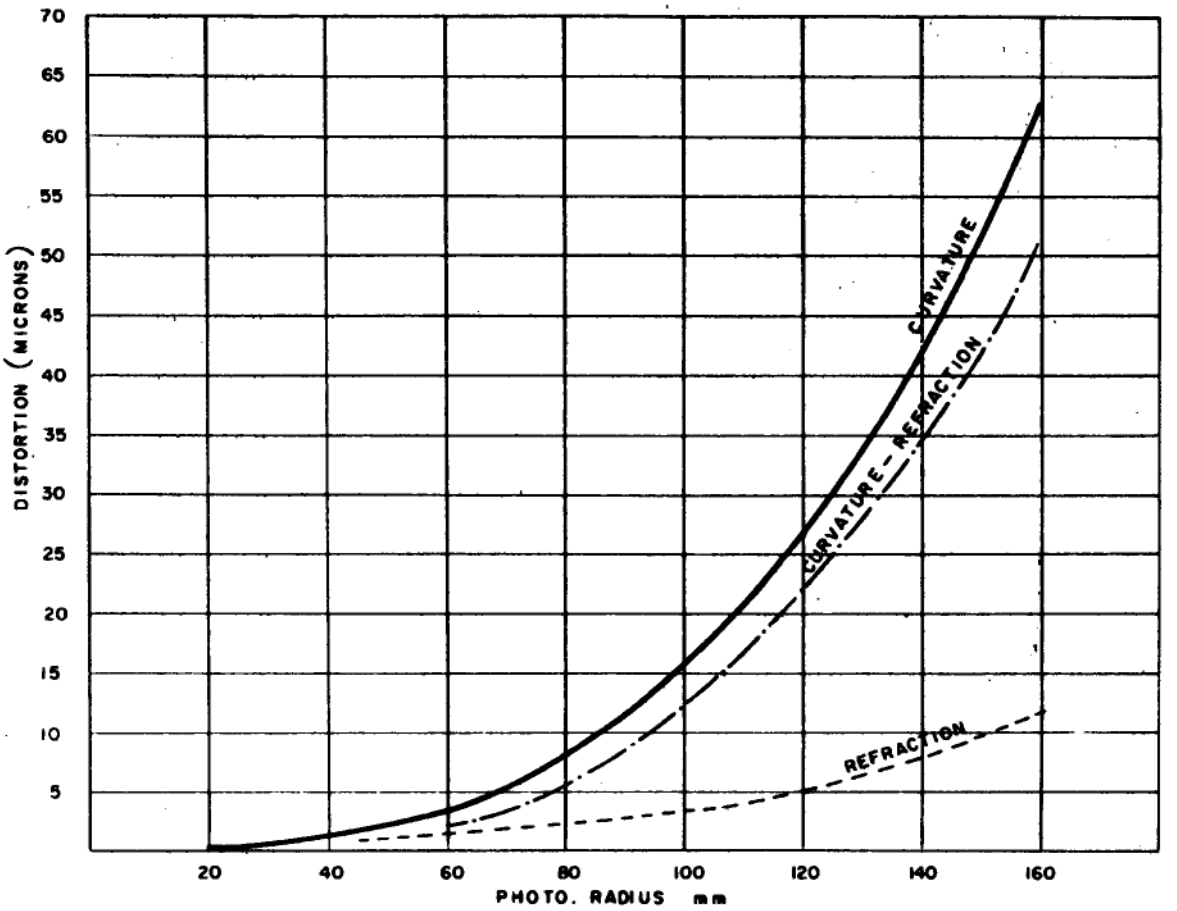

Figure 3.9 Residual Effects from
Improper Corrector Plate

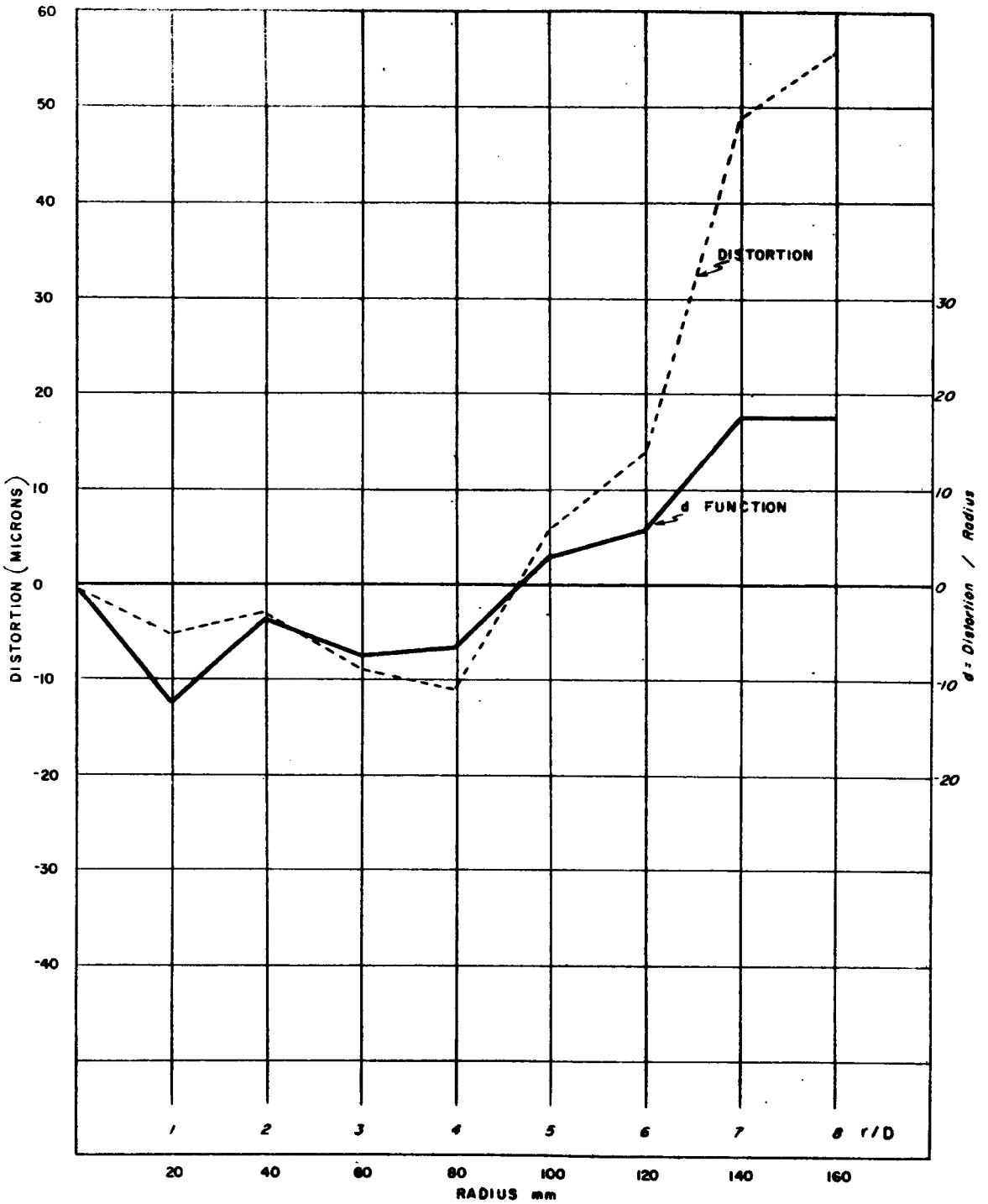

Figure 3.10 Distortion and Distortion Function with Corrector Plate

Table 3.3

Computation of Lens Distortion Function
with Corrector Plate

r(mm)	20	40	60	80	100	120	140	160
Distortion	- 5	- 3	- 9	-11	+ 6	+ 14	+ 49	+ 56
r/D	1	2	3	4	5	6	7	8
$d=\frac{\text{Dist.}}{r}$.								
$(10^{-4}\frac{mm}{mm})$	- 2.5	- .75	- 1.5	- 1.38	0.60	1.17	3.5	3.5
r/D Bracket	0-1	1-2	2-3	3-4	4-5	5-6	6-7	7-8
d(S)	- 2.5	1.75	- .75	.12	1.98	.57	2.33	0
d(I)	0	- 4.25	.75	- .9	- 9.3	- 2.25	- 12.81	3.5
d(S)·104.85	-262	184	-79	13	208	60	249	0
d(I)·(26.21)	0	- 111	20	- 24	- 244	- 59	- 336	92
d(S)+1024	762	1208	945	1037	1232	1084	1268	1024
d(I)·2048	0	- 227 328	40 960	- 49 152	- 499 712	- 120 832	- 688 128	188 416
(Add-d(I)to 67 108 864)		66 881 536		67 059 712	66 609 152	66 988 032	66 420 736	
Σ(d(I)+d(S)	762	66 882 744	41 905	67 060 749	66 610 384	66 989 116	66 422 004	189 440

Function d = distortion/r ; r = radial distance ; d(S) = slope of d - curve ; d(I) = intercept of d - curve

rigorous method for correcting for atmospheric refraction and earth curvature could be done on the AP/C with slight modifications in existing programs. The above procedure would not be applicable for convergent photography.

The computations for the distortion effects, discussed above, are shown in Appendix B. An error was made in computing the refraction and curvature effects with h = 5000 ft. The 5000 ft. was the flight height above terrain elevation of approximately 1000 ft. Thus, 6000 ft. was the actual flight elevation which should have been used. This error did not become evident until the models were set. So in addition to showing the computations for refraction (example No. 1 of Appendix B), a computation was made using tables combining refraction and curvature (example No. 2 of Appendix B).

For use of these curvature and refraction tables [29], the following procedure was followed. The centesimal seconds were converted to sexagesimal seconds by multiplying by 0.324. The units are required in radians and this factor is indicated in the examples. To obtain the distortion on the photographic plate as a function of r - the radial distance- where $r = f \tan \theta$, we have $dr = f \cdot \sec^2\theta \cdot d\theta$.

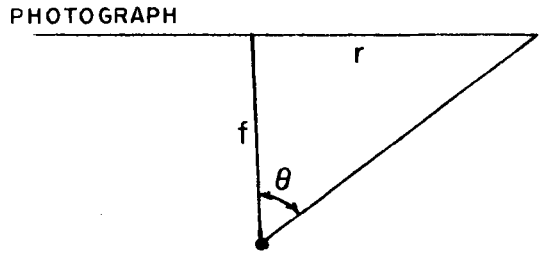

Figure 3.11 Plate Distortion as Function of Central Angle

A table is required for the values of r to cover the limit of the photograph and their corresponding distortions, dr.

In the test photography, the 1000 ft. error in altitude amounts to 12 microns at r = 144 mm. ($\theta = 58.5^{o}$) and 8 microns for r = 121 mm. ($0 = 54^{o}$) - the extremes in radial distances on the photographs. These are both significant differences.

3.6 Relative Orientation in the AP/C

Relative orientation in the AP/C provides options to the operator. He can apply a Y-parallax correction to a specific orientation parameter. Or, he can read the Y-parallax at the six locations (Figure E-1); store these in the computer which, on his command, computes the correction to each parameter by a least squares solution of parallax equations. He then applies these corrections to the parameters by another command to the computer.

In practice, the operator finds it advantageous to apply the initial corrections to the proper parameters himself. Then, by successively applying numerical orientation procedures whereby he can make multiple readings at each of six locations, he is able to better complete his relative orientation. Moving to the six locations is done by pressing proper switches. The averaging of the multiple readings is done by the operator, or his assistant, using the panel display. When the corrections are computed and applied, the operator is required to repeat the procedure of measuring the py's at each of the six locations. The formation and solution of the normal equations is, however, practically an instantaneous procedure at the AP/C computer.

Being able to do numerical relative orientation for each model is a great facility of the system. By following the sequence of hurridly going from coarse to fine corrections, the procedure can be speeded. No doubt a better numerical relative orientation can be more readily obtained than on analogue devices. This is generally done in two or three iterations after the initial corrections.

Experience on this test strip indicates that the operator may be able to apply corrections for known systematic errors at this step--he has better numerical data available for this than is the usual case.

The formulas solved by the computer in relative orientation are the normal equations shown by Hallert (Appendix E-1). The procedure

requires computation of the coefficients (Appendix E-2) by the operator and/or his assistant after the values of b and d for the photographs have been scaled. One set of values will generally suffice for all photographs of a strip. The coefficient must be computed and an input tape prepared for the AP/C. It seems feasible to stock these tapes for each focal length for assorted b and d values--where f, b, d are the arguments in the computation of coefficients.

The solution of relative orientation supplies a set of corrections to up-date the orientation elements for one or more of the pair of photographs. For this test, dependent relative orientation was used throughout so only orientation elements of one of the photographs was changed. The orientation corrections are applied when the operator pushes the INITIATE button of the control panel.

The "base-out" mode requires the solution of a different set of equations in which the coefficients are different than with "base-in". Thus computations are done and tapes are prepared for both modes--if aero-triangulation is to be done.

3.7 Absolute Orientation in the AP/C

The absolute orientation, comprising scaling and leveling the model, is accomplished using a least squares technique. It requires at least three stations--all with X, Y, and E coordinates, but it can have a possible input of many control stations. The ground coordinates must first be reduced to the working model scale for X, Y, and Z (or E). There is also a practical upper limit of the number of stations in order to prevent an overflow in the summation of coefficients for the normal equations. This is generally 30 stations.

The program, as at present, seems limited on the minimum condition because it does not provide for inclusion of partial control--that with only horizontal or only vertical coordinates. However, the operator can level the model by convantional methods. Here one line is used for scaling and three properly distributed vertical points are used for leveling. For this case the automatic computer is not to be used initially. Instead the operator changes the base component to obtain desired scale. Having done this, he enters as control data the model

planimetric coordinates (X_m, Y_m) with ground value E for the three vertical control points. The AP/C then computes the absolute orientation and applies the corrections for orientation elements for the two cameras--as before. This saves the operator the time of having to level the model and to compute and apply orientation elements to the cameras. The operator can, however, compute the necessary corrections himself and apply them through his panel controls as in analogue machines.

Absolute orientation does not comprose any translation of coordinates--the model coordinates get changed due to scaling and leveling but they remain in the same model system as before absolute orientation was begun. Next the model is translated vertically by applying a common b_z correction through the operator's panel.

To begin absolute orientation, ground control is first reduced to the selected working scale of the models. This must be done because the AP/C cannot presently handle the number size required for ground coordinates in a standard system.

In performing absolute orientation, the operator must observe each control point in the model in the same sequence that he enters the ground (reduced) coordinates. It is better to choose as the number one control station, the one nearest the model center. The operator can enter the ground coordinates either concurrently as he sets his measuring dot to the image; or beforehand as a block, but in the required number sequence.

There is not a print-out or display of residuals from absolute orientation but the operator has an excellent facility to test his results. He can initialize his "D" scale to the No. 1 control station and directly obtain a model distance, to microns, to any of the other control stations. During these tests the accuracy of reading a distance with the "D" scale was found to be near the limit of measuring capability of the instrument.

4. TEST OF PROCEDURE

4.1 Absolute Orientation--Test Strip--at AP/C

Two models of the test strip 16-17 and 17-18 had four combination horizontal and vertical control stations with approximately 40 additional vertical control stations. (Figure 3.1.) These were well distributed about the models to furnish data on the vertical accuracy of the system. Measuring the points in individually controlled models would not introduce any propagation of error as might occur in aerotriangulation. It thus could furnish some measure of the inherent accuracy of the system.

One of the models was measured twice with different operators--Figure 4.2a and b)--so as to furnish a comparison and to validate the program. Also, one of the models was measured once without any distortions applied in the AP/C (Figure 4.1). Thus there was obtained a measure of the residual distortions after printing with the corrector plates--before applying the data of Figure 3.9.

The procedure followed in setting up the models for this study is as follows:

1) The program was initialized each time a new model was begun. Interior Orientation was performed as described in Section 3.

2) Dependent relative orientation was performed by applying initial corrections to the proper orientation element as in analogue devices--using the overcorrection factor on the "omega" element. The residual y-parallaxes were removed by successive iterations using redundant observations at the six locations.

3) Absolute orientation was performed to four control stations--horizontal and vertical. These were in an approximate square distribution about the model center--and covered about half the model width. The relative orientation was checked after each absolute orientation. Absolute orientation was repeated if relative orientation was in any way disturbed. The y-parallax was rechecked when measurements within each model were completed.

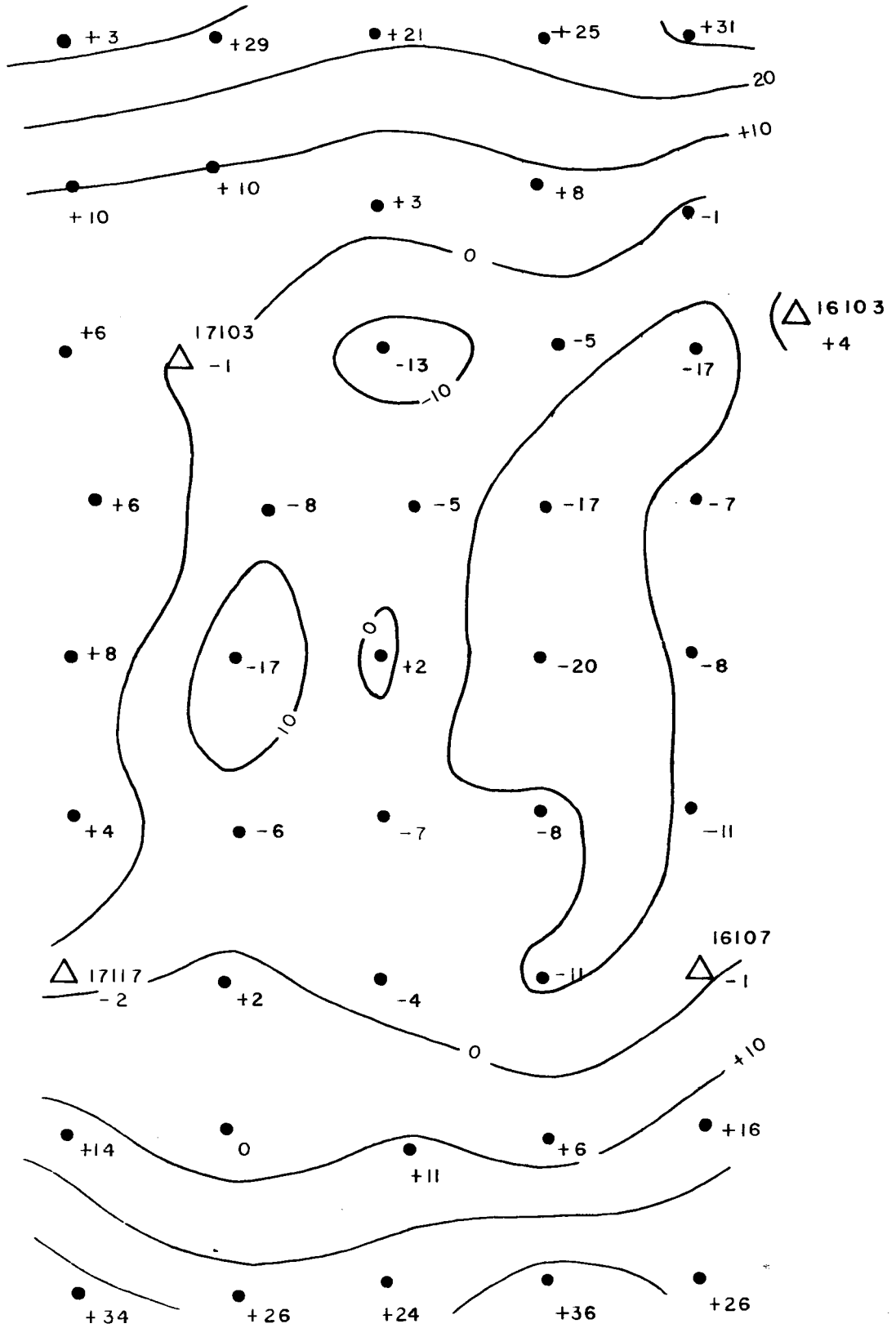

Figure 4.1 Elevation Errors in Microns in Model 16-17 with Distortions Partially Corrected

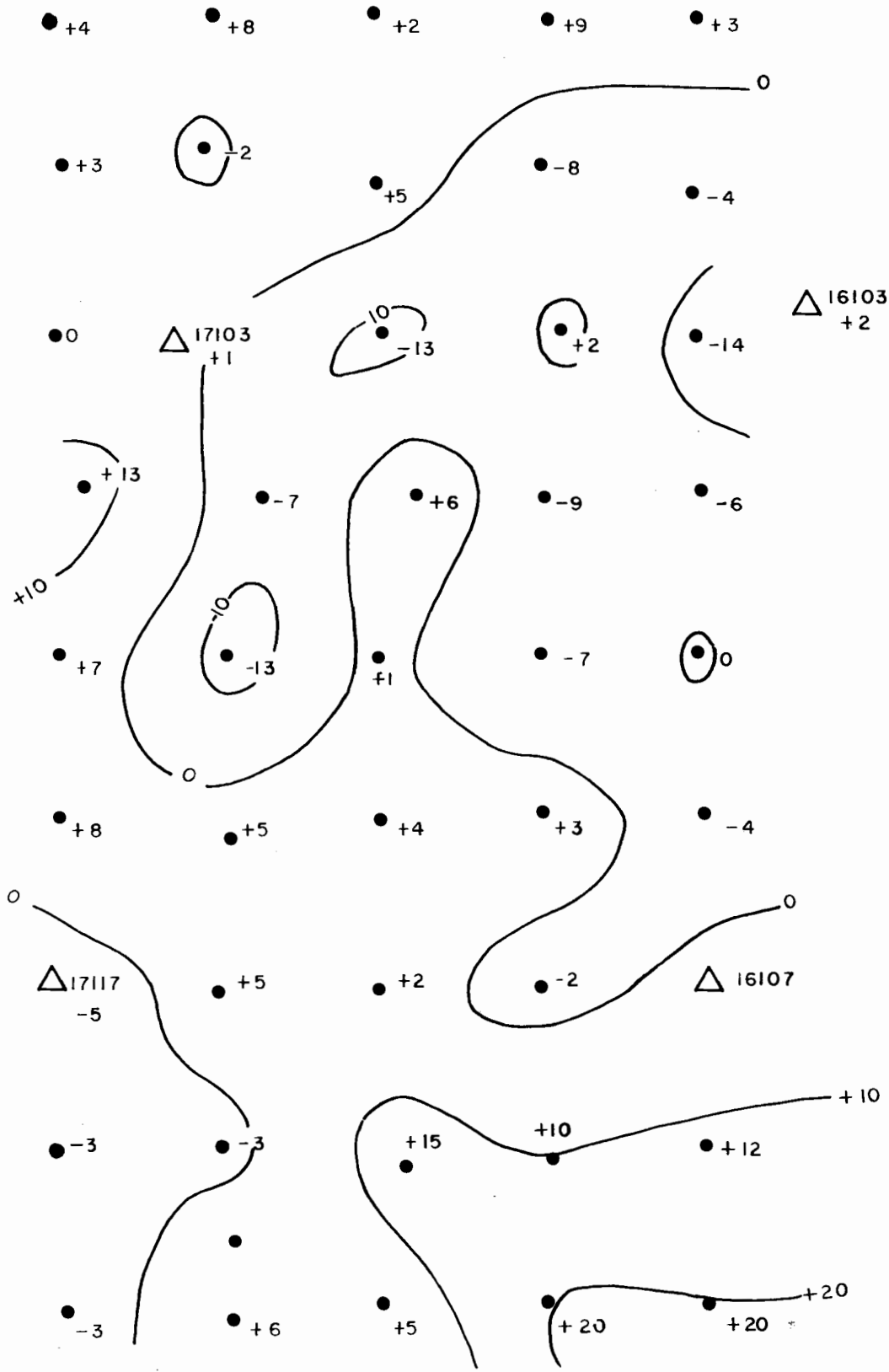

Figure 4.2a Elevation Errors in Microns in Model 16-17 with Distortions Corrected, with Different Operators

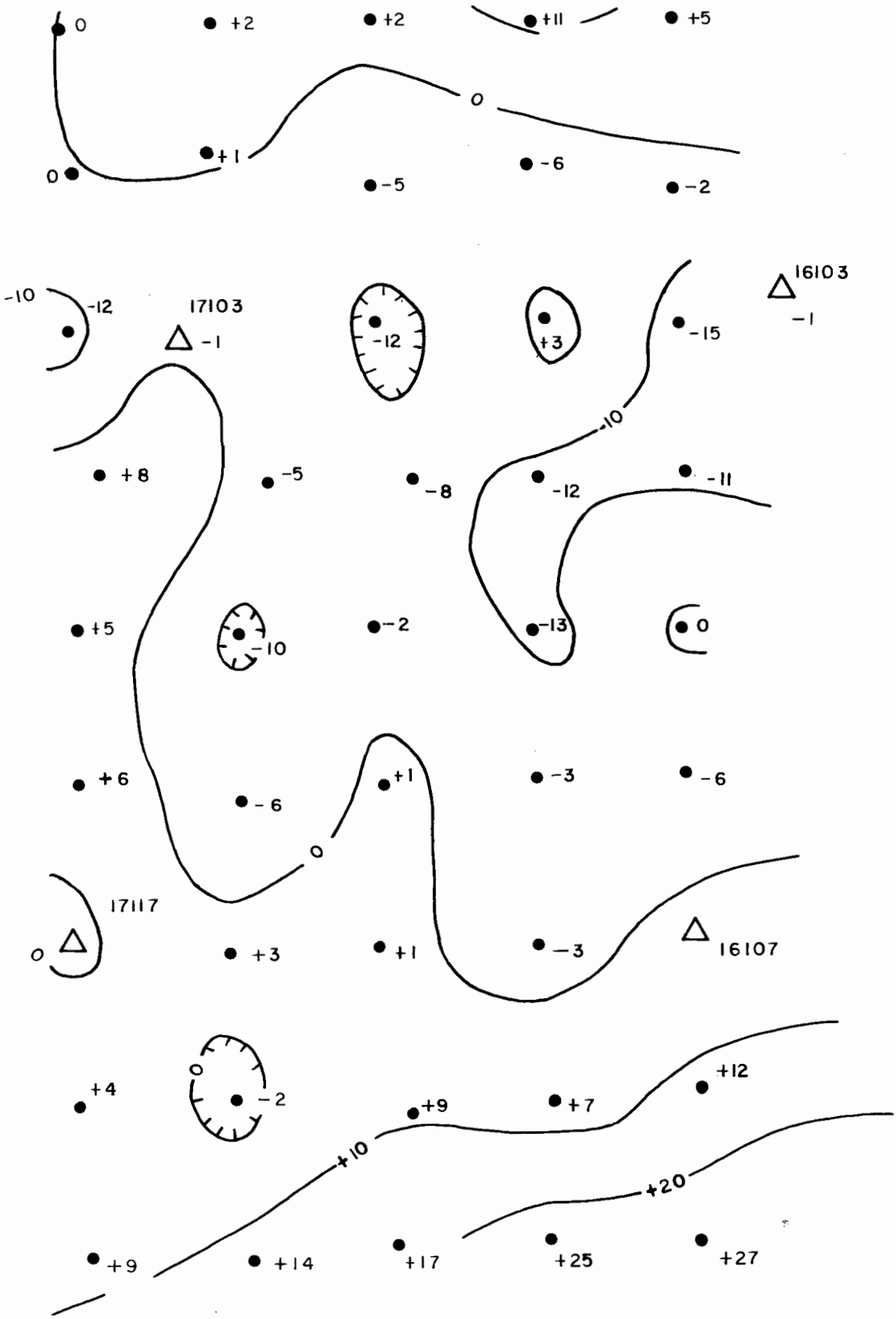

Figure 4.2b Elevation Errors in Microns in Model 16-17 with Distortions Corrected, with Different Operators

4.2 Results of Tests

(The model scale was 1:17,200 -- the value as given by USGS.) Only elevation (vertical) errors were considered for this test in absolute orientation.

A comparison was made in the two sets of measurements of Model 16-17, which were made by different operators at different times and with slightly different solutions. Ignoring the systematic effects of different solutions, the standard deviation m from the mean for a single measurement of these two sets is only ±3.7 microns, (where $m = \pm\sqrt{\frac{[dd]}{2n}}$ and d is the differences between sets). The differences were random--approximately equal positives and negatives. Thus the m of 3.7 microns should indicate a reliable value for the standard error of observation for a single observation.

Another similar comparison was made for a partial set with 28 points of the same model by the same operator on different days. (The partial set resulted from computer malfunction.) Here the standard deviation from the mean was ±3.1 microns -- slightly less but approximately the same as before.

The models were next examined for closures to control and a plot was made for each model. The model measured without any corrections entered in the AP/C -- or with partial corrections for distortions by use of the corrector plates in the printing process -- showed a remarkable systematic pattern of distortions (Figure 4.1). The standard deviation to control (misclosure at control points) was 16 microns.

Model 16-17, with corrections added as discussed, was measured by two operators. The closures to control and error curves, as depicted in Figures 4.2a and 4.2b, shows even more vividly the close agreement between operators. The standard deviations to control for these two sets were ±7.9 and ±9.2 microns, respectively. Thus, the applied corrections further reduced the standard error in elevation by one-half that with only the corrector plates. Model 17-18 showed about the same standard deviation -- ±8.4 microns. For this analysis, two measurements were excluded because their deviations were so excessive. They are shown in dashed outline in Figure 4.3.

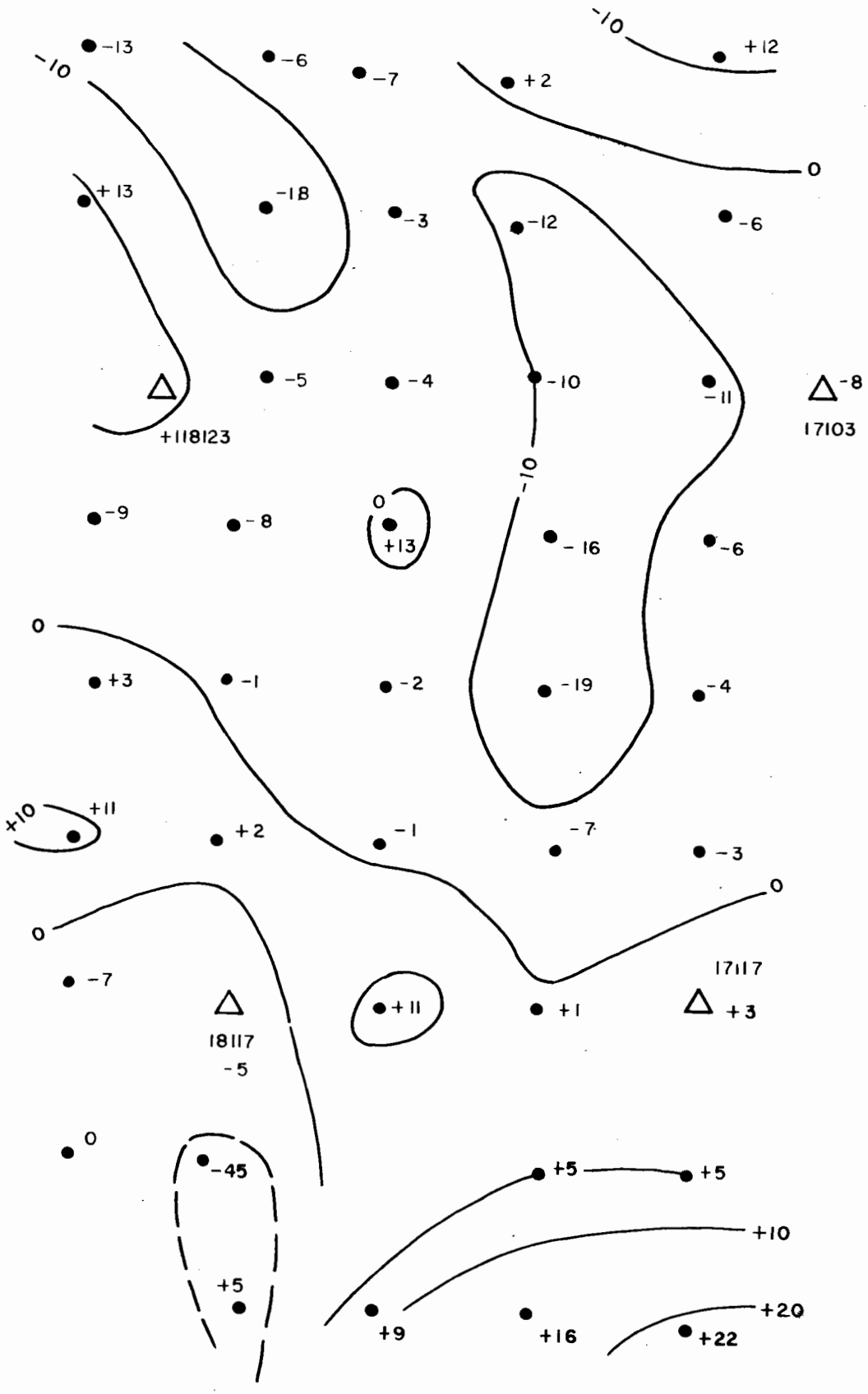

Figure 4.3 Elevation Errors in Microns in Model 17-18 with Distortions Corrected

The above standard deviations could be lessened by 1 to 2 microns if the models were translated. However, this would not be entirely valid in this study. The models were controlled absolutely to four control stations covering about one-half of the model area. Then by including deviations to all stations in the model areas, the systematic patterns are better depicted. Not always evident in these studies is the quality of the images. Some were definitely of lower quality due to the background of the targets, resolution, etc.

The juncture of the two models, 16-17 and 17-18, is rather poor with differences as great as 25 microns. However, when the models are superimposed by fitting the rectanglar patterns of control (a very convenient tool for this study), the correspondence of error patterns is remarkable. See Figure 4.4. The pattern is noticeably asymmetric with extremes in corners No.2 and No.3 (numbers as defined in Appendix A-2) which go in the same direction. This pattern prevails in the aerotriangulation adjustment (see Section 5). This indicates that the central part of the photograph should be used in order to minimize propagation effects.

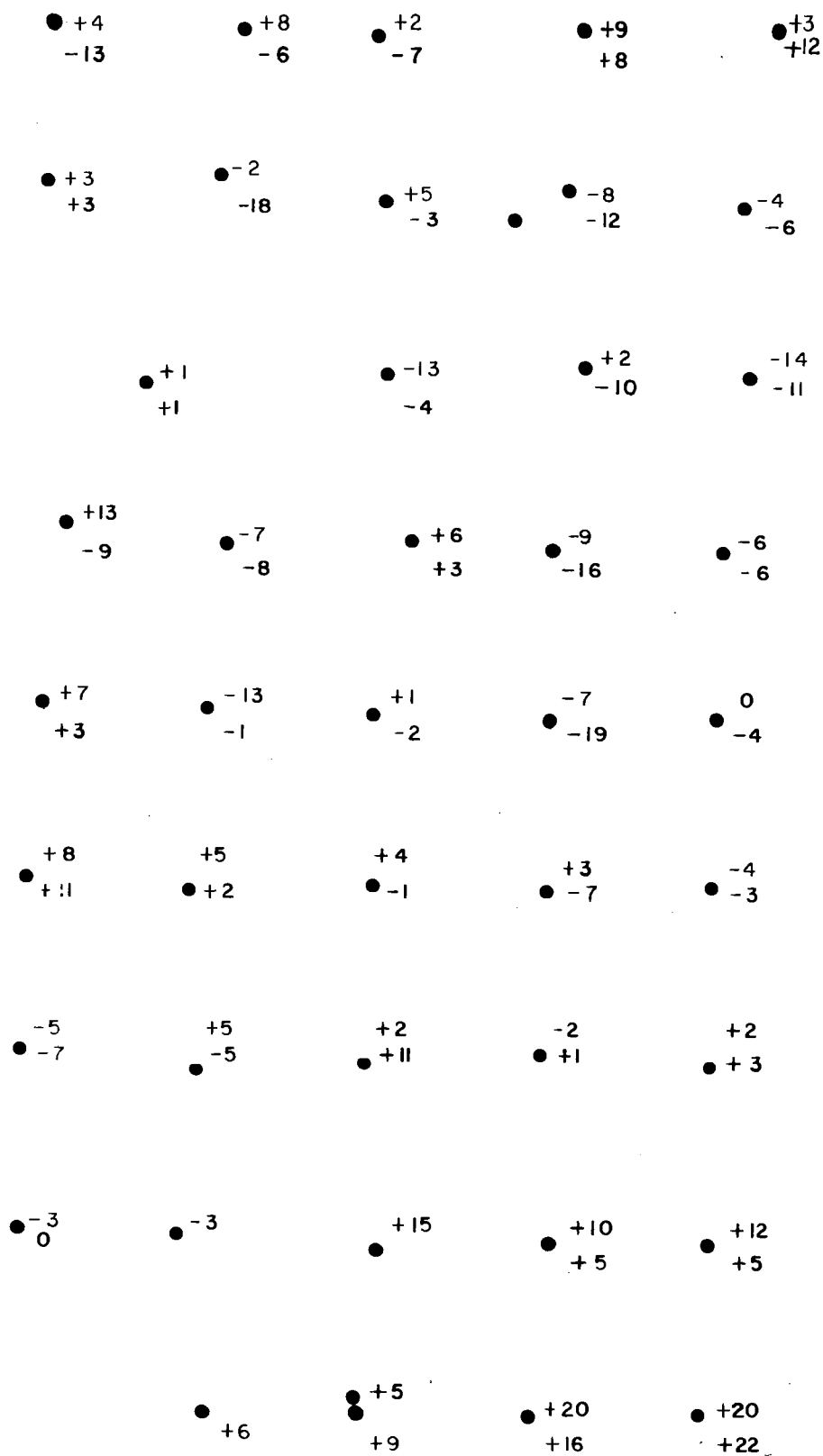

Figure 4.4. Comparison of Errors in Different Models.

The upper values are from model 16-17 and the lower values are from model 17-18; all values are in microns in the model scale.

5. AEROTRIANGULATION

5.1 Aerotriangulation on AP/C

Aerotriangulation procedures with the AP/C closely parallel those with a first-order analogue instrument. "Base-in" and "base-out" models are achieved by a single switch located just above the operator's control panel. Junctioning of models is done by first setting the E_m for a common point by the footwheel. The measuring dot is then brought to ground level in the model by changing the bx element by means of the "incremental" switch. These steps are done after dependent relative orientation is achieved.

At this point the operator must take a precautionary step. All elements of orientation for the model are merely stored quantities in the computer--only translation movements in x and y have occurred with the photographs. If anything now disturbed the stored computer memory, the model would be lost and perhaps the bridge. Thus the operator saves his work by obtaining from the computer a "dump" tape with all orientation data. He also reads coordinates on some well-defined point in the model. By reading into the computer the "dump" tape and setting on the model point, he is able to reset a model. This facility for re-setting a model can have many applications.

The adjustment program at the Ohio Highway Department, using an IBM-1620 computer, makes model ties based on a mean fit to all common tie points [3]. It is thus advantageous, in normal practice, for the operator to spend some time to make a best tie for models in an aerotriangulation procedure. The operator must be mindful of this procedure to insure that points of poor quality are not given the same code number in the program. Otherwise, the solution is weakened. It is better to treat a common point as separate points for two successive models.

The formulation for the strip adjustment program is that of the Coast and Geodetic Survey as amended by Horsfall [18]. To conserve computer storage, a ceiling in the number of control stations for adjustment is imposed, 5 for horizontal and 7 for vertical. Thus the selection of these stations should be done with care to obtain the best solution. An even distribution along the strip and one covering the

extremes of the strip are factors to strive for. Exclude control of poor quality if possible; And although the first model is controlled absolutely in scale, it should not be heavily weighted in the solution as it might introduce an erroneous slope in the polynomial adjustment.

Formulas used in the adjustment are

$$x' = x - \Delta z(2Ix + J) + Ax^3 + Bx^2 + Cx - 2Dxy - Ey + F$$

$$y' = y - \Delta z(Lx + M) + 3Ax^2y + 2Bxy + Cy + Dx^2 + Ex + G, \text{ and}$$

$$z' = z\,[1 + (2Ix + J)^2 + (Lx + M)^2]^{1/2} + Ix^2 + Jx + Lxy + My + N.$$

Here the primed quantities (x', y', z') are the newly transformed or adjusted coordinates, the unprimed quantities (x, y, z) are strip coordinates transformed to an axis-of-flight system, and the Δz is the increment in the z-coordinates of a point from the reference datum of the strip. The primed quantities must undergo an inverse transformation (translation, rotation, scaling) to ground coordinates. The coefficients A, B, C, etc., are the parameters of the transformation and are determined for the strip from the control stations. An equation in x and one in y can be formed for each horizontal control station and one equation each can be formed for each vertical control station.

5.2 Aerotriangulation of the Test Strip

The test strip comprises only four models with control as depicted in Figure 3.1. It was begun by doing absolute orientation of Model 16-17 (discussed in Section 4). The strip was cantilevered by adding successive models by co-orientation (i.e., dependent relative orientation and scaling as outlined in Section 4). A close fit to three tie points generally could not be achieved because a large amount of systematic error was evident. So scale transfer was made by using the center tie point--with an approximate fit to the other two points.

The closures to control (horizontal and vertical) before adjustment are depicted in Figure 5.1. The horizontal closures were obtained by doing a linear transformation for the control of the strip to two stations in Model 16-17. (Appendix D.) Even so, very little propagation of error is evident--only 44 microns in planimetric and 29 microns in vertical. The pattern of systematic effects is evident. Also, the poor model tie between the first and second models contributes 7 microns to error.

Data of the adjustment on the IBM-1620 computer is included in Appendix D. The closures to control after adjustment are shown in Figure 5.2. The standard deviations to control at model scale of 1:17,200 were as follows: x - 4 microns, y - 6 microns, or 7 microns in planimetry and 10 microns in z, or elevation. With this model scale (photograph scale - 1:20,500) the results obtained appear quite good. However, the control selected for elevations was not optimum because it did not cover the full width of the strip. It is evident from Figures 5.1 and 5.2 that the northwest corner of the strip was improperly controlled. So a graphical adjustment using methods of Brandenberger [4] was performed with nine control stations, as shown in Figure 5.3a. The longitudinal profiles were selected to avoid the extreme edge of the models. With this adjustment and without any corrections for junctions of models, a standard deviation to control of only $\pm$ 7.0 microns was obtained. It is obvious in comparing Figure 5.3a with Figure 5.2 that a better adjustment was made.

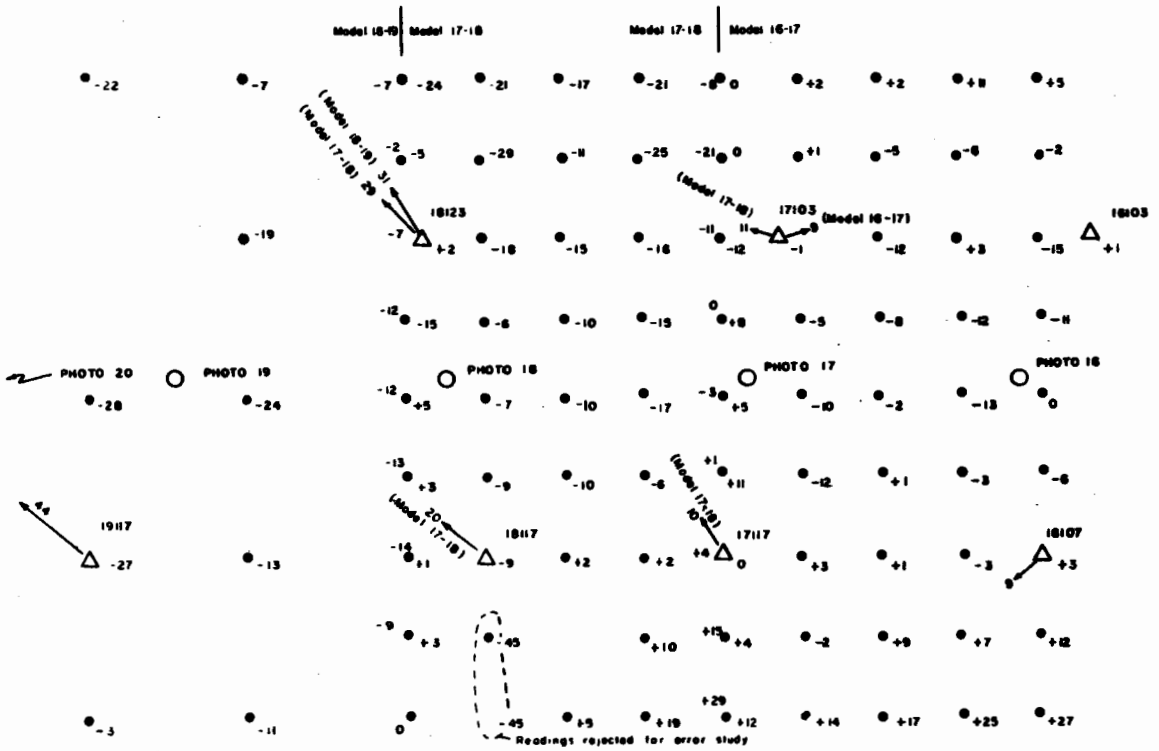

Figure 5.1 Aerotriangulation--Closures to Control before Adjustment (Horizontal misclosure shown at arrowheads, others are vertical misclosures; all values are in microns at scale of the model.)

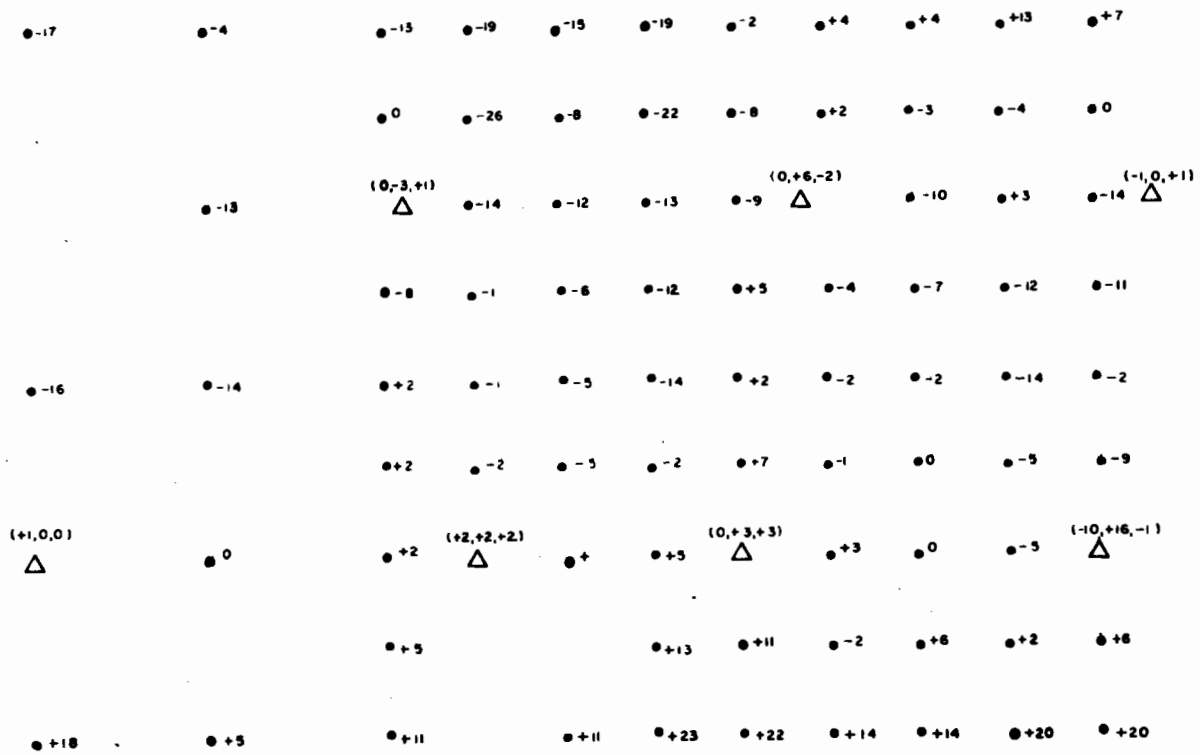

Figure 5.2 Aerotriangulation--Closures to Control after Adjustment

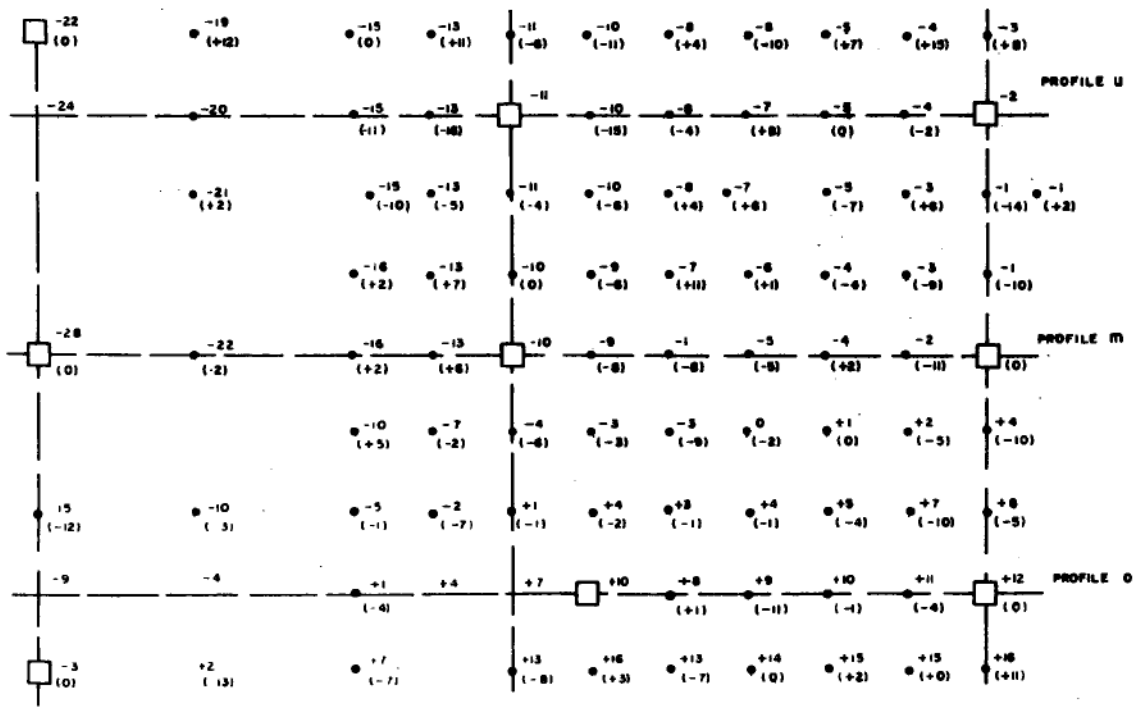

Figure 5.3a Aerotriangulation--Graphical Adjustment of Elevations

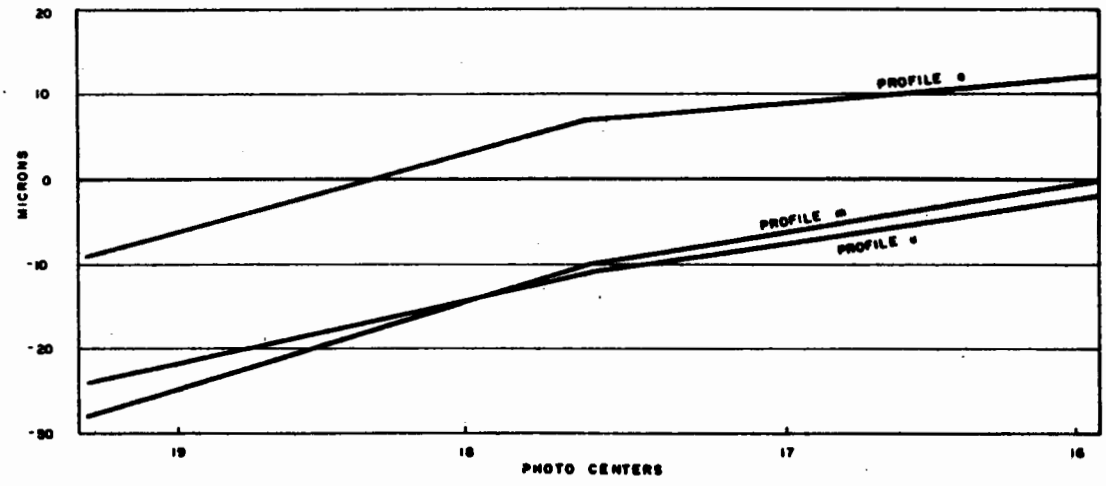

Figure 5.3b Aerotriangulation--Graphical Adjustment of Elevations

5.3 Aerotriangulation on the Wild Autograph A7

With a view to study the workability of SWA photography at a stereo plotter, not equipped for this kind of photography, and with a view to compare the results with those obtained from the AP/C, the same test strip was triangulated at the Wild Autograph A7 in the Ohio State University, Department of Geodetic Science. The aeropolygon method of aerotriangulation was performed in this case.

The calibrated focal length 88.23 mm cannot be introduced into the projector cameras of the Wild A7 because the range of focal length column here is 98 mm to 215 mm. In this case a focal length of 105.88 mm was used. This means that an increase of 1/5 times the actual (88.23 mm) is used. The photography being vertical (i.e., the camera axis being nearly coincidental with the Z coordinate direction) this increment in the focal length of the cameras would cause an affine deformation in the stereo models. Thus, the planimetric coordinates (X and Y) will have a scale different from that of the elevation coordinate (Z) which, in this case is enlarged by 1/5 times. On account of this the observed elevations (Z) are reduced to the system of X and Y by multiplying with a factor 0.833 333 33. The elevation gears were set at "B" and "a" and the elevation lever was set at meter, which enabled the reading of all the three coordinates (X, Y and Z) in millimeters in the model scale which was 1:6000.

The least count of the coordinates in the model was 0.01 mm. Further, each coordinate was read in two rounds of observation. Considering that the model scale was approximately three times the scale of the picture (i.e., the same as the model scale in the AP/C) it may be considered that the reading accuracy of all the coordinates was about the same ($\sim 3\ \mu$) in this case as at the AP/C.

The starting model in this aerotriangulation was 16-17. The relative orientation of each model was performed by the numerical method [see 11]. After the relative orientation was performed the residual y-parallaxes were measured at 8 different locations in each of the 5 models. From these 40 observations was computed the standard residual error in y-parallax which was $\pm$ 0.019 mm. This, reduced to

the picture scale was approximately $\pm$ 0.006 mm i.e., 6 μ. This is reasonably good for any analogue system.

The observed coordinates (X, Y and Z) were next reduced to the ground system by performing linear transformation based on the ground coordinates of points 16107, 17117, 16103 and 17103 (see Figure 3.1). Only at this stage could the closing errors be found in the observed coordinates at the points. An analytical-graphical method of adjustment was performed for each of the coordinates.

Table 5.1 presents the adjusted ground coordinates of all points in each method (with Wild A7 and with AP/C). Their differences are also tabulated here and are represented graphically in Figures 5.4, 5.5 and 5.5a.

TABLE 5.1

The Differences Between A7 Adjusted Ground Coordinates

and

AP/C Adjusted Ground Coordinates

Point No.	X_{A7} X_{APC}	Diff. $=X_{A7}$ $-X_{APC}$	Y_{A7} Y_{APC}	Diff. $=Y_{A7}$ $-Y_{APC}$	Z_{A7} Z_{APC}	Diff. $=Z_{A7}$ $-Z_{APC}$
16201	148 256.4 292.5	- 36.1	248 463.5 463.6	-0.0	349.5 349.6	-0.1
2	148 260.4 289.8	- 29.4	248 008.9 008.9	-0.0	349.6 349.0	+0.6
3	148 268.4 292.6	- 24.2	247 659.2 659.1	+0.1	349.8 349.2	+0.7
4	148 273.5 291.8	- 18.3	247 250.8 250.4	+0.5	350.1 349.6	+0.5
5	143 272.4 284.3	- 11.9	246 861.0 860.8	+0.2	350.2 349.1	+1.1
6	148 284.8 291.3	- 6.5	246 458.9 458.8	+0.1	350.6 349.9	+0.7
107(S-20)	148 292.8 292.6	+ 0.3	246 024.0 023.7	+0.3	350.9 350.9	+0.0
208	148 289.5 289.9	- 0.4	245 634.6 634.8	-0.1	350.1 350.3	-0.2
16103(S-19)	148 559.2 559.2	+ 0.0	247 731.8 731.8	-0.0	349.5 349.6	-0.0
5-16	148 207.4		246 946.8		350.2	
16211	147 890.1 919.6	- 29.5	248 468.3 467.6	+0.7	348.8 349.0	-0.2
12	147 871.4 894.6	- 23.2	248 080.2 080.2	+0.0	348.9 348.2	+0.7
13	147 933.9 952.0	- 18.0	247 666.3 666.1	+0.2	349.2 348.7	+0.5
14	147 888.8 899.9	- 11.2	247 249.2 249.1	+0.1	349.4 348.6	+0.8
15	147 895.7 891.4	+ 4.3	246 854.5 854.3	+0.2	349.6 349.3	+0.3
16	147 892.6 892.5	+ 0.1	246 457.1 457.0	+0.0	349.9 349.7	+0.2

TABLE 5.1

(Continued)

16217	147 891.1 889.1	+ 1.9	246 030.0 030.0	-0.1	350.2 349.7	+0.5
18	147 911.8 911.8	+ 0.0	245 605.2 604.9	+0.3	350.5 350.1	+0.4
221	147 466.5 490.0	- 23.5	248 463.6 463.2	+0.4	348.0 348.2	-0.3
22	147 465.3 480.7	- 15.4	248 037.5 037.5	-0.1	348.1 347.3	+0.8
23	147 482.7 492.3	- 9.6	247 658.1 657.5	+0.6	348.4 347.3	+1.0
24	147 581.5 586.7	- 5.2	247 240.9 241.1	-0.2	348.8 347.7	+1.1
25	147 489.5 490.3	- 0.8	246 853.3 854.3	-1.0	349.1 349.9	-0.8
26	147 488.9 488.9	- 0.0	246 451.6 451.8	-0.2	349.2 349.4	-0.2
27	147 489.0 489.0	+ 0.0	246 027.6 027.5	+0.1	349.5 349.2	+0.2
28	147 541.8 542.0	- 0.2	245 588.5 588.5	-0.0	349.9 349.8	+0.1
17201	147 077.1 092.0	- 14.9	248 464.4 463.8	+0.6	347.3 347.4	-0.2
202	147 077.4 086.0	- 8.5	248 086.0 085.9	+0.1	347.4 346.6	+0.7
17103	146 983.4 983.4	+ 0.0	247 628.9 628.8	+0.1	347.5 347.5	+0.0
204	147 201.0 201.2	- 0.2	247 244.1 244.2	-0.1	348.2 348.1	+0.1
205	147 116.8 116.9	- 0.1	246 848.3 848.5	-0.2	348.3 348.6	-0.3
206	147 114.6 114.8	- 0.2	246 399.6 399.7	-0.1	348.6 348.4	+0.2
207	147 090.8 090.8	- 0.0	246 023.5 024.0	-0.5	348.8 348.7	+0.0
208	147 086.2 086.6	- 0.4	245 643.9 643.8	+0.1	349.0 348.7	+0.3

TABLE 5.1

(Continued)

17211	146	680.8 687.9	-	7.1	248	463.6 463.3	+0.3	346.7 346.8	-0.2
12	146	697.4 698.6	-	1.2	248	073.5 073.1	+0.4	346.7 345.8	+1.0
13	146	687.4 687.3	+	0.1	247	658.9 658.6	+0.4	347.1 347.2	-0.1
14	146	757.3 756.7	+	0.7	247	263.8 263.3	+0.5	347.5 348.0	-0.5
15	146	685.9 685.5	+	0.4	246	853.1 853.0	+0.1	347.5 347.7	-0.1
16	146	685.2 685.0	+	0.2	246	451.0 451.1	-0.1	347.8 348.0	-0.2
117	146	689.2 689.6	-	0.4	246	071.8 071.7	+0.1	348.1 348.1	-0.1
218	146	676.6 676.4	+	0.2	245	621.3 621.7	+0.4	348.3 348.2	+0.1
5-17	146	766.2			246	914.5		347.5	
17221	146	146.8 146.7	+	0.2	248	400.9 400.9	+0.0	345.7 345.6	+0.1
22	146	181.9 181.6	+	0.3	248	036.5 036.4	+0.2	344.8 344.3	+0.5
23	146	249.0 248.9	+	0.1	247	650.5 650.1	+0.4	346.6 346.2	+0.5
24	146	284.4 284.3	+	0.1	247	256.4 256.1	+0.4	346.8 346.4	+0.5
25	146	284.2 284.2	+	0.0	246	854.1 853.9	+0.1	347.0 346.8	+0.3
26	146	320.8 319.8	+	1.0	246	452.2 452.3	-0.1	347.4 348.1	-0.7
27	146	300.5 300.7	-	0.2	246	064.4 065.1	-0.7	347.3 347.4	-0.1
28	146	303.1 302.8	+	0.3	245	610.8 611.6	-0.8	347.7 347.9	-0.2
18201	145	780.2 780.8	-	0.7	248	419.8 419.3	+0.5	345.4 344.9	+0.5
02	145	866.6 866.6	+	0.1	248	056.1 055.8	+0.4	345.7 344.1	+1.6

TABLE 5.1

(Continued)

18203	145	878.8 878.7	+ 0.1	247	639.6 639.1	+0.4	346.2 345.8	+0.4
204	145	882.8 882.7	+ 0.1	247	255.7 255.7	-0.0	346.4 346.2	+0.2
205	145	882.3 881.8	+ 0.5	246	854.0 854.1	-0.1	346.6 346.6	-0.1
206	145	871.5 870.7	+ 0.8	246	451.1 451.2	-0.1	346.7 346.6	+0.1
207	145	876.9 876.7	+ 0.3	246	033.4 033.5	-0.1	346.9 347.1	-0.2
208	145	965.6		245	550.6		347.3	
211	145	546.1 546.2	- 0.1	248	448.7 448.5	+0.2	344.2 344.1	+0.1
212	145	547.6 547.4	+ 0.2	248	069.6 069.3	+0.3	344.6 343.6	+1.0
213	145	565.9 565.8	+ 0.1	247	636.5 636.6	-0.0	346.6 345.5	+1.0
214	145	479.7 479.5	+ 0.2	247	254.6 254.9	-0.3	345.9 345.8	+0.0
215	145	479.9 479.6	+ 0.3	246	854.0 854.4	-0.4	346.1 346.9	-0.7
216	145	469.3 468.8	+ 0.5	246	450.2 450.4	-0.2	346.2 346.2	0.0
117	145	509.0 509.0	+ 0.0	246	029.9 029.9	+0.0	346.4 346.4	+0.0
218	145	434.7 434.6	+ 0.1	245	638.9 639.4	+0.6	346.6 346.5	+0.1
221	145	107.3 107.1	+ 0.3	248	465.3 465.2	+0.2	344.3 343.8	+0.5
222	145	107.1 106.9	+ 0.2	248	062.9 062.3	+0.6	344.7 344.0	+0.7
123	145	293.7 293.7	+ 0.0	247	597.1 597.2	-0.1	345.6 345.5	+0.0
224	145	138.0 138.0	- 0.0	247	256.3 257.3	-1.1	345.6 346.0	-0.4
225	145	152.1 152.2	- 0.1	246	836.1 837.3	-1.2	345.7 345.9	-0.2

TABLE 5.1

(Continued)

18226	145 104.6 104.6	- 0.0	246 449.5 451.4	-1.9	345.8 345.9	-0.0
18227	145 099.7 099.6	+ 0.1	246 067.2 069.1	-1.9	346.1 346.0	+0.0
18228	145 104.9 104.8	+ 0.0	245 646.0 647.5	-1.5	346.4 346.3	+0.1
5-18	145 325.9		246 880.9		345.7	
19201	144 261.4 261.7	- 0.4	248 430.4 433.8	-3.5	343.0 341.7	+1.3
19203	144 295.5 295.7	- 0.2	247 660.8 666.3	-5.5	344.2 344.5	-0.3
205	144 270.0 270.3	- 0.3	246 818.3 823.9	-5.5	344.0 343.8	+0.2
207	144 282.7 283.4	- 0.8	246 023.3 029.3	-6.0	344.0 343.9	+0.1
5-19	143 915.8		246 862.3		344.5	
19211	143 501.8 501.7	+ 0.1	248 491.1 501.5	-10.4	342.0 341.7	+0.3
215	143 504.3 504.9	- 0.6	246 818.4 828.1	-9.7	344.0 343.0	+0.9
117	143 450.6 450.6	- 0.0	246 009.7 009.7	+0.0	342.2 342.2	+0.0

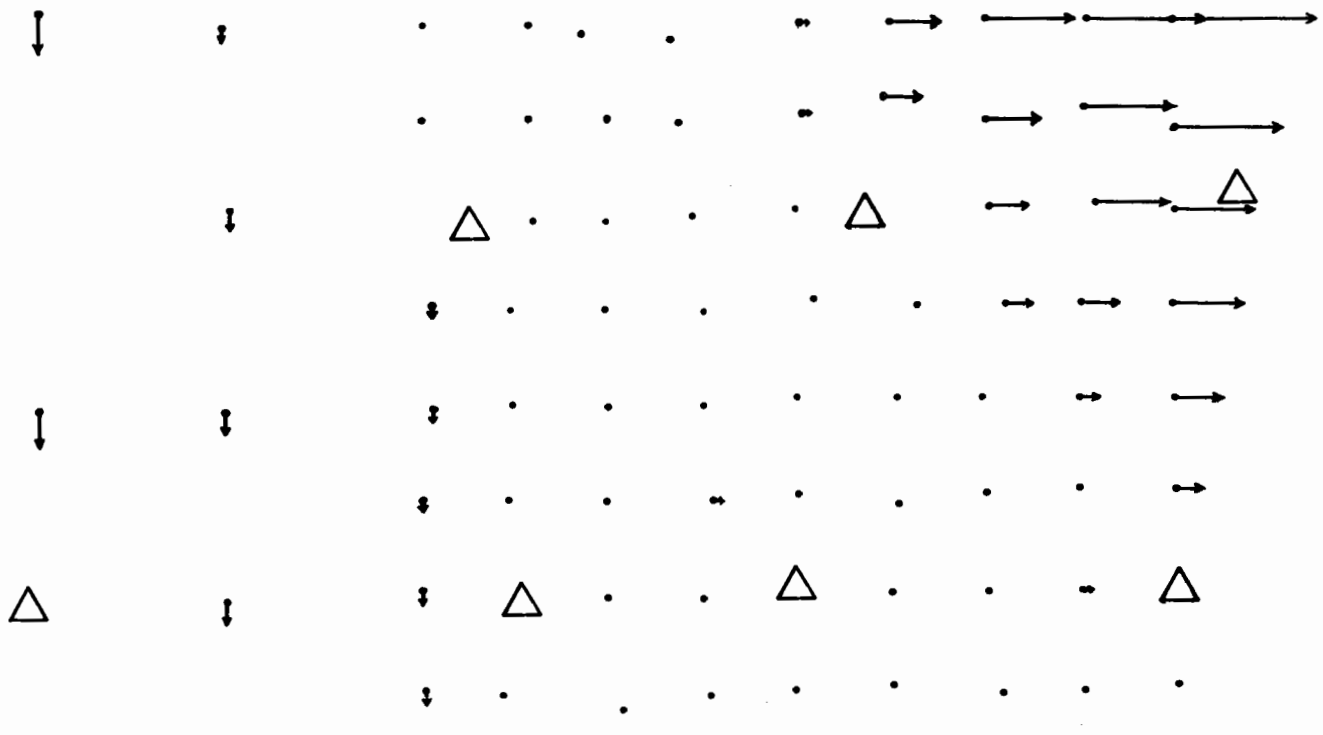

Figure 5.4 ΔX and ΔY Difference between A7 and AP/C

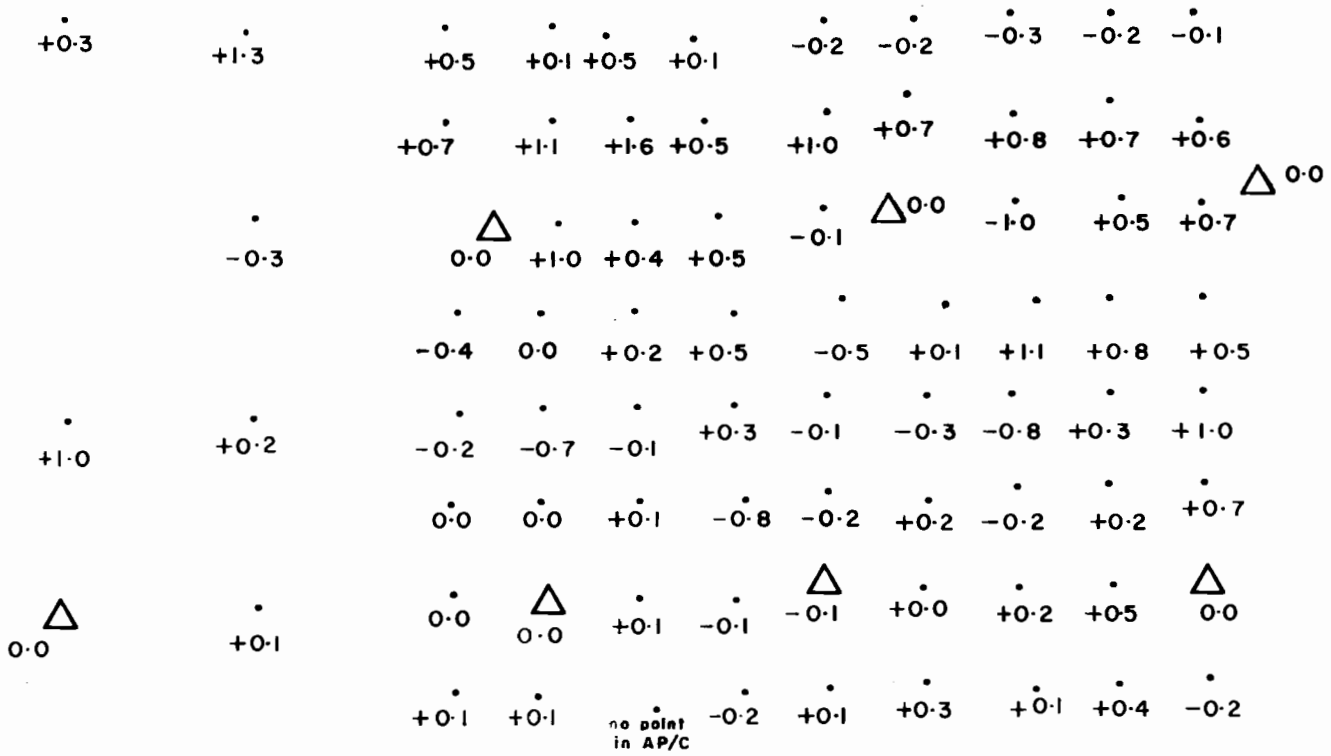

Figure 5.5 Elevation Differences in Meters between A7 and AP/C

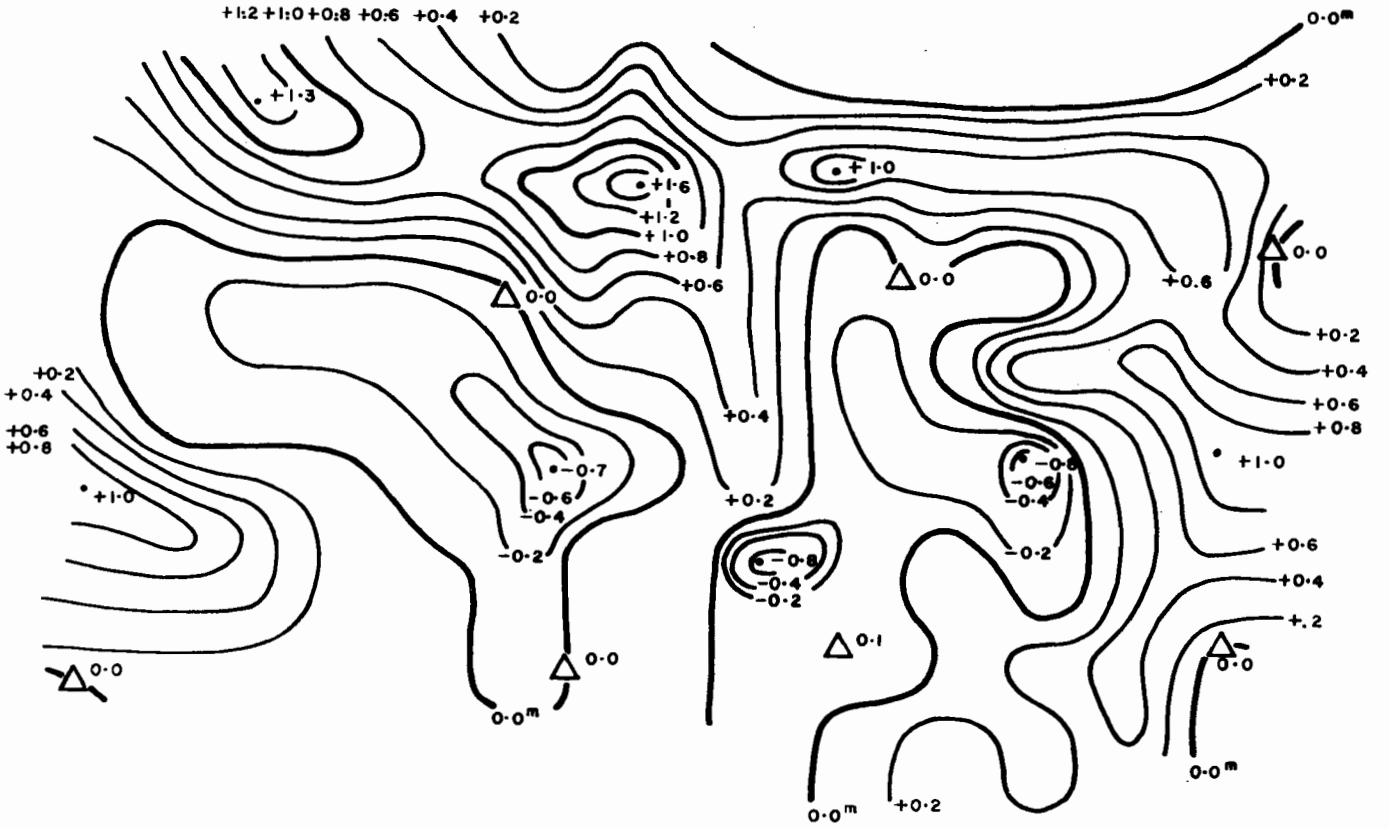

Interval : 0.2 m Scale 1:34000

Figure 5.5a Elevation Differences between A7 and AP/C

It will be noticed from a study of Table 5.1 and Figures 5.4, 5.5 and 5.5a that considerable difference in planimetry is noticed in the extreme edges of the strip due to reasons directly unknown, whereas in elevations the agreement is fairly good. It can be concluded that the discrepancies in the N.E. and N.W. edges are due to extrapolation in adjustment in the area beyond the framework of the control points.

In the N.E. area the discrepancies may be due to some gross error (blunder) in recording the X coordinate of point 16103 (which is one of the control points used in the adjustment) in either the AP/C or the A7. A blunder in the A7 value is most likely. By way of calculating back it was found that most probably an error was made in reading the X- coordinate at this point the 4th digit (in the 6 digit figure) i.e., the mm was read as 8 instead of 2 which could easily happen on account of the circular ring type counters. The standard deviation between the A7 and AP/C adjusted data are as follows:

Considering only the points within the framework of the control points (ignoring 16103):

in X = $\pm$ 0.14 m

in Y = $\pm$ 0.98 m

in Z = $\pm$ 0.14 m

It may be pointed out here that in the Wild A7 no attempt was made to compensate for the residual errors in refraction and earth curvature. It is also apparent that those residuals are negligible.

6. CONCLUSIONS AND RECOMMENDATIONS

The test performed in using the analytical procedures that have been outlined was very limited both in the size of the test data and in the control of error sources. However some conclusions are evident:

1) The analytical procedure provides a means to measure and to control systematic errors in a photograph. In the test photography printed with corrector plates to remove effects of lens distortion, earth curvature, and atmospheric refraction, the analytical procedure removed much of the residual systematic effects. The standard deviation to ground control was reduced about one-half.

2) The analytical procedure must include proper calibration programs in order to have accurate standards for correcting the data.

3) Even though some known systematic errors remained uncorrected, the AP/C analytical procedure gave results superior to those which normally could be obtained by a precise analogue device.

4) Super-wide-angle photography can produce results of very high quality in an analytical procedure with the AP/C. The standard deviation to vertical control in a test model was approximately 1:20000, using photographs of approximately 1:17000 scale. The dished-shaped distortion pattern was largely removed (Figures 4.1 through 4.3).

5) The test demonstrates that the propagation of error in an aerotriangulation is lessened. It must be realized that more study and more testing is needed in this area. It is possible, for instance, that adjustment procedures may better remove systematic effects which propagate errors.

6) Very high quality measuring is possible with the AP/C system. Additional study of error sources are needed in this area. However, the tests show that the measuring capability is much better than 0.01 mm--the least count for most analogue machines. In fact, if the full capability of the instrument and of the analytical system are not utilized, it might be better to use good analogue

instruments. It follows that the personnel must fulfill a higher role in getting the results of better quality.

7) The tests may be considered as adequate to validate the AP/C analytical system for SWA photography.

8) The tests on the Wild Autograph A7 indicates that SWA photography can be handled satisfactorily at the analogue instruments in normal aerial stereo photogrammetric mapping. This necessitates the introduction of a focal length longer than the actual one, this causing affine deformation. Proper corrections for such deformations yield satisfactory results. These effects, however, should be tested at the optical projection type instruments e.g., Kelsh Plotter, which carries the bulk of the work load in the State of Ohio, Department of Highways. Time and funds being limited in the current project, the effect of affine deformation in the Kelsh Plotter (in so far as the handling of SWA photography is concerned) could not be studied.

The results obtained in these tests exceeded expectations. However, because of the limited scope and size of the test, these results should not be used for planning purposes. Thus, the following is recommended:

1) Further testing with the same set of photographs but printed without corrector plates. Distortions would then be removed in strict accord with the AP/C programs. (This test was under way at the conclusion of this study. The diapositives were superior overall in resolution, but had scattered areas of blurred images, probably due to printing malfunctions.)

2) Further testing of a well-controlled area with a similar set of photographs. Continuing with Camera No. 367 offers advantages because some calibration already has been done. Testing the same area with a similar set (same scale or same flight height) of wide-angle photographs would be most desirable for a standard of comparison. A longer strip to include some hilly terrain and at a lower flight altitude would be more realistic for highway mapping studies.

3) Further research to test the usability of the Kelsh Plotter in SWA photography. This may be done with the same photography as was used

in this test. It is very strongly believed that by modifying some working procedures the available standard angle Kelsh Plotter can be used in handling SWA photography in accomplishing the mapping more economically and efficiently. However, such modifications should be made only after extensive research in this area, after proper consideration of terrain type, situation of ground control and the required mapping accuracy.

4) After this, or in conjunction with these tests, studies in compilation procedures for super-wide-angle photographs must be done. At present, it seems more feasible to use the AP/C in the aerotriangulation phase where the facility for additional accuracy and precision can furnish high quality control for compilation instruments. Also possibly orientation elements can be obtained for the compilation phases [32]. An economy should be realized by cutting out much geodetic surveying in highway mapping.

5) Improvements in the procedures to include calibration studies of the comparators themselves (fidelity of measuring, scales along axes and perpendicularity of axes), cameras, laboratory apparatus etc., should be made. If an error can be measured, it should, if practicable, be corrected.

APPENDIX A-1

Procedure Used in Calibration for Substitute Fiducial Marks in RC-9 Camera

The principal point was first defined in a coordinate system in which all fiducial marks were measured on a C & G S comparator. The problem here was to determine the offset of the above principal point position relative to new substitute points (the end of the leg radial to the center and at the intersection of legs defining the mark). A relation of these points to the fiducial mark centers was determined by measuring with the AP/C comparator a series of five measurements on each leg and five measurements for each substitute point. Reduction of the data is as follows:

1. Translate to the centroid for observations for each line of a fiducial mark as defined by opposite legs, where

$$\bar{X} = \frac{\Sigma X}{n} \qquad \text{and } \bar{Y} = \frac{\Sigma Y}{n}$$

2. Solve for the line slope by a least squares technique where

$$\text{Slope } C = \frac{\Sigma (X_i - \bar{X})(Y_i - \bar{Y})}{\Sigma (X_i - \bar{X})^2}$$

3. With the slope C and a point on the line known $(\bar{X}, \bar{Y})$, compute the intercept b on the Y- axis as

$$b = \bar{Y} - C\bar{X}.$$

4. With slope and intercept b now known, write the equation of the line as

$$Y = CX + b.$$

Do these steps for two lines defining the fiducial intersection.

5. Solve simultaneously the two equations for the center of the fiducial marks.

6. Determine the offset $(\Delta X, \Delta Y)$ for each substitute fiducial mark using the arithmetic mean for position of the substitute point.

7. Using the fiducial mark positions as measured in the calibration by C & G S of the "flash plate", apply the ΔX's and ΔY's of Step 6. We now have the substitute marks in the calibration coordinate system of the fiducial marks.

8. Compute the principal point as the intersection of the fiducial marks.

9. Compute the centroid of the substitute fiducial marks (Point No. 5 on measurements). Compute the offset to be used in interior orientation as:

X(principal point) - X(centroid) = X (offset)

and Y(principal point) - Y(centroid) = Y (offset).

10. To compute accuracy of procedure, a residual V_y can be computed for measurements on the fiducial lines as:

$$V_i = (Y_i - \bar{Y}) - C(X_i - \bar{X})$$

The V as distance from the mean line is $V_i/\sqrt{2}$ where slope of line is 45^o. For the substitute mark,

$$V_x = X_i - \bar{X}$$

Where $\bar{X}$ here is the arithmetic mean. Likewise for V_y.

11. To compute m, the standard deviation, for measurements on line:

$$m = \sqrt{\frac{[vv]}{(n-r)}}$$

where r = 2, the number of observations to define a line.

APPENDIX A-2

Example - Calibration for Principal Point for RC-9
Using Substitute Fiducial Marks

Measurement and Reduction of Flash Plate
For Camera No. 367

FLASH PLATE
Wild SWA Camera No. 367
Measured by
H. L. Carter
U. S. Coast & Geodetic Survey

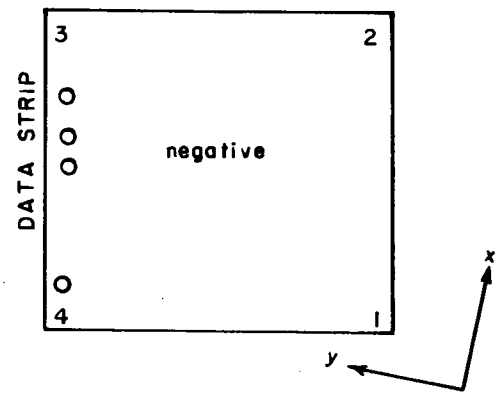

	X	Y		V_x	V_y	
67 00 001	020 227	026 438	000 001	+ 3.5	+ 1.4	
	20	36	02	- 3.5	- 0.6	mean
	20	34	03	- 3.5	- 2.6	x
	24	37	04	+ 0.5	+ 0.4	20223.5
	26	36	05	+ 2.5	- 0.6	y
	21	40	06	- 2.5	+ 3.4	26436.6
	23	30	07	- 0.5	- 6.6	
	23	36	08	- 0.5	- 0.6	Fiducial (1)
	25	40	09	+ 1.5	+ 3.4	
	26	39	10	+ 2.5	+ 2.4	
			[vv]	58.50	82.40	

67 00 002	232 214	028 336	000 011	- 3.3	+ 4.4	
	16	32	12	- 1.3	+ 0.4	mean
	19	32	13	+ 1.7	+ 0.4	x
	20	36	14	+ 2.7	+ 4.4	232217.3
	17	32	15	- 0.3	+ 0.4	y
	14	27	16	- 3.3	- 4.6	28331.6
	21	31	17	+ 3.7	- 0.6	
	16	29	18	- 1.3	- 2.6	Fiducial (2)
	19	30	19	+ 1.7	- 1.6	
	17	31	20	- 0.3	- 0.6	
			[vv]	52.10	70.40	

67 00 003	230 346	240 333	000 021	0.0	4.4	
	50	27	22	+ 4.0	- 1.6	mean
	41	27	23	- 5.0	- 1.6	x
	51	22	24	+ 5.0	- 6.6	230346.0
	44	27	25	- 2.0	- 1.6	y
	43	31	26	- 3.0	+ 2.4	240328.6
	49	29	27	+ 3.0	+ 0.4	
	42	31	28	- 4.0	+ 2.4	Fiducial (3)
	44	32	29	- 2.0	- 3.4	
	50	27	30	- 4.0	- 1.6	
			[vv]	124.00	96.40	

67 00 004	018 345	238 426	000 031	- 1.1	- 0.1	
	46	27	32	- 0.1	+ 0.9	mean
	47	24	33	+ 0.9	- 2.1	x
	44	28	34	- 2.1	+ 1.9	18346.1
	45	30	35	- 1.1	+ 3.9	y
	46	26	36	- 0.1	- 0.1	238426.1
	44	27	37	- 2.1	+ 0.9	
	48	23	38	+ 1.9	- 3.1	Fiducial (4)
	48	25	39	+ 1.9	- 1.1	
	48	25	40	+ 1.9	- 1.1	
		(vv)		22.90	36.90	

$\Sigma[vv]_x = 257.50$

$\Sigma[yy]_y = 286.10$

$n = 40 \quad m_x = \pm\sqrt{\frac{257.50}{36}} = \pm 2.7$

$u = 4 \quad m_y = \pm 2.8$

$m_{x-y} = \pm 3.9$

The above measured coordinates have been rearranged* to be compatible with the usual C & G S system.

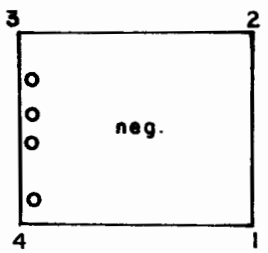

* +x = - machine y

+y = + machine x

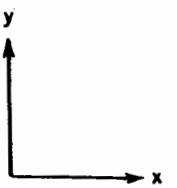

	x_1	y_1	x_2	y_2	x_3	y_3	x_4	y_4
Measured	20223.5	26436.6	232215.3	28331.6	230346.0	240328.6	18346.1	238426.1
Rearranged	323563.4	20223.5	321668.4	232217.3	109671.4	230346.0	111573.9	18346.1
Invert y coordinates for positive	323563.4	329776.5	321668.4	117782.7	109671.4	119654.0	111573.9	331653.9

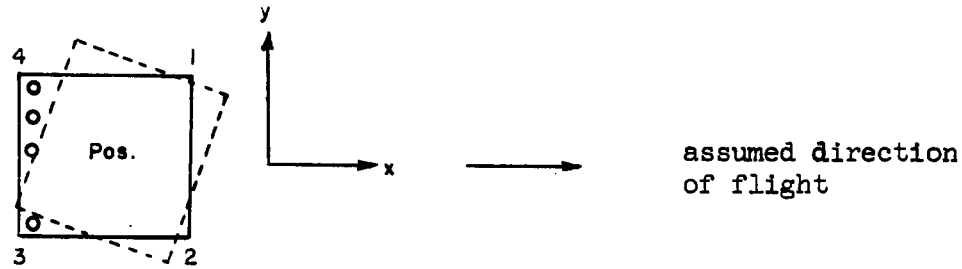

Translate to corner 3	213892.0	210122.5	211997.0	1871.3	0	0	1902.5	211999.9
Rotate for y = o @ corner 2	212028.9	212002.3	212005.3	0	0	0	31.1	212008.4

Locate principal point:

Slope 1 - 3 = $\frac{y_1}{x_1} = \frac{212002.3}{212028.9} = 0.99937455$

$x_\rho = 106017.8$

$y_\rho = 106004.5$

Slope 4 - 2 = $- \frac{212008.4}{211974.2} = - 1.0001613 4$

	x_1	y_1	x_2	y_2	x_3	y_3	x_4	y_4
Translated to principal point	+106011.6	+105997.8	+105987.5	-106004.5	-106017.8	-106004.5	105986.7	+106003.9

M for Fiducial Mark = $\frac{m}{\sqrt{n}} = \pm \frac{3.9}{\sqrt{10}} = \pm 1.2\mu$ = accuracy of mean for 10 measurements

TABLE OF COMPARATOR MEASUREMENTS FOR FIDUCIAL MARKS USED IN CALIBRATION AND COMPUTATION FOR CENTROID FOR EACH LINE
(STEP 1)

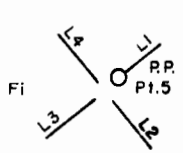

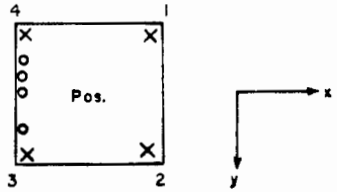

F4

	L1		L2		L3		L4		Point 5	
	X	Y	X	Y	X	Y	X	Y	X	Y
1)	-110.810	-103.999	-113.438	-103.969	-113.458	-106.602	-110.860	-106.596	-111.917	-105.088
2)	111.002	104.184	113.234	104.184	113.234	106.378	111.071	106.378	111.917	105.085
3)	111.370	104.554	112.877	104.554	112.877	106.027	111.422	106.027	111.924	105.090
4)	111.666	104.840	112.593	104.840	112.593	105.748	111.692	105.748	.923	.085
5)	111.917	105.086	112.350	105.080	112.339	105.501	111.924	105.505	.917	.086
Means	-112.1266	-105.2919	(Line 1 - 3)		(Line 2 - 4)		-112.1461	-105.2881	-111.920	-105.087

F3 Half of Line L1 - L3 Obliterated

	L1		L2		L3		L4		Point 5	
	X	Y	X	Y	X	Y	X	Y	X	Y
1)	-109.123	+107.037	-109.112	+109.444	111.516	109.475	111.542	107.060	-110.135	108.063
2)	109.319	107.245	109.319	109.246	111.292	109.246	111.292	107.307	.130	.065
3)	109.598	107.513	109.598	108.973	111.027	108.973	111.027	107.566	.127	.058
4)	109.885	107.818	109.885	108.689	110.747	108.689	110.747	107.849	.124	.067
5)	110.124	108.067	110.120	108.452	110.534	108.461	110.537	108.060	.124	.067
Means	-110.3165	+108.2528	(Line 1 - 3)		(Line 2 - 4)		-110.3179	+108.2646	-110.128	108.064

F2

	L1		L2		L3		L4		Point 5	
	X	Y	X	Y	X	Y	X	Y	X	Y
1)	+101.949	+105.139	+104.531	+105.131	+104.583	+107.736	+101.962	+107.765	+103.052	+106.234
2)	102.206	105.402	104.265	105.407	104.265	107.415	102.294	107.415	.053	.236
3)	102.517	105.710	103.972	105.710	103.972	107.134	102.577	107.134	.055	.235
4)	102.830	106.015	103.674	106.015	103.674	106.842	102.869	106.842	.055	.235
5)	103.051	106.234	103.461	106.237	103.458	106.629	103.071	106.630	.051	.232
Means	103.2505	106.4254	(Line 1 - 3)		(Line 2 - 4)		103.2676	106.4286	103.053	106.234

F1

	L1		L2		L3		L4		Point 5	
	X	Y,	X	Y	X	Y	X	Y	X	Y
1)	+100.119	-105.756	+100.102	-108.500	+102.833	-108.519	+102.866	-105.779	101.263	-106.931
2)	100.391	106.046	100.391	108.220	102.539	108.220	102.539	106.101	101.261	.934
3)	100.706	106.360	100.706	107.914	102.230	107.914	102.230	106.404	101.263	.931
4)	100.984	106.642	100.984	107.646	101.969	107.646	101.969	106.673	101.261	.931
5)	101.265	106.928	101.273	107.354	101.708	107.371	101.719	106.919	.265	.928
Means	101.4744	-107.1402	(Line 1 - 3)		(Line 2 - 4)		101.4779	-107.151	101.263	-106.931

COMPUTATION OF MEAN SLOPE OF LINES AND ERROR DATA FOR FIDUCIAL MARKS

F1 L 1-3

	(1) $X_i - \bar{X}$	(2) $Y_i - \bar{Y}$	(3) (1)x(2)	(4) $(1)^2$	(5) CX(1)	(6) V_i=(2)-(5)	(7) vv
1	-1.355	+1.384	-1.875	+1.836	+1.377	+7	49
2	-1.083	1.094	1.185	1.173	1.100	-6	36
3	.768	.780	.599	.590	.780	0	0
4	.490	.498	.244	.240	.498	0	0
5	.209	.212	.044	.044	.212	0	0
1'	+ .234	- .231	.054	.055	- .238	+7	49
2'	.495	.506	.250	.245	- .503	-3	9
3'	.756	- .774	.585	.572	- .768	-6	36
4'	1.065	1.080	1.150	1.134	-1.082	+2	4
5'	1.359	1.379	1.874	1.847	-1.381	+2	4
Σ	4.004	- .002	Σ-7.860	7.736		Σ +3	Σ 187

C=-1.016029

$m^2 = \frac{187}{8} = 23.4$

$m = \pm 4.8\mu$

L 2-4

1	-1.378	-1.349	+1.859	1.899	-1.358	9	81
2	1.087	1.069	1.162	1.182	1.071	2	4
3	.772	.763	.589	.596	.761	-2	4
4	.494	.495	.245	.244	.487	-8	64
5	.205	.203	.042	.042	.202	-1	1
1'	+ .241	+ .232	.056	.058	+ .238	-6	36
2'	.491	.478	.235	.241	.484	-6	36
3'	.752	.747	.562	.566	.741	+6	36
4'	1.061	1.050	1.114	1.126	1.045	+5	25
5'	1.388	1.372	1.904	1.927	1.368	+4	16
Σ	- .033	0 Σ	7.768	7.881		Σ+3	Σ302

C= .985662

$m^2 = \frac{302}{8} = 37.8$

$m = \pm 6.1\mu$

Average $m_{F1} = \pm 5.4$ in y or $m = \frac{5.4}{\sqrt{2}} = \pm 3.8\mu$ in normal distance to line

F2 L 1-3

	(1) $X_i - \bar{X}$	(2) $Y_i - \bar{Y}$	(3) (1)x(2)	(4) $(1)^2$	(5) C·(1)	(6) Vi=(2)-(5)	(7) vv
1	-1.302	-1.286	1.674	1.695	-1.278	-8	64
2	-1.045	1.023	1.069	1.092	-1.026	+3	9
3	- .734	.715	.525	.539	- .721	+6	36
4	- .421	.410	.173	.177	- .413	+3	9
5	- .200	.193	.039	.040	- .196	+3	9
1'	+ .207	+ .204	.042	.043	+ .203	+1	1
2'	.423	.417	.176	.179	+ .415	+2	4
3'	.721	.709	.511	.520	+ .708	+1	1
4'	1.014	.990	1.004	1.028	+ .996	-6	36
5'	1.332	1.311	1.746	1.774	+1.308	+3	9
Σ	- .005	+ .004	6.959	7.087		Σ-8	Σ178

C = .981939

$m^2 = \frac{.78}{8} = 22.2$

$m = \pm 4.7\mu$

L 2-4

1	+1.263	+1.298	-1.639	1.595	-1.291	-7	49
2	.997	-1.022	1.019	.994	-1.019	-3	9
3	.704	- .719	.506	.496	- .720	+1	1
4	.406	- .414	.168	.165	- .415	+1	1
5	.193	- .192	.038	.039	- .197	+5	25
1'	- .197	+ .201	.040	.039	+ .201	0	0
2'	- .399	.413	.165	.159	+ .408	-5	25
3'	- .691	.705	.487	.477	+ .707	-2	4
4'	- .974	.986	.960	.949	+ .996	-10	100
5'	-1.306	1.336	1.745	1.706	+1.335	+1	1
Σ	+ .004	- .004	-6.767	6.619		Σ-19	Σ215

C = -1.022518

$m^2 = 26.9$

$m = \pm 5.8\mu$

Average $m_{(F2)} = \pm 5.2$ in y or $m = \frac{5.2}{\sqrt{2}} = \pm 3.7$ distance to line

F3 L 1-3

	(1) $Xi - \bar{X}$	(2) $Yi - \bar{Y}$	(3) (1)x(2)	(4) $(1)^2$	(5) C-(1)	(6) Vi=(2)-(5)	(7) vv
1	+1.193	-1.216	-1.451	1.423	-1.212	- 4	16
2	+ .997	1.008	1.005	.994	-1.013	+ 5	25
3	+ .718	.740	.531	.516	- .730	-10	100
4	+ .431	.435	.187	.186	- .438	+ 3	9
5	+ .192	.186	.036	.037	- .195	+ 9	81
1'	- .218	+ .212	.046	.048	.222	-10	100
2'	- .431	- .436	.188	.186	.438	- 2	4
3'	- .711	.720	.512	.506	.723	- 3	9
4'	- .976	.993	.969	.953	.992	+ 1	1
5'	-1.200	1.222	1.466	1.440	1.219	+ 3	9
Σ	- .005	- .002	-6.391	6.289		Σ-8	Σ354

C = -1.016219

$m^2 = \frac{354}{8} = 44$

$m = \pm 6.6\mu$

L 2-4

1	+1.206	+1.179	1.422	1.454	+1.184	- 5	25
2	.999	.981	.980	.998	+ .981	0	0
3	.720	.708	.510	.518	+ .707	+ 1	1
4	.433	.424	.184	.187	.425	- 1	1
5	.198	.187	.037	.039	.194	- 7	49
1'	- .219	- .205	.045	.048	- .215	+10	100
2'	.429	.416	.178	.184	- .421	+ 6	36
3'	.709	.699	.496	.503	- .696	- 3	9
4'	.974	.958	.933	.949	- .956	- 2	4
5'	1.224	1.205	1.475	1.498	-1.201	- 4	16
Σ	- .001	- .004	+6.260	6.378		Σ- 5	Σ241

C + .981499

$m^2 = \frac{241}{8} = 30.1$

$m = \pm 5.5\mu$

Average $m_{(F3)} = \pm 6.1\mu$ in y . For distance to line $m = \frac{6.1\mu}{\sqrt{2}} = \pm 4.3\mu$

F4 L1 - L3 Solution for $C = \frac{\Sigma(3)}{\Sigma(4)}$

(1) $X_i - \bar{X}$	(2) $Y_i - \bar{Y}$	(3)=(1)x(2)	(4)=$(1)^2$	(5)=C·(1)	Vi=(2)-(5)	vv
1.317	1.293	1.7029	1.7345	1.293	0	0
1.125	1.108	1.2465	1.2656	1.105	+3	9
.757	.738	.5587	.5730	.743	-5	25
.461	.452	.2084	.2125	.453	-1	1
.210	.206	.0433	.0441	.206	0	0
- .212	- .209	.0443	.0449	- .208	-1	1
- .466	- .456	.2125	.2172	- .458	+2	4
- .750	- .735	.5513	.5625	- .737	+2	4
-1.107	-1.086	1.2022	1.2254	-1.087	+1	1
-1.331	-1.310	1.7436	1.7716	-1.307	-3	9
	Σ	7.5137	7.6513		Σ-2	Σ54

$C = \frac{7.5137}{7.6513} = .98201613$

$m^2 = \frac{54}{8} = 6.75$

$m = \pm 2.6\mu$

F4 L2 - L4

-1.292	+1.319	-1.704	1.669	1.312	+7	49
-1.088	1.104	-1.201	1.184	1.105	-1	1
- .731	.734	- .537	.534	.742	-8	64
- .447	.448	- .200	.200	.454	-6	36
- .204	.208	- .042	.042	.207	+1	1
+ .222	- .217	- .048	.049	- .225	+8	64
+ .454	- .460	- .209	.206	- .461	+1	1
+ .724	- .739	- .535	.524	- .735	-4	16
+1.075	-1.090	-1.172	1.156	-1.092	+2	4
+1.286	-1.308	-1.682	1.654	-1.306	-2	4
Σ-.001	- .001	-7.330	7.218		Σ-2	Σ240

$m^2 = \frac{240}{8} = 30$

$m = \pm 5.5\mu$

C - 1.015517

Average $m_{(F4)} = \pm 4.05$ in y or $m = \frac{4.05}{\sqrt{2}} = \pm 2.9\mu$ distance to lines for F4

Computation of Line Intersections for Fiducial Marks

F4

Solve for intercept for L1 - L3 : $b = Y - C\bar{X}$ where C is slope.

$$b_{(1-3)} = -105.292 - .982016 \cdot (-112.127$$

$$= -105.292 + 110.111 = +4.819$$

L2 - L4 :

$$b_{(2-4)} = -105.288 + 1.015517 \cdot (-112.146)$$

$$= -105.288 - 113.886 = -219.174$$

Use form $CX - Y = -b$

$$.982016X - Y = -4.819 \quad (1-3)$$

$$-1.015517X - Y = +219.174 \quad (2-4)$$

$$1.997533X = -223.993$$

$$X = -112.135$$

$$Y = .982016(-112.135) + 4.819 = -1-5.299$$

F1

L1 -L3 $b_{1-3} = \bar{Y} - C\bar{X} = 107.140 - (-1.016029)(101.474$

$$= -4.039$$

$$b_{2-4} = -107.151 - (.985662)(101.478)$$

$$= -207.174$$

For intersection of lines $CX - Y = -b$

$$(-1.016029)\ X - Y = +4.039$$

$$1.016029\ X + Y = -4.039$$

$$.985662\ X - Y = +207.174$$

$$2.001691\ X = +203.135$$

$$X = +101.482$$

$$(1.016029)(-101.482) + Y = -4.039$$

$$Y = -107.148$$

F2

Intercepts:

$$b = 106.425 - (.981939)(103.251 = + 5.039 \quad (1\text{-}3)$$

$$b = 106.429 - (-1.022518)(103.268) = +212.022$$

Intersection of lines:

$$.981939\ X - Y = -\ 5.039$$

$$-1.022518\ X - Y = -212.022$$

$$2.004457\ X = +206.983$$

$$X = +103.261$$

$$(.981939)(+103.261) - Y = 5.039$$

$$Y = +106.435$$

F3

$$b = y - cx$$

$$b_{1\text{-}3} = +108.253 -(-1.016219)(-110.316) = -3.852$$

$$b_{2\text{-}4} = +108.265 -(\ .981499)(-110.318) = +216.542$$

Intersection of lines:

$$CX - Y = -b$$

$$-1.016291\ X - Y = +\ 3.852$$

$$.981499\ X - Y = -216.542$$

$$1.997718\ X = -220.394$$

$$X = -110.323$$

$$(.981499)(110.323) - Y = -216.543$$

$$Y = +108.261$$

Translation Between Intersection of Fiducial Lines And Substitute Fiducial Mark

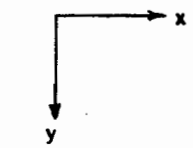

Quantities ΔX and ΔY:

F4

	X		Y
Intersection	-112.135		-105.299
Point No. 5	-111.920		-105.087
ΔX	+ .215	ΔY	+ .212

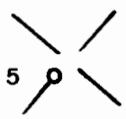

F1

	X	Y
Intersection	101.482	-107.148
Point No. 5	+101.263	-106.931
	- .219	+ .217

F3

	X	Y
Intersection	-110.323	+108.261
Point No. 5	-110.128	108.064
	+ .195	- .197

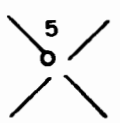

F2

	X	Y
Intersection	+103.261	+106.435
Point No. 5	103.053	106.235
	- .208	- .201

Computation of errors in measurements for Points No. 5, substitute fiducial mark, -- based on five observations each for three points. One badly obliterated by etched line is not included for analysis.

	F4		F2		F1	
	V_x	V_y	V_x	V_y	V_x	V_y
1	+3	-1	-1	0	0	0
2	+3	+2	0	+2	-2	+3
3	-4	-3	+2	+1	0	0
4	-3	+2	+2	+1	-2	0
5	+3	+1	-2	-2	+2	-3

$[VV] = 124$

$n = 30 \qquad u = 2 \quad$ (1 for each x and y)

$$m_{x,y} = \pm\sqrt{\frac{[vv]}{n-u}} = \pm\sqrt{\frac{124}{30-2}} = \pm\sqrt{4.43} = \pm 2.1$$

$m = \pm\sqrt{2} \cdot m_{x,y} = \pm 3.0\ \mu$ Standard error in planimetry

$M = \frac{m}{\sqrt{n}} = \pm\frac{3.0}{\sqrt{5}} = \pm 1.3\ \mu$ Error at mean.

Determining the Coordinates for the Substitute Fiducial Marks in C & G S Calibration System

C & G S Origin F3

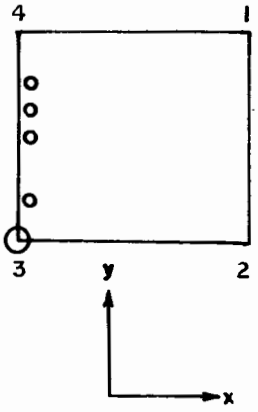

Camera Calibration

		X-axis	+	F2
F1	X_1	212 028.9	Y_1	212 002.3
	ΔX	219.		217.
F1 Sub.Pt		211 810		211 785

F2	X_2	212 005.3	0
	ΔX	208	+201
F2 Sub. Pt.		211 797	+201
F3	X_3	0	0
	ΔX	+195	+197
F3 Sub. Pt.		+195	+197
F4	X_4	31.1	212 008.4
	ΔX	+215	-212
F4 Sub. Pt.		+246	211 796

Coordinates of Principal Point	106 018.	106 005
Centroid of Substitute Fiducial Marks	106 012.	105 995
Principal Point Offset	6	10

Offset in principal point	+ 6 in X
for AP/C System	+10 in Y

Calibrated Lengths in mm : as required for Film distortion

ΔX : Line 4-1 : 211.564
Line 3-2 : 211.602 ΔX_m = 211.583

ΔY : Line 4-3 : 211.599
Line 1-2 : 211.584 ΔY_m = 211.592

CALIB Y ÷ CALIB X = 1.000043

Measurements at Approximate Equal Intervals Along Lines

APPENDIX B

EXAMPLES IN USE OF TABLES for CURVATURE AND REFRACTION

Example No. 1 in use of Tables [29]

Photogrammetric Refraction

h = 5000 ft ≅ 1.5 km

$h_{(\text{corrector plate})}$ ≅ 3.0 km

H = 1100 ft ≅ 0.3 km

f = 88.23 mm

Angle θ(Nadir)	5^g	10	15	20	25	30	35	40	45	50	55	60	65^g
= degrees	4.5^o	9	13.5	18	22.5	27	31.5	36	40.5	45	49.5	54	58.5^o
$r = f \cdot \tan\theta$ (mm)	6.9	14.0	21.2	28.7	36.6	45.0	54.1	64.1	75.4	88.2	103.3	121.4	144.0
For Ground Elevation 0 km (values below in centesimal seconds)													
$h_{(km)}$													
(1) 1.5	0.9	1.9	2.9	3.9	4.9	6.1	7.3	8.6	10.2	11.9	13.9	16.4	19.4^{cc}
(2) 3.0	1.7	3.5	5.3	7.2	9.2	11.3	13.6	16.1	19.0	22.2	26.0	30.6	36.2^{cc}
For H_G = 0 km, $h_{3.0} - h_{1.5}$													
(3)=(2)-(1)	0.8	1.6	2.4	3.3	4.3	5.2	6.3	7.5	8.8	10.3	12.1	14.2	16.8^{cc}
For Ground Elevation 0.5 km (actual E_M ≅ 1100 ft ≅ .34 km)													
h													
(4) 1.5	0.6	1.3	1.9	2.6	3.3	4.0	4.8	5.7	6.7	7.9	9.2	10.9	12.9^{cc}
(5) 3.0	1.4	2.9	4.4	5.9	7.5	9.3	11.2	13.2	15.5	18.2	21.3	25.1	29.7^{cc}
For H_G = 0.5 km, $h_{3.0} - h_{1.5}$													
(6)=(5)-(4)	0.8	1.6	2.5	3.3	4.2	5.3	6.4	7.5	8.8	10.3	12.1	14.2	16.8^{cc}
Thus, computing the difference in refraction is not much effected by ground elevation. Use line (6). Convert to radians. Factor 1.5707963×10^{-6} for centesimal second.													
(6)=(dθ)	.146	.242	.388	.533	..679	.825	1.019	1.164	1.407	1.600	1.892	2.231	2.638
Distortion: $dr = f \sec^2\theta \cdot d\theta$ where r' = radial distance													
$f \cdot \sec^2\theta$ (μm)	88777	90443	93316	47545	103368	111136	121362	134803	152589	176460	209185	255376	323187
dr (μm)	.1	.2	.4	.5	.7	.9	1.2	1.6	2.2	2.8	4.0	5.7	8.5

These values are plotted on graph (Fig. 3.9) with computed values for curvature effects.

Example No. 2 in use of Tables [29]

Photogrammetric Refraction and Curvature

h = 6000 ft = 1828.8 meters

H = 1100 ft = 334 mm.

$h_{(corrector\ plate)}$ = 10,000 ft = 3.0 km

Angle θ (Nadir)		5g	10	15	20	25	30	35	40	45	50	55	60	65g
	For Altitude 3.0 km, H = .33 km													
	H													
	0.0	+1.6	+2.9	+3.3	+2.6	+0.1	-4.4	-11.4	-21.5	-34.9	-52.7	-75.4	-104.3	-141.4
(1)	0.33	1.4	2.6	3.0	2.2	0.0	-4.0	-10.3	-19.2	-31.2	-47.0	-67.3	- 92.9	-125.9
	0.5	+1.3	+2.4	+2.8	+2.0	-0.1	-3.8	- 9.7	-18.1	-29.4	-44.2	-63.2	- 87.3	-118.3
	For Altitude 2.0 km, H = .33 km													
	0.0	+1.2	+2.1	+2.4	+1.9	+0.3	-2.6	- 7.2	-13.8	-22.8	-34.4	-49.5	-68.6	- 93.1
(2)	0.33	1.0	1.7	2.0	1.6	0.3	-2.2	- 6.2	-11.8	-19.4	-28.5	-42.1	-58.4	- 79.2
	0.5	0.9	1.5	1.8	1.4	0.3	-2.0	- 5.5	-10.4	-17.2	-25.9	-37.2	-51.6	- 70.0
	For Altitude 1.5 km, H = .33 km													
	0.0	0.9	1.6	1.9	1.6	0.4	-1.8	- 5.2	-10.2	-16.8	-25.5	-36.8	-51.0	- 69.4
(3)	0.33	0.7	1.2	1.5	1.3	0.3	-1.4	- 4.2	- 8.2	-13.5	-20.5	-29.5	-40.9	- 55.5
	0.5	0.6	1.1	1.2	1.1	0.3	-1.2	- 3.5	- 6.8	-11.3	-17.1	-24.6	-34.1	- 46.3
	For Altitude 1.83 km and H = 0.33 km [lines (2) and (3)]													
(4)	0.33	0.9	1.3	1.8	1.5	0.3	-1.9	- 5.4	-10.4	-17.0	-25.3	-37.1	-51.4	- 69.7
	For Difference in Corrector Plate h = 3.0 km and h = 1.83 km [(1) - (4)]													
	.33	+0.4	+1.1	+1.0	+0.5	-0.4	-1.9	- 4.3	- 7.7	-12.4	-18.9	-26.1	-35.9	- 48.6
	These are Centesimal Seconds. To convert to radians use factor 1.5707963×10^{-6}:													
	.33	+0.6	+ .17	+ .16	- .08	- .06	- .30	- .68	- 1.21	- 1.95	- 2.97	- 4.10	- 5.64	$- 7.63 \times 10^{-5}$
Angle θ (degrees)		4.5°	9	13.5	18	22.5	27	31.5	36	40.5	45	49.5	54	58.5°
$f \sec^2\theta$ (μm)		88 777	90 443	93 316	97 545	103 368	111 136	121 362	134 803	152 589	176 460	209 185	255 376	323 187
	Distortion $dr = f \sec^2\theta \cdot d\theta$ (in microns)													
dr		+0.1	+ .2	+ .1	- .1	- .1	-0.3	0.8	1.6	3.0	5.2	8.6	14.4	24.7
	For radius on plate, $r = f \cdot \tan\theta$													
$r_{(mm)}$		6.9	14.0	21.2	28.7	36.6	45.0	54.1	64.1	75.4	88.2	103.3	121.4	144.0

APPENDIX C

FORMULAS FOR ABSOLUTE ORIENTATION IN THE AP/C

Absolute orientation comprises the scaling and leveling as is done in an analogue device. It does not include any translation and rotation as would be required to bring the model into the same coordinate system as the ground. The output of absolute orientation includes the orientation elements of Φ and Ω that are required to rotate the model. These, plus the scale factor, serves to update the elements of orientation for each photograph.

Formulas involved are as follows [2]:

For scaling,

$$\text{Scale factor} = \frac{\Sigma(\text{control distances})}{\Sigma(\text{measured distances})} \qquad \text{(C-1)}$$

where

$$\text{Control distance} = \sqrt{(X_i - X_1)^2 + (Y_i - Y_1)^2 + (E_i - E_1)^2}$$

and

$$\text{Measured distance} = \sqrt{(X_{M_i} - X_{M_1})^2 + (Y_{M_i} - Y_{M_i})^2 + (E_{M_i} - E_{M_1})^2} \ .$$

Here, the subscript 1 is the first control station entered in the computer and i denotes a general station used in the solution. The ground coordinates are X, Y and E and the model coordinates are X_m, Y_m and E_m.

The base elements of each photograph (b_x, b_y, b_z) are multiplied by the scale factor to scale the model. The rotation required to level the model is determined by forming an observation equation for each vertical control station. The parameters are determined by a least squares solution if redundant observations are made. The basic equation [2]:

$$[A(X_{M_i} - X_{M_1}) + B(Y_{M_i} - Y_{M_1}) + C(E_{M_i} - E_{M_1})] \cdot \text{scale factor} \qquad (C\text{-}2)$$

$$= E_i - E_1$$

where

$A^2 + B^2 + C^2 = 1$ - the orthogonality condition.

The quantities A, B, C are related to the quantities Ω and Φ and the complete transformation equations for X, Y and E are as follows in matrix form [2].

$$\begin{bmatrix} \frac{C}{\sqrt{1-B^2}} & 0 & -\frac{A}{\sqrt{1-B^2}} \\ -\frac{AB}{\sqrt{1-B^2}} & \sqrt{1-B^2} & -\frac{BC}{\sqrt{1-B^2}} \\ A & B & C \end{bmatrix} \begin{bmatrix} X_{M_i} \\ Y_{M_i} \\ E_{M_i} \end{bmatrix} = \begin{bmatrix} X_i \\ Y_i \\ E_i \end{bmatrix} \qquad (C\text{-}3)$$

$$R_\Omega \cdot R_\Phi \cdot X_M = X$$

and

$$\begin{bmatrix} \cos\Phi & 0 & -\sin\Phi \\ \sin\Phi\sin\Omega & \cos\Omega & \sin\Omega\cos\Phi \\ -\sin\Phi\cos\Omega & -\sin\Omega & \cos\Omega\cos\Phi \end{bmatrix} \begin{bmatrix} X_{M_i} \\ Y_{M_i} \\ E_{M_i} \end{bmatrix} = \begin{bmatrix} X_i \\ Y_i \\ E_i \end{bmatrix} \quad \text{(C-4)}$$

This rotation matrix is applied to the base elements of each camera to obtain a new position for the camera elements by substituting b_x, b_y, b_z in place of X_m, Y_m, E_m. Thus,

$$\begin{bmatrix} b_x' \\ b_y' \\ b_z' \end{bmatrix} = R_\Omega \cdot R_\Phi \cdot \begin{bmatrix} b_x \\ b_y \\ b_z \end{bmatrix} \cdot \text{(scale factor)} \quad \text{(C-5)}$$

The orientation elements for each camera require changes resulting from the model rotation. The required orientation angles can be obtained by substituting the inverted rotation matrix from above into the old orientation matrix for each photograph. The relations for these orientation angles [2] are

$$
\begin{aligned}
B' &= B\cos\kappa - A\sin\kappa \\
\sin\Omega' &= \cos\Omega \cdot B' + \sin\Omega \cdot C \\
A' &= A\cos\kappa + B\sin\kappa \\
\sin\Delta\Phi &= -\frac{A'}{\cos\Omega'} \\
\Phi' &= \Phi + \Delta\Phi \\
\sin\kappa' &= \frac{\sin\kappa\cos\Omega\,\frac{C}{\sqrt{1-B^2}} + \sin\Omega\,\frac{A}{\sqrt{1-B^2}}}{\cos\Omega'}
\end{aligned}
\qquad \text{(C-6)}
$$

where

κ, Ω, Φ = original orientation angles

κ', Ω', Φ' = new orientation angles

APPENDIX D-1

Linear Transformation of Strip Coordinates--Arizona Test Strip

(Using Station 16103 and Station 17117 of First Model)

Point	x_s	y_s	X*	Y*	
16103	- 19.737	45.772	219.723	73.732	
17117	88.786	-50.945	111.027	170.245	
(1)-(2)	-108.523	+96.717	+108.696	- 96.513	Δ's

$x_s \rightarrow X^*$

$\Delta x_s \cdot a + \Delta y_s \cdot b = \Delta X^*$

$\Delta y_s \cdot a - \Delta x_s \cdot b = \Delta Y^*$

$$a = \frac{\begin{vmatrix} \Delta X^* & +\Delta y_s \\ \Delta Y^* & -\Delta x_s \end{vmatrix}}{\begin{vmatrix} \Delta x_s & \Delta y_s \\ \Delta y_s & -\Delta x_s \end{vmatrix}} = \frac{\begin{vmatrix} +108.696 & +96.717 \\ -96.513 & +108.523 \end{vmatrix}}{\begin{vmatrix} -108.523 & +96.717 \\ +96.717 & +108.523 \end{vmatrix}} = \frac{21130.463829}{-21131.419618} \qquad a = -0.99995477$$

$$b = \frac{\begin{vmatrix} \Delta x & \Delta X \\ \Delta y & \Delta Y \end{vmatrix}}{D} = \frac{\begin{vmatrix} -108.523 & 108.696 \\ 96.717 & -96.513 \end{vmatrix}}{21131.419618} = \frac{-38.870733}{-21131.419618} \qquad b = +.001839476$$

$c = X_1 - x_1 \cdot a - y_1 \cdot b = 219.723 - (19.737)(.999955) - (45.772)(.001839) = 199.903$

$d = Y_1 - y_1 \cdot a + x_1 \cdot b = 73.732 + 45.772 \cdot .999955 - 19.737 \cdot .001839 \qquad d = 119.466$

Check with Point 2 (17117)

$X_2 = x_2 \cdot a + y_2 \cdot b + c = -(88.786)(.999955) - (50.945)(001839) + 199.903 = 111.027$

$Y_2 = y_2 \cdot a - x_2 \cdot b + d = (50.945)(.999955) - (88.786)(.001839) + 119.466 = 170.245$

Transformation of Coordinates for Control Points

$$X_i = 199.903 - .999955\ x_i + .001839\ y_i$$

$$Y_i = 119.466 - .001839\ x_i - .999955\ y_i$$

Point	x_i	y_i	X_i	Y_i	X	Y	ΔX	ΔY
18123 (2)	170.119	37.622	29.861	82.533	29.867	81.563	- 6	-30
17103 (1)	71.867	39.627	128.112	79.709	128.104	79.713	+ 8	- 4
19117	277.147	-54.881	- 77.332	173.835	- 77.293	173.856	-39	-21
18117 (2)	157.443	-53.497	42.369	172.671	42.386	172.681	-17	-10
16107	- 4.424	-53.557	204.228	173.029	204.235	173.023	- 7	+ 6
17103 (2)	71.878	39.634	128.101	79.702	128.104	79.713	- 3	-11
17117 (2)	88.791	-50.936	111.022	170.236	111.027	170.245	- 5	- 9
18123 (3)	170.130	37.615	29.850	81.540	29.867	81.563	-17	-23

APPENDIX D-2

AEROPOLYGON STRIP ADJUSTMENT
for
ARIZONA TEST STRIP
using
ELECTRONIC COMPUTER

OHIO DEPARTMENT OF HIGHWAYS
AEROTRIANGULATION STRIP ADJUSTMENT PROGRAM WRITTEN BY C. T. HORSFALL OF THE U. S. COAST AND GEODETIC SURVEY IN MARCH, 1965
PROJECT NUMBER 1800 STRIP NUMBER 1

THIS IS A SIMULTANEOUS ADJUSTMENT TO THE THIRD DEGREE HORIZONTALLY AND TO THE SECOND DEGREE VERTICALLY.

THE FOLLOWING POINTS WERE USED FOR HORIZONTAL CONTROL--

POINT	PHOTO X	PHOTO Y	PHOTO Z	GROUND X	GROUND Y	GROUND Z	TYPE
16103	-19.737	45.772	20.323	219.723	73.732	20.322	6
17117	88.786	-50.946	20.238	111.027	170.245	20.236	6
18123	170.118	37.612	20.085	29.867	81.563	20.088	6
19117	277.139	-54.891	19.880	-77.293	173.856	19.897	6

THE FOLLOWING POINTS WERE USED FOR VERTICAL CONTROL--

POINT	PHOTO X	PHOTO Y	PHOTO Z	GROUND X	GROUND Y	GROUND Z	TYPE
16103	-19.737	45.772	20.323	219.723	73.732	20.322	6
16107	-4.424	-53.557	20.405	204.235	173.023	20.402	7
17103	71.870	39.624	20.200	128.104	79.713	20.205	7
17117	88.786	-50.946	20.238	111.027	170.245	20.236	6
18117	157.438	-53.508	20.131	42.386	172.681	20.140	7
18123	170.118	37.612	20.085	29.867	81.563	20.088	6
19117	277.139	-54.891	19.880	-77.293	173.856	19.897	6

THE POINTS USED FOR DETERMINING THE AXIS OF FLIGHT WERE--

16000	.124	-.384
20000	330.707	-5.536

THE GROUND TO MODEL SCALE RATIO IS 304.760 TO 1

FOLLOWING IS THE DATA COMPUTED FROM THE 4 HORIZONTAL CONTROL POINTS

POINT	CORRECTIONS DELTA X	CORRECTIONS DELTA Y	COMPUTED COORDINATE GROUND Z	RESIDUALS RESIDUAL X	RESIDUALS RESIDUAL Y	TYPE
16103	.0000	-.0000	20.3234	-.0010	-.0008	6
17117	.0156	.0003	20.2398	-.0009	.0033	6
18123	.0110	-.0091	20.0894	.0009	-.0033	6
19117	-.0000	-.0000	19.8969	.0010	.0008	6

FOLLOWING IS THE DATA COMPUTED FROM THE 7 VERTICAL CONTROL POINTS

POINT	CORRECTION DELTA Z	COMPUTED COORDINATES GROUND X	COMPUTED COORDINATES GROUND Y	RESIDUAL RESIDUAL Z	TYPE
16103	-.0225	219.7219	73.7311	-.0014	6
16107	-.0245	204.2245	173.0391	.0015	7
17103	-.0170	128.1039	79.7198	.0029	7
17117	-.0235	111.0261	170.2483	-.0038	6
18117	-.0126	42.3833	172.6834	.0020	7
18123	-.0191	29.8679	81.5596	-.0014	6
19117	-.0046	-77.2919	173.8568	.0000	6

NOTE -- ALL VALUES IN THIS PRINTOUT ARE IN MILLIMETERS.

FOLLOWING ARE THE COMPUTED GROUND COORDINATES FOR ALL OTHER POINTS

	CORRECTIONS (Actual - Computed)			COMPUTED COORDINATES			ACTUAL COORDINATES			
POINT	DELTA X	DELTA Y	DELTA Z	GROUND X	GROUND Y	GROUND Z	GROUND X	GROUND Y	GROUND Z	TYPE
16103	.001	.000	-.001	219.721	73.731	20.323	219.723	73.732	20.322	6
16205	.000	.000	-.020	204.228	218.392	20.397	.000	.000	20.377	2
16107	.010	-.016	.001	204.224	173.039	20.400	204.235	173.023	20.402	7
16208	.000	.000	-.006	204.062	195.653	20.364	.000	.000	20.358	2
16206	.000	.000	.009	204.143	147.745	20.341	.000	.000	20.351	2
16203	.000	.000	.014	204.221	77.957	20.300	.000	.000	20.315	2
16204	.000	.000	.011	204.176	101.549	20.326	.000	.000	20.338	2
16201	.000	.000	-.007	204.215	31.188	20.324	.000	.000	20.317	2
16202	.000	.000	.000	204.061	57.622	20.293	.000	.000	20.294	2
16205	.000	.000	.002	203.740	124.373	20.298	.000	.000	20.301	2
16303	.000	.000	.000	201.831	209.754	20.392	.000	.000	.000	1
16302	.000	.000	.000	199.885	119.788	20.310	.000	.000	.000	1
16000	.000	.000	.000	199.774	119.855	20.310	.000	.000	.000	8
16301	.000	.000	.000	195.591	33.627	20.315	.000	.000	.000	1
16213	.000	.000	-.003	184.416	77.554	20.272	.000	.000	20.269	2
16211	.000	.000	-.013	182.534	30.956	20.289	.000	.000	20.276	2
16218	.000	.000	-.002	182.079	197.388	20.353	.000	.000	20.351	2
16219	.000	.000	-.020	181.313	218.149	20.357	.000	.000	20.337	2
16214	.000	.000	.012	181.392	101.795	20.269	.000	.000	20.282	2
16216	.000	.000	.005	180.962	147.847	20.332	.000	.000	20.338	2
16217	.000	.000	.005	180.885	172.672	20.331	.000	.000	20.337	2
16212	.000	.000	.004	181.082	53.476	20.243	.000	.000	20.248	2
16215	.000	.000	.014	180.895	124.752	20.309	.000	.000	20.324	2
16224	.000	.000	.007	163.178	102.262	20.213	.000	.000	20.221	2
16228	.000	.000	-.006	160.583	198.341	20.337	.000	.000	20.331	2
16229	.000	.000	-.014	157.480	218.338	20.326	.000	.000	20.312	2
16223	.000	.000	.010	157.691	78.039	20.194	.000	.000	20.205	2
16227	.000	.000	.000	157.498	172.820	20.305	.000	.000	20.306	2
16226	.000	.000	-.000	157.499	148.156	20.314	.000	.000	20.314	2
16225	.000	.000	.002	157.531	124.787	20.342	.000	.000	20.345	2
16221	.000	.000	-.004	157.556	31.209	20.247	.000	.000	20.243	2
16222	.000	.000	.003	157.018	55.957	20.191	.000	.000	20.195	2
17204	.000	.000	.004	140.766	102.081	20.238	.000	.000	20.243	2
17205	.000	.000	.009	135.869	125.089	20.268	.000	.000	20.278	2
17206	.000	.000	.001	135.746	151.180	20.255	.000	.000	20.257	2
17209	.000	.000	-.013	135.230	220.811	20.270	.000	.000	20.257	2
17207	.000	.000	-.003	134.348	173.064	20.276	.000	.000	20.273	2
17201	.000	.000	-.004	134.418	31.177	20.200	.000	.000	20.196	2
17208	.000	.000	.002	134.102	195.129	20.275	.000	.000	20.278	2

17202	.000	.000	-.002	134.067	53.145	20.154	.000	.000	20.152	2
17103	.000	-.006	.002	128.103	79.719	20.202	128.104	79.713	20.205	7
17303	.000	.000	.000	117.592	207.757	20.258	.000	.000	.000	1
17302	.000	.000	.000	115.811	120.561	20.231	.000	.000	.000	1
17214	.000	.000	-.005	114.922	100.972	20.230	.000	.000	20.225	2
17301	.000	.000	.000	113.459	33.569	20.156	.000	.000	.000	1
17219	.000	.000	-.022	111.442	219.558	20.266	.000	.000	20.244	2
17212	.000	.000	.008	111.549	53.889	20.102	.000	.000	20.111	2
17117	.000	-.003	-.003	111.026	170.248	20.239	111.027	170.245	20.236	6
17213	.000	.000	.009	110.892	77.990	20.185	.000	.000	20.195	2
17216	.000	.000	-.007	110.756	148.191	20.234	.000	.000	20.227	2
17215	.000	.000	-.002	110.783	124.828	20.214	.000	.000	20.212	2
17211	.000	.000	.002	110.925	31.203	20.165	.000	.000	20.168	2
17218	.000	.000	-.011	110.256	196.413	20.243	.000	.000	20.232	2
17226	.000	.000	.002	89.552	148.123	20.240	.000	.000	20.243	2
17228	.000	.000	-.013	88.537	196.998	20.227	.000	.000	20.214	2
17227	.000	.000	-.005	88.411	170.632	20.200	.000	.000	20.195	2
17225	.000	.000	.014	87.452	124.772	20.162	.000	.000	20.177	2
17224	.000	.000	.012	87.460	101.392	20.137	.000	.000	20.150	2
17229	.000	.000	-.023	87.216	218.427	20.257	.000	.000	20.234	2
17223	.000	.000	.013	85.403	78.485	20.126	.000	.000	20.140	2
17222	.000	.000	.022	81.488	56.026	20.018	.000	.000	20.041	2
17221	.000	.000	.019	79.458	34.834	20.095	.000	.000	20.115	2
18204	.000	.000	.006	64.109	101.411	20.126	.000	.000	20.133	2
18205	.000	.000	.005	64.059	124.759	20.152	.000	.000	20.158	2
18209	.000	.000	-.011	63.885	218.350	20.199	.000	.000	20.188	2
18207	.000	.000	-.007	63.759	172.471	20.180	.000	.000	20.174	2
18203	.000	.000	.012	63.878	79.701	20.102	.000	.000	20.115	2
18206	.000	.000	.005	63.441	148.186	20.153	.000	.000	20.159	2
18202	.000	.000	.008	63.173	54.316	20.007	.000	.000	20.016	2
18201	.000	.000	.015	58.188	33.761	20.051	.000	.000	20.067	2
18213	.000	.000	.014	45.684	79.268	20.079	.000	.000	20.094	2
18219	.000	.000	.000	44.775	217.656	20.152	.000	.000	.000	1
18212	.000	.000	.026	44.617	54.109	19.976	.000	.000	20.003	2
18211	.000	.000	.019	44.547	32.062	20.005	.000	.000	20.025	2
18117	.002	-.002	.002	42.383	172.683	20.137	42.386	172.681	20.140	7
18215	.000	.000	.001	40.676	124.744	20.166	.000	.000	20.168	2
18214	.000	.000	.001	40.670	101.461	20.106	.000	.000	20.108	2
18216	.000	.000	.002	40.049	148.233	20.126	.000	.000	20.129	2
18218	.000	.000	.000	38.059	195.381	20.147	.000	.000	.000	1
18303	.000	.000	.000	32.082	210.203	20.111	.000	.000	.000	1
18302	.000	.000	.000	31.861	123.063	20.188	.000	.000	.000	1

18301	.000	.000	.000	31.606	36.584	19.951	.000	.000	.000 1
18123	-.000	.003	-.001	29.867	81.559	20.089	29.867	81.563	20.088 6
18225	.000	.000	-.002	21.637	125.736	20.113	.000	.000	20.111 2
18224	.000	.000	.008	20.816	101.317	20.117	.000	.000	20.124 2
18228	.000	.000	-.005	18.886	194.913	20.131	.000	.000	20.126 2
18226	.000	.000	-.002	18.874	148.176	20.108	.000	.000	20.106 2
18222	.000	.000	.000	19.005	54.517	19.999	.000	.000	20.000 2
18221	.000	.000	.013	19.016	31.095	19.989	.000	.000	20.003 2
18229	.000	.000	-.011	18.645	218.313	20.048	.000	.000	20.037 2
18227	.000	.000	-.002	18.582	170.399	20.119	.000	.000	20.117 2
19209	.000	.000	-.005	-27.989	218.317	19.973	.000	.000	19.968 2
19203	.000	.000	.013	-28.155	77.542	20.030	.000	.000	20.044 2
19207	.000	.000	.000	-28.870	172.714	19.992	.000	.000	19.993 2
19205	.000	.000	.014	-29.633	126.520	19.988	.000	.000	20.003 2
19201	.000	.000	.004	-30.132	32.916	19.865	.000	.000	19.870 2
19301	.000	.000	.000	-48.858	37.461	19.965	.000	.000	.000 1
19303	.000	.000	.000	-49.408	209.702	19.933	.000	.000	.000 1
19000	.000	.000	.000	-50.112	123.878	20.009	.000	.000	.000 1
19312	.000	.000	.000	-51.053	129.374	19.975	.000	.000	.000 1
19215	.000	.000	.016	-74.133	126.268	19.944	.000	.000	19.961 2
19211	.000	.000	.017	-74.319	28.981	19.868	.000	.000	19.886 2
19219	.000	.000	-.018	-74.709	218.232	19.903	.000	.000	19.885 2
19117	-.001	-.000	.000	-77.291	173.856	19.896	-77.293	173.856	19.897 6
20301	.000	.000	.000	-129.644	29.186	19.821	.000	.000	.000 1
20000	.000	.000	.000	-130.765	124.418	19.870	.000	.000	.000 9
20303	.000	.000	.000	-133.742	212.618	19.818	.000	.000	.000 1
20302	.000	.000	.000	-135.002	126.582	19.852	.000	.000	.000 1

THE STANDARD ERROR OF X IS .0039 mm , BASED ON THE 7 X GROUND COORDINATES KEYPUNCHED ON THE DATA CARDS.

THE STANDARD ERROR OF Y IS .0063 mm , BASED ON THE 7 Y GROUND COORDINATES KEYPUNCHED ON THE DATA CARDS.

THE STANDARD ERROR OF Z IS .0104 mm , BASED ON THE 88 Z GROUND COORDINATES KEYPUNCHED ON THE DATA CARDS.

THE SEVEN HORIZONTAL ADJUSTMENT CONSTANTS WERE

.C0000000 -.00000024 -.00008785 -.00000018 .00000622 .01056261 -.00219822

THE FIVE VERTICAL ADJUSTMENT CONSTANTS WERE

.C0000004 .00005099 -.00000054 -.00004057 -.01616827

ALL COMPUTATIONS FOR THIS STRIP HAVE BEEN COMPLETED

APPENDIX E-1

Relative Orientation Formulas as Solved in AP/C

These formulas are much the same as presented in Appendix B-7, Photogrammetry, 1960, a textbook by Bertil Hallert and shown in [2].

In the AP/C we define our model points for relative orientation as follows:

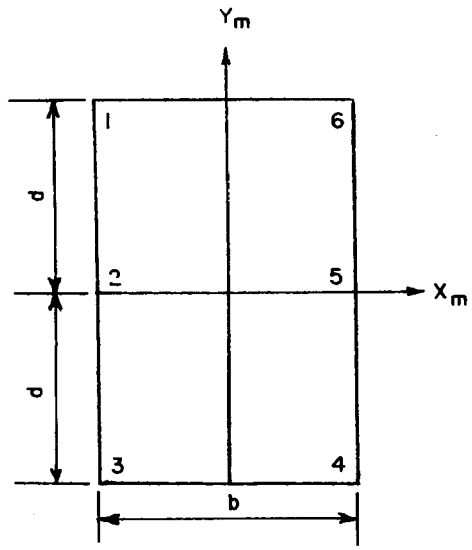

MODEL

Point	X_M	Y_M
1	bx_1	+d
2	bx_1	0
3	bx_1	-d
4	bx_2	-d
5	bx_2	0
6	bx_2	+d

COORDINATES

Figure E-1. Designation of Model Points in AP/C System

The equation for differential y-parallax for the dependent case, where $py = y_2 - y_1$ is:

$$py = dby_2 + (x-b)d\kappa_2 - \frac{y}{h}\,dbz_2 + \frac{(x-b)}{h}\,d\varphi_2 - (1 + \frac{y_2^2}{h})\,hd\omega_2 \qquad (E\text{-}1)$$

This is changed from an expression of error to a correction equation in parallax by simply changing signs of the right hand side. Then an observation equation can be written for each point in the model where parallax is measured as follows:

$$v = -dby_2 - (x-b)d\kappa_2 + \frac{y}{h}\,dbz_2 - \frac{(x-b)y}{h}\,d\varphi_2 + (1+\frac{y_2^2}{h})hd\omega_2 - py \qquad (E\text{-}2)$$

The problem is greatly simplified by selecting points in the model as shown on the preceding page. With redundant observations, more than five, a least squares solution is required, which is done in the AP/C. For six points located as above, the observation equations are presented in the following table (note that $b = bx_2 - bx_1$ and py is the observed quantity in each case):

Point	dby_2	$d\kappa_2$	dbz_2	$d\varphi_2$	$d\omega_2$	py	= v
1	-1	b	d/h	$\frac{bd}{h}$	$h + \frac{d^2}{h}$	$-p_1$	v_1
2	-1	b	0	0	h	$-p_2$	v_2
3	-1	b	-d/h	$\frac{-bd}{h}$	$h + \frac{d^2}{h}$	$-p_3$	v_3
4	-1	0	-d/h	0	$h + \frac{d^2}{h}$	$-p_4$	v_4
5	-1	0	0	0	h	$-p_5$	v_5
6	-1	0	d/h	0	$h + \frac{d^2}{h}$	$-p_6$	v_6

The solution of the normal equations from this set of observations is as follows:

$$1)\quad d\kappa_2 = \frac{1}{3b}(p_1 + p_2 + p_3 - p_4 - p_5 - p_6)$$

$$2)\quad d\omega_2 = \frac{h}{4d^2}(p_1 - 2p_2 + p_3 + p_4 - 2p_5 + p_6)$$

$$3)\quad d\varphi_2 = \frac{h}{2bd}(p_1 - p_3 + p_4 - p_6) \qquad \text{(E-3)}$$

$$4)\quad dby_2 = \frac{1}{12d^2}\{(p_1 + p_3)(3h^2 + 2d^2) + (p_4 + p_6)(3h^2 - 2d^2)$$

$$-p_2(6h^2 + 4d^2) - p_5(6h^2 + 8d^2)\}$$

$$5)\quad dbz_2 = \frac{h}{2d}(p_6 - p_4)$$

These equations are expressed in generalized form to better present the coefficients in a tabular form for computation as scheduled for AP-C, even though some coefficients are zero:

$$\Delta\kappa_2 = a_1p_1 + a_2p_2 + \quad \cdots \quad + a_6p_6$$

$$\Delta\omega_2 = b_1p_1 + b_2p_2 + \quad \cdots \quad + b_6p_6$$

$$\Delta\varphi_2 = c_1p_1 + c_2p_2 + \quad \cdots \quad + c_6p_6 \qquad \text{(E-4)}$$

$$\Delta by_2 = d_1p_1 + d_2p_2 + \quad \cdots \quad + d_6p_6$$

$$\Delta bz_2 = e_1p_1 + e_2p_2 + \quad \cdots \quad + e_6p_6$$

These coefficients are evaluated and are presented in Table E-1 with columns and rows designated by number and letter respectively.

TABLE E-1

Values of Coefficients for Solution

of Relative Orientation

Coefficient	1	2	3	4	5	6	Pt. No.
a	$1/3b$	$1/3b$	$1/3b$	$-\frac{1}{3b}$	$-\frac{1}{3b}$	$-\frac{1}{3b}$	
b	$\frac{h}{4d^2}$	$-\frac{h}{8d^2}$	$\frac{h}{4d^2}$	$\frac{h}{4d^2}$	$-\frac{h}{8d^2}$	$\frac{h}{4d^2}$	
c	$-\frac{h}{2bd}$	0	$\frac{h}{2bd}$	$-\frac{h}{2bd}$	0	$\frac{-h}{2bd}$	
d	$\frac{3h^2+2d^2}{12d^2}$	$\frac{-6h^2+4d^2}{12d^2}$	$\frac{3h^2+2d^2}{12d^2}$	$\frac{3h^2-2d^2}{12d^2}$	$\frac{-6h^2+8d^2}{12d^2}$	$\frac{3h^2-2d^2}{12d^2}$	
e	0	0	0	$\frac{h}{2d}$	0	$-\frac{h}{2d}$	

For AP/C, generally h = f. For "base-out", substitute (-b) for (+b). as is the case for dependent orientation where the left photograph is oriented to the right.

These equations are well adapted to error analysis for the individual parameters. If μ represents the error in parallax measurement and all measurements are equal in quality, then the errors in the orientation parameters are:

$$m_\kappa = \mu \cdot \sum_{n=1}^{6} |a| \qquad m_{by} = \mu \cdot \sum_{n=1}^{6} |d|$$

$$m_\varphi = \mu \cdot \sum_{n=1}^{6} |c| \qquad \text{(E-5)}$$

$$m_\omega = \mu \cdot \sum_{n=1}^{6} |b| \qquad m_{bz} = \mu \cdot \sum_{n=1}^{6} |e|$$

APPENDIX E-2

Computed Coefficients (AP/C Machine Units) for Relative Orientation as Shown in Table E-1 for Photographs in Arizona Test Strip

TAPE FORMAT

Base In	1 02 041
d	720 000
d_1	426 666
d_2	- 853 332
d_3	426 666
d_4	77 175
d_5	-1 203 765
d_6	77 175
e_1	0
e_2	0
e_3	0
e_4	514 012
e_5	0
e_6	- 514 012
a_1	2 225 147
a_2	2 225 147
a_3	2 225 147
a_4	-2 225 147
a_5	-2 225 147
a_6	-2 225 147

Base Out	1 02 041
d	720 000
d_6	77 175
d_5	-1 203 765
d_4	77 175
d_3	426 666
d_2	- 853 332
d_1	426 666
e_6	- 514 012
e_2	0
e_4	514 012
e_3	0
e_5	0
e_1	0
a_6	-2 225 147
a_5	-2 225 147
a_4	-2 225 147
a_3	2 225 147
a_2	2 225 147
a_1	2 225 147

Base In		Base Out	
b_1	-1 637 147	b_6	-1 634 147
b_2	+3 268 294	b_5	+3 268 294
b_3	-1 634 147	b_4	-1 634 147
b_4	-1 634 147	b_3	-1 634 147
b_5	+3 268 294	b_2	+3 268 294
b_6	-1 634 147	b_1	-1 634 147
c_1	-3 268 295	c_6	3 268 295
c_2	0	c_2	0
c_3	3 268 295	c_4	-3 268 295
c_4	-3 268 295	c_3	3 268 295
c_5	0	c_5	0
c_6	3 268 295	c_1	-3 268 295

F = 88.23 mm

B = 90.00 mm

D = 90.00 mm

BIBLIOGRAPHY

1. Anderson, James M., "Analytical Aerotriangulation Applied to Photogrammetric Mapping for Highway Design", Photogrammetric Engineering, March, 1961, Vol. XXVII, No. 1.

2. Bendix Corporation, "AP/C Control Computer Operating Procedures and Programs," April 10, 1964.

3. Brandenberger, Arthur J., "Aero-Triangulation for Ohio Highway Department Surveys and Right-of-Way Acquisition," Technical Report, July, 1963.

4. Brandenberger, Arthur J., "Class Notes--Analytical Photogrammetry," 1965.

5. Brock, Robert H., Jr. and Faulds, Arthur H., "Atmospheric Refraction and its Distortion on Aerial Photography", Photogrammetric Engineering, March, 1964, Vol. XXX, No. 2, Pages 292-298.

6. Brown, Duane C., "Decentering Distortion and the Definitive Calibration of Metric Cameras," Presented at American Society of Photogrammetry, Annual Meeting, 1965, Washington, D.C.

7. Cunietti, M.; Inghilleri, G.; Togliatti, G.; "Aerotriangulation on the AP/C", Report, Roma, 1964.

8. DeAngelis, Q. C., "Tests and Evaluation of Ultra-Wide-Angle Mapping Photography." Technical Report No. 6-TR; USAE/GIMRADA, June, 1962.

9. Eden, J. A., "The Conditions Necessary for Plotting Stereo Models in which the Set Principal Distance is not the Same as That of the Taking Camera," Photogrammetric Eng., March, 1962, Vol. XXVIII, No. 1.

10. Friedman, S. J., "The AP/1 System", Photogrammetric Engineering, July, 1962, Vol. XXVIII, No. 3.

11. Ghosh, S. K., "Investigation into the Problems of Relative Orientation in Stereo-Aerial Photogrammetry"; Technical Report, Ohio State University Research Foundation submitted to USAE/GIMRADA, August, 1964.

12. Ghosh, S. K., "Photogrammetric Research and Measurement of Spheres", Technical Report, Ohio State University Research Foundation, June, 1965.

13. Gruner, H. E., "Super-Wide-Angle Projection Mapping Instrumentation", Photogrammetric Engineering, September, 1964, Vol. XXX, No. 5, Pages 661-866.

14. Halbrook, J. W., "Ultra-Wide-Angle Mapping," Photogrammetric Engineering, September, 1962, Vol. XXVIII, No. 4, Pages 657-660.

15. Harris, W. D.; Tewinkel, G. C.; and Whitten, C. A.; "Analytic Aerotriangulation", Coast and Geodetic Survey Technical Bulletin No. 21, July, 1962.

16. Helava, U. V., "Analytical Plotter", Canadian Surveyor, June, 1963, Vol. XVII, No. 2.

17. Helava, U. V., "Analytical Plotter Using Incremental Computer", Photogrammetric Engineering, June, 1960, Vol. XXVI, No. 2.

18. Horsfall, C. T., "Aerotriangulation Strip Adjustment Using FORTRAN and the IBM-1620 Computer", Report, Coast and Geodetic Survey, March, 1965.

19. Jaksic, Z., "Aerial Triangulation on the Analytical Plotter", Canadian Surveyor, June, 1963, Vol. XVII, No. 2.

20. Johnson, E. C., "System Design of a Digital Control Computer for an Analytical Stereoplotter", Photogrammetric Engineering, September, 1961, Vol. XXVII, No. 4.

21. Johnson, E. C. and Kamm, V. C., "Computer and Programs for AP/C", Canadian Surveyor, June, 1963, Vol. XVII, No. 2.

22. Kasper, Hugo, "Photogrammetry and Electronic Computing in Highway Engineering", Journal of the Society of Swiss Highway Engineers.

23. Kasper, H., "Super-Wide-Angle Photos for Large-Scale Mapping", Photogrammetric Eng., July, 1965, Vol. XXXI, No. 4, Pp. 635-637.

24. Kasper, H. and Neumaier, K., "Aerial Triangulation Tests with Super-Wide-Angle Photography", OEEPE, Special Publication, No. 2, 1965, (Organization Européenae d'Etudes Photogrammetriques Expérimentales).

25. Keller, M. and Tewinkel, G. C., "Aerotriangulation Strip Adjustment", Coast and Geodetic Survey Technical Bulletin No. 23, Aug., 1964.

26. Keller, M. and Tewinkel, G. C., "Aerotriangulation: Image Coordinate Refinement", Coast and Geodetic Survey Technical Bulletin No. 25, March, 1965.

27. Lampton, B. Frank, "The Mathematical Compensation of Film Distortion for Analytical Photogrammetry", Presentation 1965 ACSM--ASP Convention, Washington, D. C.

28. Laurila, Simo, Textbook--"Electronic Surveying and Mapping", 1960.

29. Leijonbufuud, Alex, "On Astronomic, Photogrammetric and Trigonometric Retraction", Stockholm, Sweden, 1950.

30. Löscher, W., "Optimum Field Angle for Aerial Cameras", Photogrammetric Engineering, July, 1964, Vol. XXV, No. 4, Pp. 613-621.

31. Prescott, Wm. G., "The Orientation of Kelsh Plotter Stereo Models Utilizing Aerial Triangulation Data from the Analytical Plotter AP/C", The Ohio State University, Thesis, 1965.

32. Pryor, William T., "Evaluation of Aerial Photography and Mapping Highway Development," Photogrammetric Eng., Jan., 1964, Vol. XXX.

33. Pryor, William T., "Highway Engineering Influences on Aerial Surveys", Photogrammetric Engineering, March, 1964.

34. Schmid, Hellmut, "Precision Photogrammetry, a Tool of Geodesy", Photogrammetric Engineering, December, 1961, Vol. XXVII, No. 5.

35. Schmid, Hellmut, "Analytical Photogrammetric Instruments", Photogrammetric Engineering, July, 1964, Vol. XXX, No. 4, Pages 497-660.

36. Tewinkel, G. D., "Film Distortion Compensation for Photogrammetric Use", Coast and Geodetic Survey Technical Bulletin No. 14.

37. Van Wijk, M. C., "The Use of the A9 - B9 System in Aerial Surveying", Photogrammetric Engineering, January, 1964, Vol. XXX, No. 1, Pages 1-164.

38. Washer, F. E., "The Precise Evaluation of Lens Distortion", Photogrammetric Engineering, March, 1963, Vol. XXIX, No. 2, Pages 213-356.

39. Zeller, M., "Textbook of Photogrammetry", 1952.

Project Supervisor _____ Date Sept. 27, 1966

Executive Director Robert C. Stephenson Date 10-5 — 1966